EPOXIDIZED SUCROSE SOYATE AS A PRIMARY BINDER IN PARTICLEBOARD

A Thesis
Submitted to the Graduate Faculty
of the
North Dakota State University
of Agriculture and Applied Science

By

Andrew James Norris

In Partial Fulfillment of the Requirements
for the Degree of
MASTER OF SCIENCE

Major Program:
Mechanical Engineering

May 2018

Fargo, North Dakota

North Dakota State University
Graduate School

Title

EPOXIDIZED SUCROSE SOYATE AS A PRIMARY BINDER IN PARTICLEBOARD

By

Andrew James Norris

The Supervisory Committee certifies that this ***disquisition*** complies with North Dakota State University's regulations and meets the accepted standards for the degree of

MASTER OF SCIENCE

SUPERVISORY COMMITTEE:

Dr. Dilpreet Bajwa
Chair

Dr. Sreekala Bajwa

Dr. Dean Webster

Approved:

August 17, 2018
Date

Dr. Alan Kallmeyer
Department Chair

ABSTRACT

Wood composites industry has been growing for decades. However, wood composites have been associated with some health concerns due to the presence of formaldehyde. A promising bio-based resin Epoxidized Sucrose Soyate (ESS) was investigated as a potential primary binder in particleboards. The goal of this research was to find a strong and durable resin for wood composite. Several ESS-MDI based formulas were found that were able to match the performance criteria for particleboard.

ACKNOWLEDGEMENTS

I would like to acknowledge all the people that helped make this possible. Dr. Dilpreet Bajwa for pushing me to go to graduate school, without his influence I probably would have never gone. My committee, Dr. Dilpreet Bajwa, Dr. Sreekala Bajwa, and Dr. Dean Webster, for dedicating their time and for their patience with this project. Grant Engeman, Josh Liaw, Brian Barta, and NDSU's statistician Curt Doetkott for giving a helping hand in moving the project along. Also, I owe a big thank you to Broadview Technologies who not only donated considerable supplies to this project but also Jason Tuerack and Phillip Rhoades taking the time to discuss with us any issues with the products we were experiencing. Finally, I would like to thank the North Dakota Soybean Council for financially backing this project.

TABLE OF CONTENTS

LIST OF TABLES

LIST OF FIGURES

LIST OF ABBREVIATIONS

MDI or M.....Methylene diphenyl diisoycanate.

ESS.....Epoxidized Sucrose Soyate.

Form2 or F2 .....Formula 2.

MUF.....Melamine urea formaldehyde.

UF .....Urea formaldehyde.

PF .....Phenol formaldehyde.

MHHPA .....Methylhexahydrophthalic Anhydride.

MTHPA.....Methyltetrahydrophthalic Anhydride.

DSC.....Differential Scanning Calorimetry.

FTIR.....Fourier Transform Inferred Spectrometry.

LIST OF SYMBOLS

100A	100% of the resin in the board is resin A with a standardized resin content of 4%.
75A	75% of the standard resin content is used in this board and is of resin composition A.
25A/75B	25% of the boards resin content is resin A and 75% of the boards resin content is resin B. Standard resin content of 4% total resin content is used.
50A/50B	50% of the boards resin content is resin A and 50% of the boards resin content is resin B. Standard resin content of 4% total resin content is used.
75A/25B	75% of the boards resin content is resin A and 25% of the boards resin content is resin B. Standard resin content of 4% total resin content is used.

LIST OF APPENDIX TABLES

LIST OF APPENDIX FIGURES

1. INTRODUCTION

Wood composites is approximately a 100-billion-dollar industry that is poised to grow [1]. This is predicted to be true for the next 15 years, and one of the reasons for this is that there are many applications in which wood products could be used that haven't been explored yet [2,3] Furthermore, this growth shows no signs of being hindered because currently the demand for wood products has not outpaced the rate of forest growth across North America and this is expected to continue the for next 15 year period [2,4]. Additionally, wood composites, especially fiberboard and particleboard, can be made by using the waste streams from other lumber mills further reducing the ecological impact of the industry [5]. However, the industry does have some obstacles to overcome for this growth to be fully realized, namely in trying to eliminate the health risk associated with the current synthetic resin binder systems used in the industry. Removing these health risks will overcome a major issue in creating an industry that is safe, ecological, and economical. This is where plant-based resins are looking to fill a niche.

Vegetable oils have shown promise in recent years as a substitution or replacement for synthetic or petroleum-based resins. This is due to their abundance, making them relatively cheap when compared to other options [6]. Soybean oil has been the predominate oil of study due to its availability from high production volume compared to other vegetable oils such as linseed [7]. A soy-based epoxy, Epoxidized Sucrose Soyate (ESS), has been shown to have similar properties to the primary binders used in particleboard urea-formaldehyde (UF), melamine-urea-formaldehyde (MUF), phenol-formaldehyde (PF), and Methylene diphenyl diisoycanate (MDI) making it a possible bio-based replacement for these resins [8]. ESS has been shown to work with the existing equipment used in the manufacturing of particleboard, making it easy and efficient to adopt as the new alternative resin [8]. However, the main

drawback has been that the processing time was significantly longer than the current resins in use, thus making the change uneconomical [9].

1.1. Objectives

Therefore, the goal of this study is to find a resin binder system using ESS that can eliminate or reduce the amount of Methylene diphenyl diisoycanate (MDI) used, while maintaining the properties of the particleboard at low cure times of 5 min and 10 min. To accomplish this several resin systems, comprising of ESS, crosslinker, and catalyst, were tested, along with a mixing of those systems with MDI. These formulas were tested at different times, 5 min and 10 min, and temperatures, 175^{o}C and 190^{o}C, to account for any influence these parameters had on the particleboard properties.

2. LITERATURE REVIEW

2.1. Resins

2.1.1. Standard industrial wood composite resins

The most common binders used in the industry are urea-formaldehyde (UF), melamine-urea-formaldehyde (MUF), phenol-formaldehyde (PF) and Methylene diphenyl diisoycanate (MDI) [10,11]. Unfortunately, all of these pose a health hazard, and governments and health agencies want to move away from these health damaging chemicals [10]. Formaldehyde is defined by the EPA as a carcinogenic, compound and limits its emission in the US from 0.05 ppm to 0.13 ppm depending on the product, while the World Health Organization (WHO) has a recommendation of 0.008 ppm to mitigate health risk [11,12]. These emissions are a problem because UF products continue to emit formaldehyde over the life time of the product [10]. While products like MUF and PF can greatly reduce these emission, they come with their own set of issues [10]. MUF has the same issue as UF with it emitting formaldehyde over its lifetime though at a lower emission rate [10,13]. However, it is unclear as to whether this lower emission rate is actually a reduction in overall emissions, or if the emissions are the same and simply take place over a longer period of time [10]. Meanwhile PF has added the chemical phenol to the formaldehyde mixture and which does lower the emission when compared to UF and MUF, but phenol is defined as being an immunotoxicant by the National Institute of Health and therefore has an additional health risk associated with it [10]. The last resin MDI does not emit formaldehyde or any other compound over its lifetime but, is still labeled a cariogenic by the EPA for people working with the uncured form of MDI [14]. Along with this, MDI is an occupational hazard causing respiratory issues and can even lead to asthma in 5% to 10% of workers [10].

2.1.2. Epoxidation

An epoxy is characterized by the epoxide reaction group being the reactive structure. The epoxide is a cyclic ether in which an oxygen atom is contained in a three-member ring [15]. High epoxide functionality leads to a more rapid cure and higher crosslink density creating a stronger material [16].

Epoxidation is the process of adding epoxy groups to a molecule [15]. Epoxidized Sucrose Soyate (ESS), as the name suggests, is synthesized by epoxidation of the double bonds in sucrose soyate, which has been made by esterification of soybean fatty acids with sucrose. The sucrose soyate used has an average degree of substitution of 7.7 of the 8 hydroxyl groups on sucrose with the soybean fatty acids. This leads to a highly functional epoxy resin as can be seen in Figure 1. This structure thus allows for a high degree of crosslinking which with its unique properties has potential to replace petroleum-based epoxies [18].

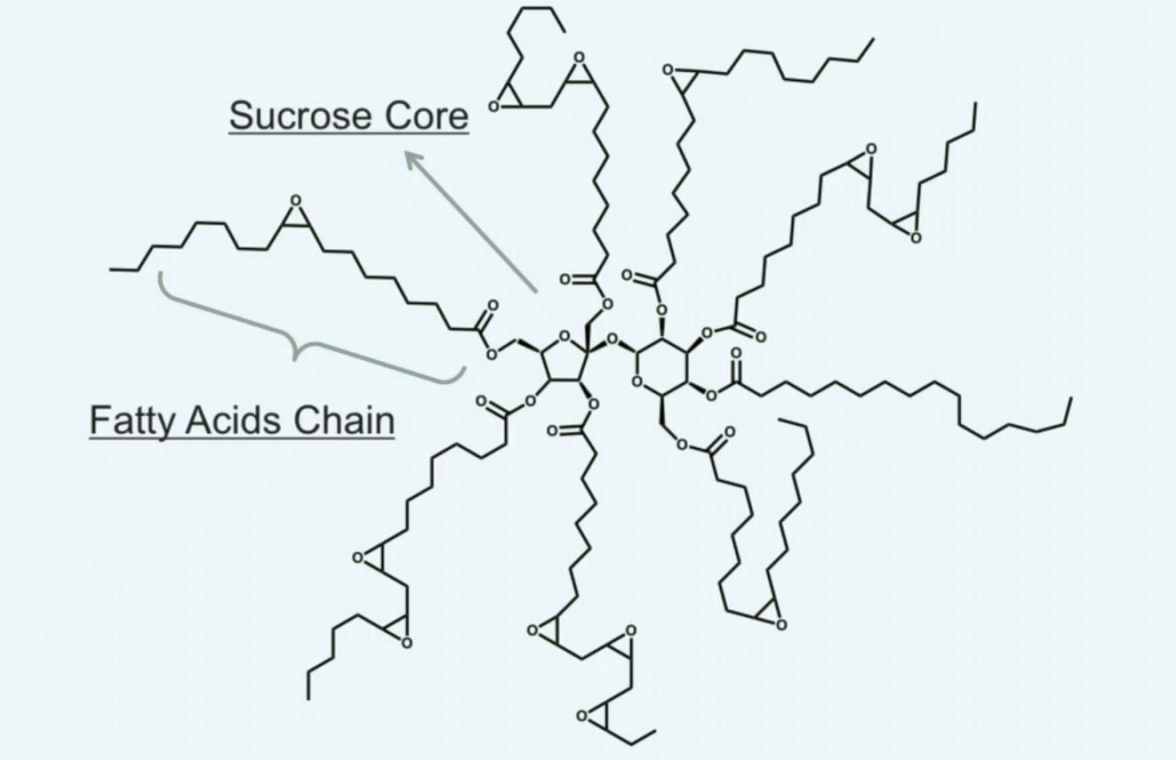

Figure 1: Molecular structure of fully substituted sucrose molecule [19]

2.1.3. Crosslinkers and catalysts

ESS is a bio-based resin with the potential for super high crosslinking density which happens to pair well with anhydrides [18,19]. Anhydrides have been shown to effectively crosslink with bio-based epoxies [7,19,20,21]. This is due to their highly reactive structure which places 6 carbons relatively close to each other which facilities crosslinking during a reaction as the ring opens [20,21]. Anhydrides have relatively good thermal and moisture stability [20,21]. This tied in with them being less hazardous then other curing agents, makes anhydrides a great candidate for a crosslinker [20,21]. The most common anhydride found throughout research are Methylhexahydrophthalic Anhydride (MHHPA) and Methyltetrahydrophthalic Anhydride (MTHPA) [7,9,18,19,20]. Based on previous studies they stand as a good starting point for this research [7,9,18,19,20].

The catalysts used in this study were quaternary ammonium salts supplied by Broadview Technologies, NJ. These were found in a previous study to be effective on catalyzing the crosslinking in an ESS - anhydride based resin [19]. On top of that they have been shown to have lower cure times than other catalyst and since low cure times is a primary objective in this study it is a natural fit. Past experiments have used 1,8-Diazabicyclo[5.4.0]undec-7-ene (DBU) but due to its expensive nature and it being a slow curing catalyst leading to long cure times makes it not fit the criteria as compared to the quaternary ammonium salt [9]. Combining ESS with these crosslinkers and catalyst leads to a larger array of mechanical properties that can fill a host of unique applications [19].

2.1.4. Epoxidized sucrose soyate in particleboard

Several studies showed that vegetable oil derived resins can be applied in wood particleboards [22,23]. Specifically, when looking at Epoxidized Sucrose Soyate (ESS) based

composites the ESS based composites exceeded expectations for both flexural and tensile properties and both studies were able to conclude that ESS has potential in structural materials [22,23]. Along with this an ESS-MDI mixture was used as a particleboard binder and showed promise [9]. These results indicate that a substitution of MDI might be achievable even if a full replacement is not.

2.2. Particleboard

2.2.1. Particleboard manufacturing process

To get to the finished product of a particleboard it must go through several processes to move from wood chips and lumber mill waste to the finished product. It starts by drying the material to around a 2.5% moisture content [24]. This is to prevent an excess of water vapor from forming during the pressing process that can lead to compromising the strength of the material by creating internal stresses and sometimes forming cracks [25,26]. After drying the materials are sifted into either a fine or coarse category [24]. The coarse category is generally to be used as the core of the board while the fine is used on the surfaces [24]. Then glue is sprayed to the fibers this can be done in a drum which agitates them or by conveyer belt both are coated by atomized sprayer [24]. The advantage to the drum method is that the glue is distributed more evenly across the particles due to more surface area of the particles being exposed during this process as well as any excess resin being able to transfer between different particles through contact [25]. The resin distribution can be increased further by increasing the atomization, or how fine the sprayer sprays, this has diminishing returns with finer sprays taking more time to spray for nominal strength gains [25]. The amount of resin added to the material depends on the type of resin with MDI being about 2% of the weight content of the board while resins like UF can be as much as 8% to 12% of resin content [24]. As resin content increases so does cost so

keeping the resin content as low as possible is an important factor [24]. Also, at this stage in the process any other additives are added a common one being wax which is usually added at about 0.5% to 1% total weight which helps increase resistance to moisture absorption [24]. After the particles are coated in resin they are laid as a mat on a hot platen and pressed at desired temperatures and pressures [24]. There are two different types of particleboard layups single layer and multi-layer [24]. While both are still made multi-layer is far more common than the single layer version [24].

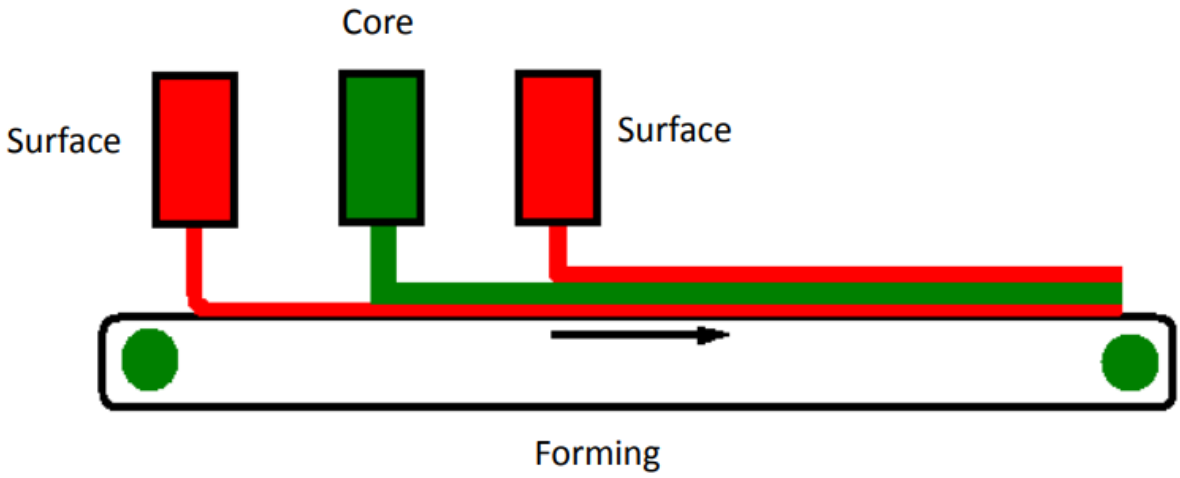

Figure 2: Basic diagram showing multi-layer particleboard layup [24]

The single layer layup is just one layer of material with the same coarseness and other properties all the way through the board [24]. While multi-layer layup uses a coarser material for the core of the particleboard and a finer material for the surface [24]. Multi-layer boards have better properties than their single layer counterparts. The reason for this is that the outer surface which is more densely packed and harder makes the board stiff and resistant to cracking. Meanwhile the soft core allows the material to be able to bend and not act in a brittle fashion. Also, the finer material along the surface has a higher moisture content then the core of the board usually around 10% to 15% [24]. This extra moisture helps transfer the heat through the entire

board to speed up the curing process while also increasing the amount of cure when being pressed [24,26]. After pressing they are conditioned by cooling and then shipped to market [24].

2.2.2. Board processing procedure

Particleboard formation is function of temperature, press time, press load, and moisture content that all influence the particleboards properties [26,27,28,29,30]. Temperatures and press time both deal with the same core issue that leads to the same result lower overall board strength [29,31,32]. This is because the fibers have degraded from too much heat or the resin isn't cured fully due to a lack of heat [29,31,32]. Press load mainly influences the density and by extension stiffness of the board along with the amount of spring back that occurs [26,29] Spring back is the relaxation of the structure after pressing that occurs because of a reduction in the load, and internal stress relaxation due to water vapor escaping that was trapped in the material [26,29]. The amount of water vapor is a function of the moisture content within the material [26,29]. This water vapor is important factor in helping cure the board as wood is naturally an insulator, the vapor helps in the heat transfer throughout the board allowing for an evenly distributed cure [26,29,30]. However, too much vapor pressure within the board will lead to explosive decompression during spring back destroying the board [26,29].

2.2.3. Particle vs Fiber vs OSB vs Plywood

Wood based composites includes materials such as fiberboard, particleboard and plywood that are commonly used in many settings both residential and commercial based on their density and grade [33]. This section looks to define the difference between particleboard, fiberboard, Oriented Strandboard (OSB), and plywood as defined by ASTM D1554. Particleboard is made up of particles as the name suggests where a particle is a catch all for any wood product that is a small subdivision of the starting product [34]. This includes chips, flakes,

curls, sawdust, shavings, slivers, strands, wood flour, and wood wool [34]. Wood flour was refined raw material used for the boards in this research. Wood flour comes in the form of wood particles that were reduced in size through hammer milling until they resembled wheat flour and could pass through 40-mesh screen [34]. Similarly, fiberboard is compositionally fibers which are defined as slender threadlike elements or groups of fibers made through chemical or mechanical defiberization [34]. OSB is made of strands defined as a wood flake having a length to width ratio of 2:1 [34]. Plywood uses veneers or plys that are the full length and width of the board and builds up several layers of them to create its depth varying from the other boards that are made with particulates. This is only one way to classify the wood composite boards however their density and other characteristics can be used to further define what applications a product might have.

2.2.4. Wood products and classification

Classification of particleboard, fiberboard, and composition boards are further broken down by their density and grade to better define what applications they are best suited for. Instead of going in-depth on the applications of each of the different board types and their different classifications, for this research particleboard were selected as the most relevant to this research. Medium density particleboard is defined as having a density of 640 kg/m^3 to 800 kg/m^3 according to the ANSI 208.1 while it defines low density particleboard as anything under 640 kg/m^3 and anything above 800 kg/m^3 is defined as high density particleboard [33,35,36]. These classes of density are further broken down into grades with properties that fill a niche application. Grades such as 1-M-1, 2-M-2 and 2-M-3 are well suited to being floor underlayment due to its smooth level surface that is particularly indent resistant with the 2 series being more for industrial use in buildings like factories [33]. While grades 1-M-2 and 1-M-3 are used as the

cores of furniture such as laminate kitchen countertops [33]. The 2-M grades (2-M-1, 2-M-2, and 2-M-3) have also been found to be useful as sheeting for roofs and exterior walls and as siding [33]. However, the added weight of particleboard makes it difficult to install over a waferboard or OSB by comparison and as such their use as sheeting is quite limited [33]. As for the low-density grades, they mainly find use as door cores since weight is a more defining factor over parameters such as toughness in those products [33].

Table 1: Property requirements for type 1 and 2 mat-formed particleboards (ANSI 208.1)

Grade	Modulus of Rupture	Modulus of Elasticity	Internal Bond	Hardness	Linear Expansion	Screw Withdrawal
1-H-1	16 MPa	2413 MPa	896 kPa	2225 N	n/a	1780 N
1-H-2	20 MPa	2413 MPa	896 kPa	4450 N	n/a	1891 N
1-H-3	23 MPa	2757 MPa	965 kPa	6675 N	n/a	2002 N
1-M-1	11 MPa	1723 MPa	413 kPa	2225 N	0.35%	n/a
1-M-2	14 MPa	2240 MPa	413 kPa	2225 N	0.35%	1001 N
1-M-3	16 MPa	2757 MPa	551 kPa	2225 N	0.35%	1112 N
1-L-1	5 MPa	1034 MPa	137 kPa	n/a	0.30%	556 N
2-H-1	16 MPa	2413 MPa	861 kPa	2225 N	n/a	1780 N
2-H-2	23 MPa	2757 MPa	2068 kPa	8010 N	n/a	2002 N
2-M-1	12 MPa	1723 MPa	413 kPa	2225 N	0.35%	1001 N
2-M-2	17 MPa	3102 MPa	413 kPa	2225 N	0.35%	1112 N
2-M-3	20 MPa	3447 MPa	413 kPa	2225 N	0.35%	n/a

**Table 1 is adapted from the table found in [33] and has had its units converted to SI from English units.

3. OBECTIVES

The objectives of this research are to find a resin binder system using ESS that can cure within a set time window, be used as a binder in particleboards, and be blended with Methylene diphenyl diisoycanate (MDI) to make particleboards that maintaining the properties of MDI based particleboards. To accomplish this several resin systems, comprising of ESS, crosslinker, and catalyst, were tested, along with mixing of those systems with MDI. These formulas were tested and different times, 5 min and 10 min, and temperatures, 175^{o}C and 190^{o}C, to account for any influence these parameters had on the particleboards properties.

H1: An ESS resin binder system that includes a crosslinker and a catalyst can be made that can cure within a 5 to 10 min cure window.

H2: An ESS based resin system can be used as the sole binder in particleboards and be comparable to industrial resins (MUF, UF, PF, MDI).

H3: An ESS resin system can be partially substituted for MDI in particleboards while maintaining its properties.

4. METHOD

4.1. Resin Analysis

4.1.1. Design of experiment for resin analysis

Each resin was run through a series of tests to determine their viability as a primary binder in particleboard. The different resin systems were analyzed through by using DSC and lap shear testing. DSC was used to determine if the resin cured within the designated time window. Meanwhile, lap shear testing was used to determine if the resins were strong enough to be used as a primary resin binder. After a resin system was determined to be useful as a primary resin binder, Fourier Transform Inferred Spectrometry (FTIR) was performed to determine what the chemical composition of the material is.

4.1.2. Materials for resin analysis

A 1.5 mm thick Finnish birch plywood was acquired from Aircraft Spruce (Corona, CA) for lap shear testing. The crosslinkers (MHHPA, MTHPA) and catalysts (BV-CAT7, BV-CAT7FC, AC-8) were provided by Broadview Technologies (Newark, NJ). The control (MDI) was supplied by Primeboard Masonite Corporation (Wahpeton, ND) and the epoxy (ESS) was supplied by NDSU through previous research testing pilot scale production [17].

4.1.3. ESS resin formulation selection

For this experiment ESS was paired with two different crosslinkers, MHHPA and MTHPA, and three different catalyst, AC-8, BV-CAT7 and BV-CAT7FC. These different resin systems were made by mixing 100 parts by weight ESS with 80 parts by weight crosslinker and then adding 2 or 4 parts by weight to create two different mixtures for the BV-CAT7 and BV-CAT7FC while AC-8 was 10 parts by weight as recommended by the manufacturer due to higher amounts being required to properly function. This was then combined with the control, 100%

MDI resin, which was used as a control to compare with the different studies that have been conducted in the past [9,10]. All these resins can be seen in Table 2.

Table 2: Resin-crosslinker-catalyst ratio chart

Primary Resin	Catalyst	Crosslinker	Mixture Ratio	Name
ESS	BV-CAT7FC	MHHPA	50:40:02	Formula 1
			50:40:01	Formula 2
		MTHPA	50:40:02	Formula 3
			50:40:01	Formula 4
	BV-CAT7	MHHPA	50:40:02	Formula 5
			50:40:01	Formula 6
		MTHPA	50:40:02	Formula 7
			50:40:01	Formula 8
	AC-8	MHHPA	50:40:05	Formula 9
		MTHPA	50:40:05	Formula 10

Another aspect that was evaluated included identifying what impact mixing an ESS based resin from the above table would have with MDI. Three ratios of 3:1, 1:1 and 1:3 ESS:MDI were selected for evaluation and testing. Instead of testing every one of the aforementioned resins in these three different mixtures the best performing resin from the Table 2, which happened to be Formula 2, was taken and run through the screening process outlined in the procedure.

Table 3: Control based formulations

Name	Composition	Ratio
25F2/75M	Formula2/MDI	1:3
50F2/50M	Formula2/MDI	1:1
75F2/25M	Formula2/MDI	3:1

Resins mass was weighed on an Adventurer Analytical scale made by Ohaus (Parsippany, NJ). The resins were mixed by first portioning out the proper amount of epoxy and then adding the crosslinker and finally the catalyst. The mixture was immediately stirred for 5

min manually by using an uncontaminated stir stick. A resin mixture was prepared and used on the same day to manufacture test samples.

4.1.4. Differential scanning calorimetry

To characterize if the resin system cured within the desired cure time and temperature a Differential Scanning Calorimetry (DSC) technique was employed. The DSC was run at a ramp rate of 10^{o}C per minute from 25^{o}C to 200^{o}C to see if any exothermic activity occurred in that range characterized by a rising slope. If so, then an isothermal test was conducted.

The settings for the isothermal involved quickly ramping from 25^{o}C to the desired temperature with a ramp rate of 20^{o}C per min and then holding at that temp for 20 min. The four temperatures tested were 130^{o}C, 150^{o}C, 175^{o}C, and 190^{o}C. The reason these four temperatures were tested was that they cover most of the exothermic range of the samples. In addition, the lower two temperatures followed Broadview Technologies recommendations for the three catalysts that were selected, while the higher two temperatures are a more typical cure temperature for industrial resins (MDI, UF, PF). So, this set of four temperatures would be able to test both the manufactures specifications and industrial ones.

The testing was performed on a TA Instruments Q20 Differential Scanning Calorimeter (Newcastle, DE). The chamber was purged with nitrogen gas at a rate of 50 ml/min. There were fourteen (14) unique formulas run through this process. If a formulas degree of curing was within the time and temperature constraints, then lap shear testing was conducted on that formulation.

4.1.5. Lap shear testing

Lap shear testing was done in accordance with ASTM Standard D2339-2011 [37]. Sample blanks were cut to dimensions of 25 mm x 76 mm x 1.5 mm of birch plywood. These sample blanks were then glued together with a 25 mm x 25 mm lap joint. This joint was formed

by applying the resin to the both sides of the joint area spread to cover the whole area to be joined. The resin coated samples were then joined and put into a clamp that had been pre-heated to the curing temperature, either 175ºC or 190ºC. The clamped samples were then placed into a Carver Press Model 4122 (Wabash, IN) hot press and pressed until both platens were touching the clamp, but without any pressure being applied. The clamp used in the experiment can be seen in Figured 3 below.

The samples were then cured for the desired time of 5 min or 10 min, and then removed from the hot press and clamp. The samples were allowed to cool down and condition for a minimum of 24 hours under open lab conditions before being tested. Figure 3 and Figure 4 show the clamp with samples in it and the Carver Press that the samples were cured in.

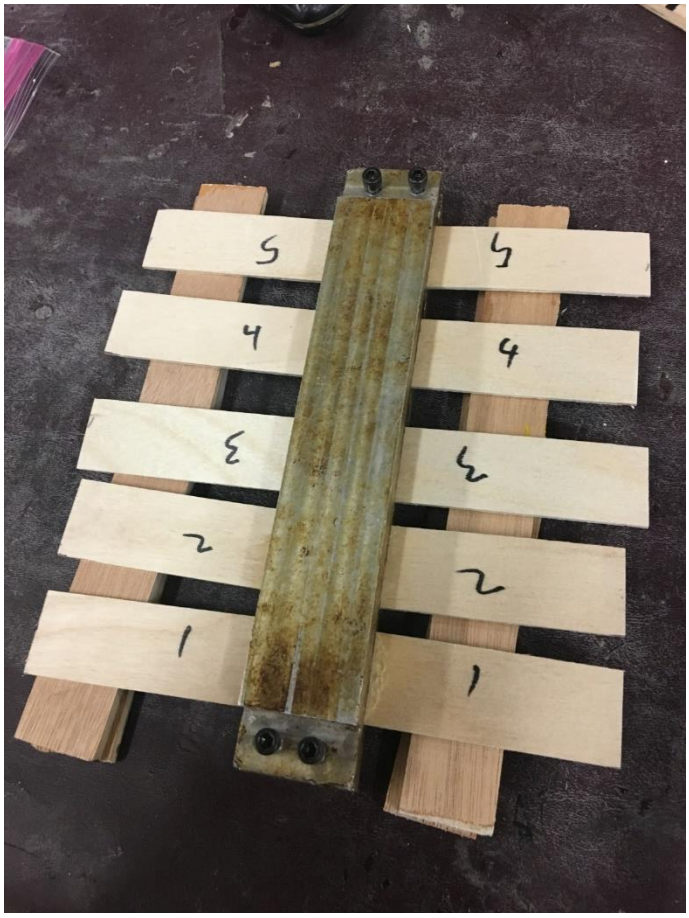

Figure 3: Lap shear clamp for curing samples

Figure 4: Carver press model 4122

Once the samples had cured for the allotted time the shear strength of the samples could be tested. The Samples were tested on an Instron load frame Model 5567 using tension test grips. Extra pieces of plywood were used on either side of the lap shear sample to make sure the sample was aligned vertically 90^{o}.

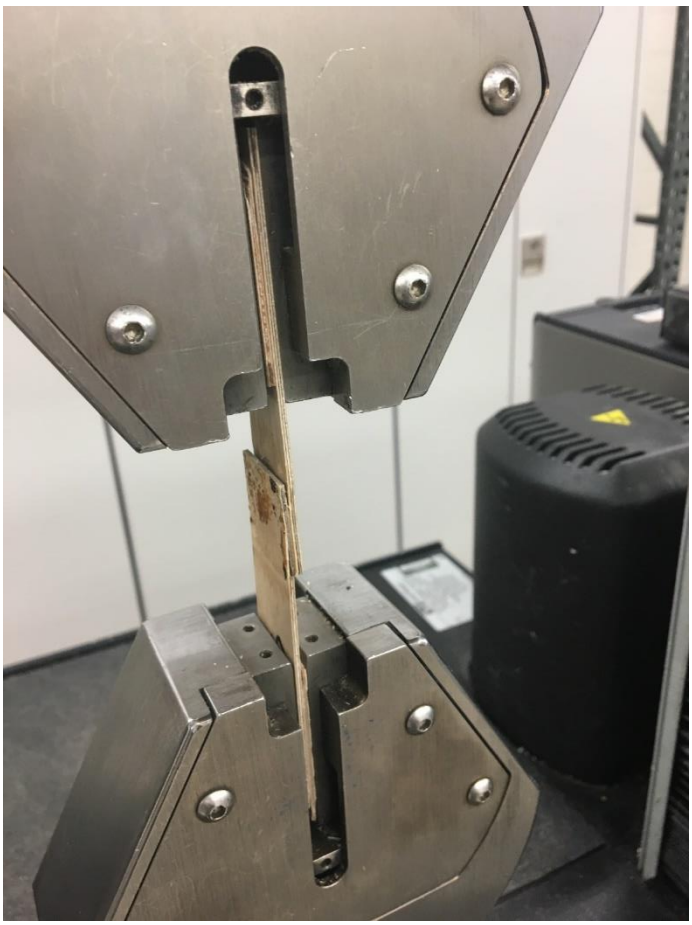

Figure 5: Lap Shear sample being tested in Inston load frame model 5567

The strain rate was set to 1mm/min instead of the load-controlled rate stated in the standard as was performed by [9]. Each sample was tested until failure. If the sample had anything but adhesive dominated failure, then the sample was excluded from the results. The adhesive shear strength was found using the following equation.

$$\tau = \frac{F}{ab} \qquad \text{(Equation 1)}$$

Where τ is the shear stress in MPa, F is the force in N, and a and b are the length and width of the bond area respectively and are given in mm. If a samples shear strength was comparable to that of MDI, then particleboard characterization tests were run for the sample. Five (5) samples were tested for each unique formulation.

4.1.6. Fourier transform infrared spectroscopy

Fourier Transform Infrared Spectrometry was performed to determine if mixing Formula 2 with MDI created any new distinct bonds. To determine this FTIR was run on Formula 2 and all the mixtures Formula 2 and MDI those being, 25F2/75M, 50F2/50/M, and 75F2/25M. The FTIR for the MDI was pulled from literature as it is an established resin that has already been extensively tested [38]. The FTIR machine used was Nicolet 8700 produced by Thermo Scientific (Waltham, MA) using the ATR-FTIR method with a diamond crystal in normal atmospheric conditions. Each sample was scanned 64 times with a resolution of 4 cm^{-1} to generate the spectra.

4.2. Particleboard Manufacture

4.2.1. Design of experiment for particleboard testing

A full factorial design was used to determine the effect of resin, time and temperature on board properties. The resin used in the production of the boards were the ones that showed comparable results to MDI in both DSC and lap shear tests. There were five (5) resin binder system tested three of which were controls. These binder systems were tested at two (2) different temperatures and times. These boards were then fully characterized by testing their density, water absorption, linear expansion, static bending, tension perpendicular to surface (internal bond), screw withdrawal, and hardness. The data generated from these tests was fully evaluated using statistics software Minitab to verify the statistical significance or insignificants of the findings.

4.2.2. Materials for particleboard manufacture

Pine wood flour grade 2020 manufactured by American Wood Fibers (Wausau, WI) was used as raw material for particleboard manufacture. The crosslinkers (MHHPA, MTHPA) and

catalysts (BV-CAT7, BV-CAT7FC, AC-8) were provided by Broadview Technologies (Newark, NJ). The control (MDI) was supplied by Primeboard Masonite Corporation (Wahpeton, ND) and the epoxy (ESS) was supplied by NDSU through previous research testing pilot scale production [17]. The wax emulsion was TRANSSEAL pre-wax manufactured by Groco Specialty Coatings (Dallas, TX) and purchased from Wood Finishers Depot (Baytown, TX).

4.2.3. Manufacturing process

The particleboards were manufactured using 1 kg batches of raw material. The composition of the raw material was 4% resin, 2% wax and 94% wood flour for all boards except 75M which used 1% less resin and 1% more wood flour. Each batch yielded two boards from which all the samples were cut. Two batches for each time and temperature combination were made for a total of four boards per set. The boards were made by placing the wood flour in a cement mixer manufactured by Kobalt (Mooresville, NC) to agitate the wood particles while resin was applied.

Figure 6: Kobalt cement mixer used to mix resin and wood flour

The resin was applied via paint HLVP spray gun made by Vaper (Renton, WA) and was applied on the order of MDI, ESS formula, and TRANSSEAL pre-wax wax emulsion with the spray gun being cleaned between each spray. Once the samples had the resin properly applied to them they were put in a mold, which has been preheated to a set temperature, and pressed to 10 metric tons in the Carver Press Model 4122 (Wabash, IN) hot press which was also used during lap shear testing and is shown in Figure 4. Up to a minute was given to bring the press to the proper tonnage. The pressing time started once this tonnage was reached. The press was maintained at 10 metric tons for the whole duration of the prescribed press time. Below is the figure of the paint sprayer and the mold used to form the boards.

Figure 7: Particleboard mold and HLVP spray gun used for resin distribution

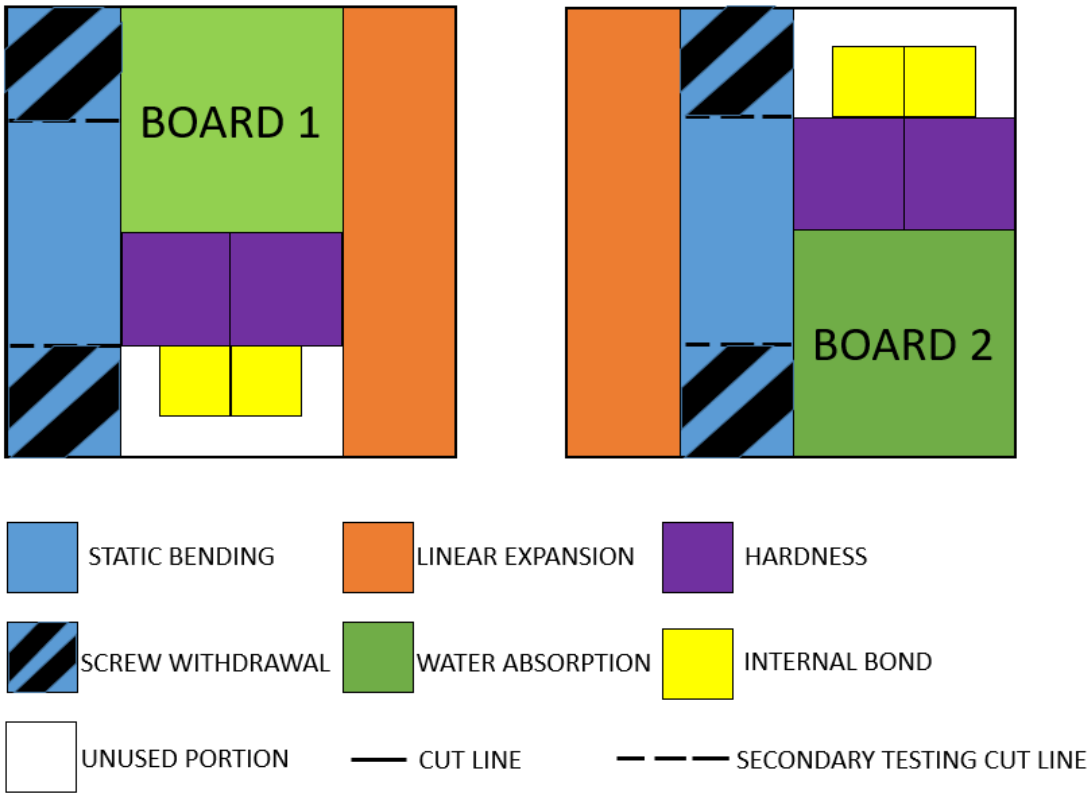

Figure 8: Particleboard sample cut out patterns for all testing samples

The boards were cut using ASTM D1037 as a baseline for the process [39]. Due to the manner of the manufacturing process only being able to produce two boards from one batch of fully resin coated material the board's cuts were designed in a manner to have any variance in batch production be accounted for during testing of the different properties. This meant that each board had to have a sample come from it to account for any such variance. Thus, the cuts in Figure 8 were decided in such a manner as to have a sample contribution from each board to minimize the effect of variance that can occur during the board manufacturing process. It should be noted for the static bending sample the full blue zone including the stiped area designated as the screw withdrawal section was used for static bending. After static bending testing was completed the test specimens were cut for use as screw withdrawal samples. The screw

withdrawal samples were cut from the static bending samples from the undamaged areas after completion of the static bending test.

4.3. Particleboard Characterization

4.3.1. Density

The density was calculated in accordance to ASTM Standard D2395 Section 8 [39]. The density was found by weighing the mass of the full-size boards to within ±0.1g. While the volume was calculated by measuring the two lengths, two widths and four thicknesses, then averaging with the measurements falling within a ±0.001 mm variance. The density was the calculated based on the following equation.

$$\rho = \frac{m}{lwt} \quad \text{(Equation 2)}$$

Where ρ is the density in kg/m^3, m is the mass in kg, l is the length, w is the width and t is the thickness all in m. Four (4) densities were measured for each unique formula.

4.3.2. Water absorption

Water absorption tests the resilience of a board when fully submerged in water. This is an important parameter when considering particleboards viability for use as exterior sheathing material in construction [33]. ASTM Standard D1037-12 Section 23 was followed for this test [39]. The test was a 2-plus-22h water submersion. So, the samples were measured after 2 hours of being submerged and then submerged again for another 22 hours before being measured a final time. The specimen dimensions were 152 mm x 152 mm x approximately 8.5 mm manufactured thickness. The specimens were submerged in water that was maintained at a temperature of 20 ± 1^{o}C. Specimens were measured by taking their length (l), width (w) and thickness (t) at the midpoint of all four sides along with a mass (m) measurement. These

measurements were used to calculate the change in mass and volume for those time periods with the following equations.

$$\%\ Change\ in\ Mass = \frac{m_f - m_i}{m_i} \quad \text{(Equation 3)}$$

$$\%\ Change\ in\ Volume = \frac{V_f - V_i}{V_i} \quad \text{(Equation 4)}$$

Where m_f and V_f are the final mass and volume respectively and m_i and V_i are the initial mass and volume respectively. Volume is given by the following equation.

$$V = lwt \quad \text{(Equation 5)}$$

Where l, w and t are the length, width and thickness of the specimens all in units of mm. Four (4) samples were tested for each unique formulation.

4.3.3. Linear expansion

Linear expansion is the measure of the dimensional stability of a material under high humidity conditions. This is an important factor when looking at structural materials because if not accounted for can lead to buckling of the material due to insufficient spacing to allow for expansion. The linear expansion test was conducted in accordance to ASTM Standard D1037-12 Section 24 [39]. The test was performed in a Binder Humidity Chamber model KBF 115-UL (Tuttlingen, Germany). First the test samples were conditioned to practical equilibrium conditions at 50% relative humidity and temperature of 20 ± 3ºC. Practical equilibrium is defined as not having a mass change greater than 0.05% over a 24-hour period. Then the samples were exposed to relative humidity 80% and temperature 20 ± 3ºC. A 80% relative humidity was used instead of 90% due to the humidity chamber not being able to maintain 90% relative humidity and so it was changed to 80% in accordance to the ASTM D 1047-12 standard. The linear expansion of the board was calculated by the following equation.

$$\%\ Change\ in\ Length = \frac{L_f - L_i}{L_i} \quad \text{(Equation 6)}$$

Where L_f is the final length and L_i is the initial length both of which were measured in mm. Four (4) samples were tested for each unique formulation. Figure 9 shows the humidity chamber and how samples were placed within it.

Figure 9: Linear expansion setup in the Binder Humidity Chamber model KBF 115-UL

4.3.4. Static bending

Three-point static bending testing was conducted to measure the stiffness of the boards. High stiffness is an important factor for load bearing applications such as floor underlayment and sheeting [33]. Each sample was tested on an Instron load frame Model 5567 in accordance to ASTM D1037-12 Section 9 [39]. A picture pf the load frame during testing can be seen in the Figure 10.

Figure 10: Three-point static bending as prescribed by ASTM D1037 being conducted on an Instron load frame model 5567

The sample dimensions were 76 mm x 305 mm x as pressed thickness. The span was set to 204 mm in accordance with the standard and the crosshead rate was set by;

$$N = \frac{zL^2}{6d} = \frac{0.005\frac{mm}{mm*min}(204mm)^2}{6(8.5mm)} = 4.1mm/min \qquad \text{(Equation 7)}$$

Where N is the cross-head rate, z is the outer fiber strain rate given by the standard as 0.005 mm/mm/min, L is the span length, and d is the thickness.

The modulus of rupture and modulus of elasticity were calculated using the following equations;

$$R_b = \frac{3P_{max}L}{2bd^2} \qquad \text{(Equation 8)}$$

$$E = \frac{L^3}{4bd^3}\frac{\Delta P}{\Delta y} \qquad \text{(Equation 9)}$$

Where for Equation 8 R_b is the modulus of rupture, P_{max} is the maximum load, L is the span length, b is the specimen width, and d is the thickness. While for Equation 9 E is the modulus of elasticity and $\Delta P/\Delta y$ is the slope of the straight-line portion of the load–deflection

curve, with L, b and d as being the same as in Equation 8. Four (4) flexural samples were tested for each unique formulation.

4.3.5. Tension perpendicular to surface (Internal bond)

ASTM Standard D1037-12 Section 11 was followed to test the internal bond strength of the specimen which is a measure of its cohesive strength [39]. For this test samples with dimensions 50 mm x 50 mm x approximately 8.5 mm pressed thickness were cut and glued to test blocks using a hot melt glue provided by PrimeBoard Masonite in Wahpeton, North Dakota. The blocks were weighted to help ensure adhesion of the blocks to the samples and then the glue was allowed to cure for a minimum of 6 hours.

Testing was performed on a universal testing machine Instron model 5576 load frame (Norwood, MA). All samples that had failure between the test block and sample were excluded from the data. Figure 11 shows a sample in the fixture undergoing testing.

Figure 11: Internal bond blocks loaded into Instron load frame model 5576

The crosshead rate was set to 1 mm/min as a substitution for the constant strain rate of 0.08 cm/cm called in the standard. This deviation from the standard was due to the unavailability of suitable equipment to measure and keep constant the strain rate of the specimen. The internal bond strength was measured by the following equation;

$$IB = \frac{P_{max}}{ab} \quad \text{(Equation 10)}$$

Where IB is the internal bond strength in MPa, P_{max} is the maximum load achieved for a specimen given in N, a is the width in mm and b is the length in mm. Eight (8) internal bond samples were tested for each unique formulation.

4.3.6. Screw withdrawal

Direct screw withdrawal test measures the ability of the material to hold a fastener such as screw when a load is applied. This is an important parameter to know for any material that is going to be used in a structural capacity. ASTM D1037-12 Section 16 was followed to determine the materials resistance to screw withdrawal [39]. Samples for this test were cut from samples used in the static bending test. Samples were cut sufficiently far from the breakage point of the flexural samples to prevent any influence from the previous test. Sample dimensions were 76 mm x 102 mm x double the manufactured thickness. This extra thickness was required to allow the screw to penetrate the required depth it needed to for the standard. This increased thickness was obtained by gluing two specimens cut from the same sample together using Weldwood contact cement as prescribed by the standard. A lead hole with diameter 3.2 mm was drilled to a depth of 17 mm before inserting the test screw. A type #10 screw was inserted into the lead hole to a depth of 17mm. The specimen was then loaded into the test fixture as shown in Figure 12. Each specimen was tested a rate of 1.5 mm/min and the maximum load required for screw withdrawal was recoded. Four (4) replicates were tested for each unique formulation.

Figure 12: Screw withdrawal fixture and test sample being tested on Instron load frame

4.3.7. Hardness

ASTM Standard D1037-12 Section 17 was followed for testing the hardness of the samples [39]. The samples were of dimensions 76 mm x 152 mm x double the manufactured thickness. To achieve the desired thickness two samples were glued together using Weldwood contact cement as called for by the standard. The test itself was a modified Janka-ball test in which the test was stopped once the ball has penetrated one half its diameter of the radius of the sample. This was modified slightly as the prescribed indentation depth for the Janka-ball indenter would be deeper than the manufactured thickness. As such an indention depth of half the prescribed depth was decided on, that depth being 4.75 mm, and whose depth can be found in a similar study [40]. The loading rate was 6 mm/min with the maximum force recorded as the hardness value. Two tests per sample were conducted leading to eight (8) tests per unique formulation. A picture of the test being conducted can be seen below in Figure 13.

Figure 13: Janka-ball hardness indenter test pre-run on the Instron load frame

4.4. Statistical Method

Analysis of variance (ANOVA) was conducted on the data obtained from all the tests to find which factors and their interactions were significant. Significance was determined through the 95% confidence interval. If any interaction effects were significant the interaction plots were used to determine if an interaction effect occurred. The interaction was then assessed whether it was a strong or weak interaction the interpretation of which is given in Section 4.4.2 Interaction Effects and Plots. Lastly, if a parameter was significant and does not have an interaction effect a Tukey Comparison Test was run to determine if the different samples within that factor differed in a significant way from one another. A more comprehensive explanation of how each of these methods works can be found in the proceeding sections.

4.4.1. Analysis of variance of a factorial design

Analysis of variance (ANOVA) is a method used to compute the error between different variables and their different interactions. This allows for a comparison of all the possible factors that are being tested within the model and determines how significant they are. The significance was determined through a confidence interval. For this study a confidence interval of 95% was chosen. Two factor factorial design and two-way ANOVA, as explained and defined by *Applied Statistics for Engineers and Scientists* [41] was used to evaluate the test results.

Common annotation used throughout this explanation are as follows. A and B are two distinct primary factors, r is the number of levels of factor A, c is the number of levels of factor B, n' is the number of replications for each cell, and n is the total number of observations in the experiment and is equal to rcn'. X_{ijk} is the value of the kth observation for level i of factor A and j of factor B. Common functions that will be seen are as follows:

$$\bar{\bar{X}} = \frac{\sum_{i=1}^{r}\sum_{j=1}^{c}\sum_{k=1}^{n'} X_{ijk}}{rcn'} \quad \text{(Equation 11)}$$

$$\overline{X_{i..}} = \frac{\sum_{j=1}^{c}\sum_{k=1}^{n'} X_{ijk}}{cn'} \quad \text{(Equation 12)}$$

$$\overline{X_{.J.}} = \frac{\sum_{i=1}^{r}\sum_{k=1}^{n'} X_{ijk}}{cn'} \quad \text{(Equation 13)}$$

$$\overline{X_{iJ.}} = \sum_{k=1}^{n'} \frac{X_{ijk}}{n'} \quad \text{(Equation 14)}$$

Where $\bar{\bar{X}}$ is the overall or grand mean. $\bar{X}_{i..}$ is the mean of the ith level of factor A, where i=1, 2, …, r. $\bar{X}_{.j.}$ is the mean of the jth level of factor B, where j=1, 2, …, c. $\bar{X}_{ij.}$ is the mean of the cell ij, the combination of the jth level of factor B. All the variables are defined in the above paragraph for reference. The total variance for all observations is

$$SST = \sum_{i=1}^{r}\sum_{j=1}^{c}\sum_{k=1}^{n'}\left(X_{ijk} - \bar{\bar{X}}\right)^2 \quad \text{(Equation 15)}$$

Where SST is. This can be further split up into the constituent parts to find the sum of squares for factors A and B.

$$SSA = cn' \sum_{i=1}^{r} \left(\bar{X}_{i..} - \bar{\bar{X}}\right)^2 \quad \text{(Equation 16)}$$

$$SSB = rn' \sum_{j=1}^{c} \left(\bar{X}_{.j.} - \bar{\bar{X}}\right)^2 \quad \text{(Equation 17)}$$

Where SSA is the sum of squares due to factor A and SSB is the sum of squares due to factor B. The interaction effect between these two factors is defined as

$$SSAB = n' \sum_{i=1}^{r} \sum_{j=1}^{c} \left(X_{ij.} - \bar{X}_{i..} - \bar{X}_{.j.} + \bar{\bar{X}}\right)^2 \quad \text{(Equation 18)}$$

Where SSAB is the sum of squares due to the interaction of A and B. Meanwhile the error caused by random factors is defined as

$$SSE = \sum_{i=1}^{r} \sum_{j=1}^{c} \sum_{k=1}^{n'} \left(X_{ijk} - \bar{X}_{ij}\right)^2 \quad \text{(Equation 19)}$$

Where SSE is the sum of squares of the error inherent in any system. The mean square values are found by dividing the sum of squares by their degrees of freedom within the system.

$$MSA = \frac{SSA}{r-1} \quad \text{(Equation 20)}$$

$$MSB = \frac{SSB}{c-1} \quad \text{(Equation 21)}$$

$$MSAB = \frac{SSAB}{(r-1)(c-1)} \quad \text{(Equation 22)}$$

$$MSE = \frac{SSE}{rc(n'-1)} \quad \text{(Equation 23)}$$

These equations are then used testing the hypothesis sets the first hypothesis

$$H_0: \mu_1 = \mu_2 = \cdots = \mu_r$$

Against the alternative

$$H_1: Not\ all\ \mu_i\ are\ equal$$

For the F test this is tested by

$$F = \frac{MSA}{MSE} > \alpha \quad \text{(Equation 24)}$$

Where α is a factor of the chosen confidence interval that being of the tails that lie outside the confidence interval of 95% and so α=0.05. This statement means that if F is greater than α then the null hypothesis is true. Likewise, with factor B and the interaction effects of A and B is tested against the α value to test the hypothesis

$$F = \frac{MSB}{MSE} > \alpha \quad \text{(Equation 25)}$$

$$F = \frac{MSAB}{MSE} > \alpha \quad \text{(Equation 26)}$$

4.4.2. Interaction effects and plots

The description of interaction effects comes from the text *Applied Statistics for Engineers and Scientists* [41]. If there is no interaction between two factors (A and B), then any difference in the dependent or response variable between the two levels of factor A would be the same at each level of factor B [41].

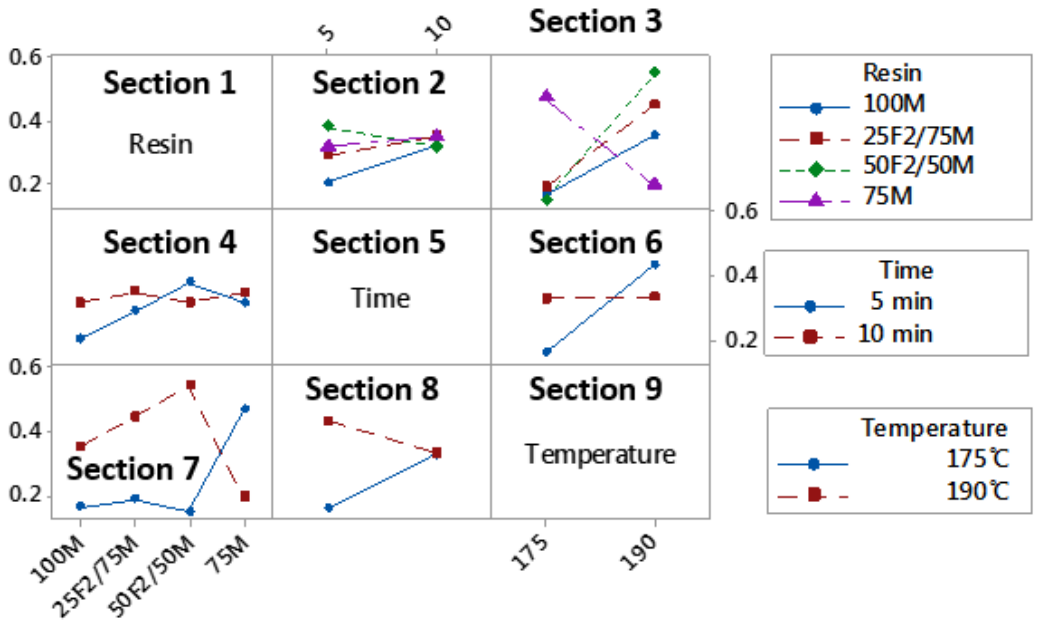

Figure 14: Example interaction plot to highlight strong and weak interaction effects between factors

In Figure 14 some of these interaction effects can be seen. Section 3 in Figure 14 is a good example of a strong interaction effect along with section two and six. Meanwhile, section 8 is a good example of a more average interaction effect while the beginning part of section seven shows a weak interaction effect. While not pictured in Figure 14 parallel lines would indicate no interaction effect.

4.4.3. Tukey Pairwise Comparison Test

The definition of Tukey's Pairwise Comparison Test was derived from *Design and Analysis of Experiments* [42]. To test the pairwise mean comparisons the following hypothesis must be tested:

$$H_0: \mu_i = \mu_j$$

$$H_1: \mu_i \neq \mu_j$$

Where H_0 is the null hypothesis, H_1 is the alternative hypothesis, μ is the mean and $i \neq j$. The Tukey test considers two means as significantly different if the absolute value of the sample difference is greater then

$$T = q_\alpha(a, f)\sqrt{\frac{MS_E}{n}} \qquad \text{(Equation 27)}$$

Where $q_\alpha(a, f)$ is the studentized range statistic whose value is obtained from a table based on the confidence interval used. MS_E is the mean square and n is the number of samples.

4.4.4. Interval plots

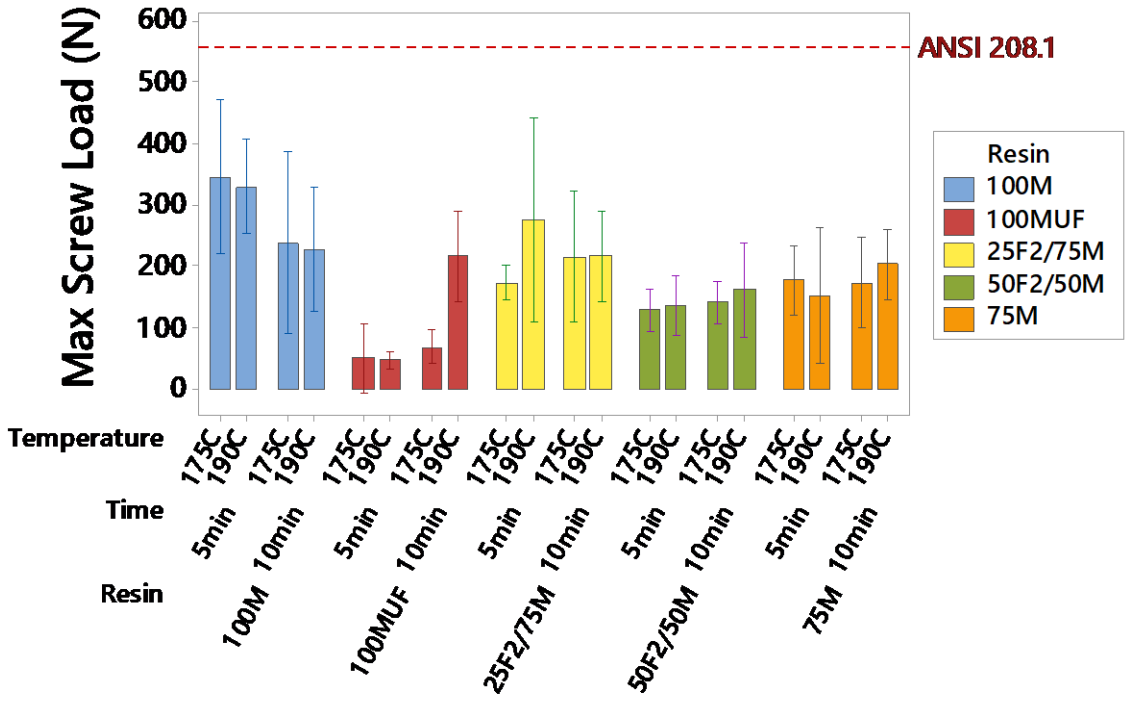

Figure 15: Example interval plot to explain key features of the graph

Figure 15 shows the mean value for the recorded data through the bar graph while the interval lines shows the expected range of data at 95% confidence interval. The ASNI 208.1 line signifies the standards required value for commercial application for a low-density particleboard. One thing to note from Figure 15 is that for 100MUF at a time of 5 min at 175^{o}C the interval plot can stretch into the negative. This was not possible for these tests in a real world setting to go past zero. These anomalies were caused by having large variance and a low mean and was not reflective of the true variance in the samples. If any of these anomalies are seen it can be assumed that the interval ends at zero.

5. RESULTS AND DISCUSSION

5.1. Resin Characterization and Analysis Results

5.1.1. Differential scanning calorimetry results

The purpose of running the DSC tests was to find the curing kinetics of the resins to determine their suitability for the lap shear tests. A DSC test will graph the exothermic energy and show if a resin will cure within the 5 min to 10 min cycle time used when curing lap shear samples allowing the exclusion of resins that will not cure.

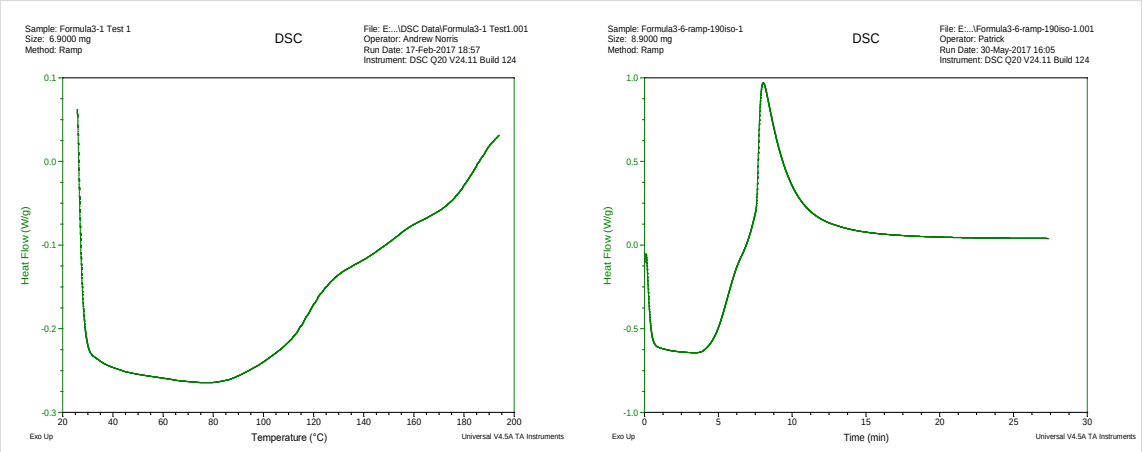

Figure 16: Example DSC curves for ramp and isothermal tests to demonstrate ideal exothermal activity curing curves

Figure 16 shows on the right the graph of the slow ramp, 10^{o}C per min, and on the left was a 190^{o}C isothermal test, both graphs demonstrating the desired exothermal activity. The total thermal energy and peak heat flow were found for the isothermal tests using the Universal Analysis software provided by the DSC manufacturer TA instruments.

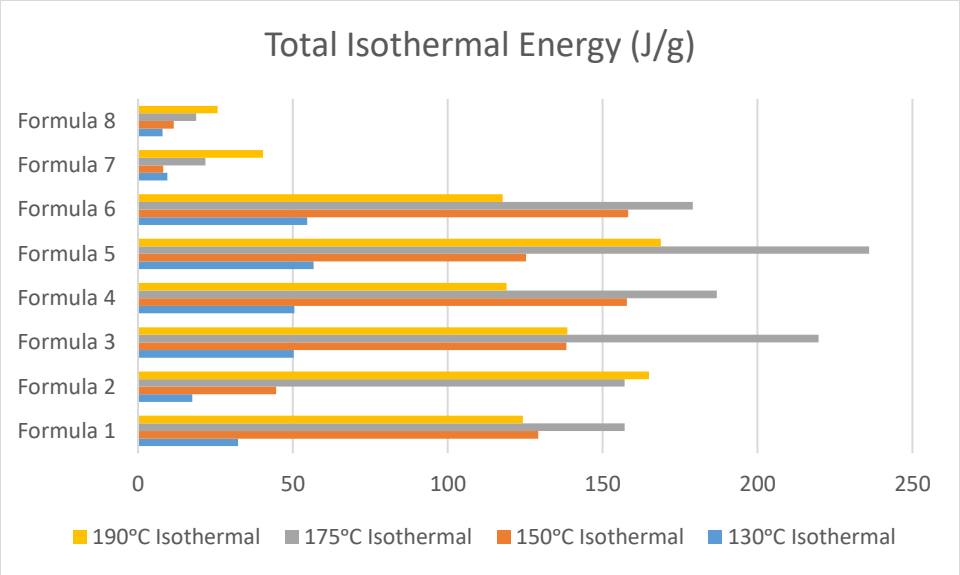

Figure 17: Total integrated isothermal energy from peak heat flow to end of test

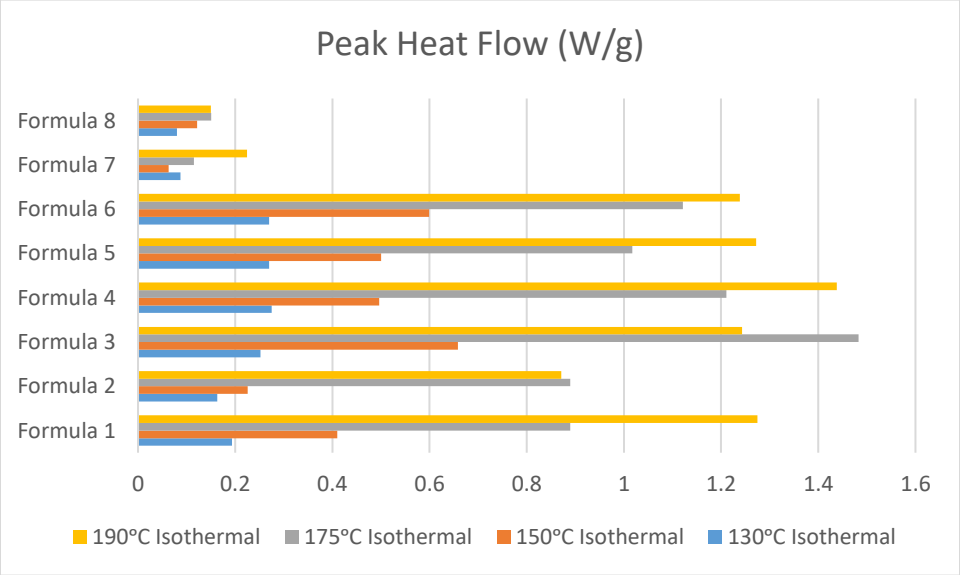

Figure 18: Peak heat flow for each isothermal test

Figure 17 and 18 show the total energy released and peak heat flow rate for various formulations at the different isothermal temperatures. From the figures it appears that peak heat flow was better at determining whether a sample will cure or not over total isothermal energy. This is best illustrated by comparing the total isothermal energy of the 150°C vs 190°C with 150°C being shown to have more total isothermal energy then 190°C for Formula 1, Formula 4,

and Formula 6. However, once the peak energy was compared between the two this was no longer the case and 190^{o}C was found to outperform 150^{o}C every time. Being that none of the samples cured at 150^{o}C this would indicate that peak heat flow was a better indicator of the curing characteristics of resins then total isothermal energy. Figure 18 shows that DSC samples need to have a peak heat flow of at least 0.8 W/g approximately to be able to cure within the 5 or 10 min time range. This was substantiated through the manufacturing process of the lap shear samples. This makes both 130^{o}C and 150^{o}C unsuitable for curing lap shear samples along with some other formulations whose suitability is shown in Table 4.

A couple of notable formulas not listed in Figures 17 and 18 were Formula 9, Formula 10 and the Formula 2-MDI mixtures. Formula 9 and 10 did not have isothermal test conducted on them because the ramp test that was performed showed no exothermal activity as was seen in all other formulations and therefore it was deemed unnecessary to run their isothermals for those formulas. As for the Formula 2 – MDI mixtures, since it was already known that each of these resins had no issues curing independently of one another it was assumed that combing these to resins would not cause the opposite effect of reducing its ability to cure and so the tests were unnecessary. This also proved to be the case as all Formula 2 – MDI mixtures showed no change in their ability to cure during the production of either lap shear samples or during particleboard manufacturing.

Table 4: DSC Performance chart for ESS based resin systems outlining if the resins will be used in further testing

Primary Resin	Catalyst	Crosslinker	Mixture Ratio	Name	DSC (P/F)
ESS	BV-CAT7FC	MHHPA	50:40:02	Formula 1	Pass
			50:40:01	Formula 2	Pass
		MTHPA	50:40:02	Formula 3	Pass
			50:40:01	Formula 4	Fail
	BV-CAT7	MHHPA	50:40:02	Formula 5	Pass
			50:40:01	Formula 6	Pass
		MTHPA	50:40:02	Formula 7	Pass
			50:40:01	Formula 8	Fail
	AC-8	MHHPA	50:40:05	Formula 9	Fail
		MTHPA	50:40:05	Formula 10	Fail

Table 4 shows the resins that qualified for lap shear testing. A pass means the samples were found to suitable cure and met the 0.8 W/g peak heat flow criteria. While a fail simply means that this standard was not met and will no longer be pursued as a possible candidate.

5.1.2. Lap shear testing results

Lap shear testing is used to evaluate the strength of a resin in relation to a control. In this study that control was MDI and all resins were assessed based on how they compared to MDI.

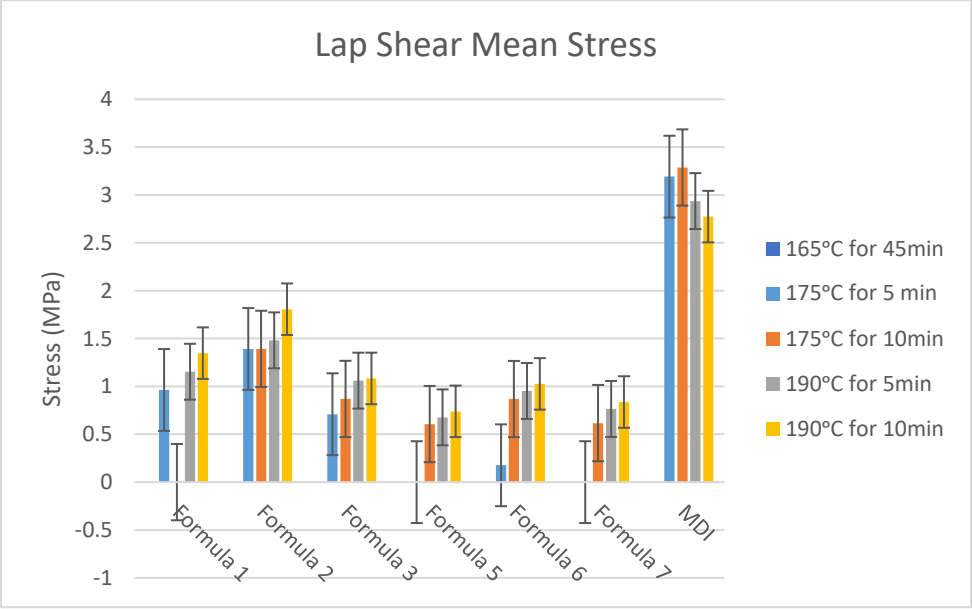

Figure 19: Mean Stress for all ESS based formulas as compared to MDI

Figure 19 shows the mean shear stress for all the different ESS based formulations that were tested. At this point all the remaining formulations from Table 5 failed to match the strength of MDI, so the next step was to check if substitution with MDI was a viable alternative to improve the performance of these formulations. For this the best preforming resin system was considered, that being Formula 2. Formula 2 was mixed with MDI in percentages of 25%-75%, 50%-50% and 75%-25% of Formula 2 – MDI. This yielded results much more comparable to the MDI as can be seen in Figure 5 and the formulas 50% Formula2 – 50% MDI (50F2/50M) and 25% Formula 2 – 75% MDI (25F2/75M) were sufficiently close enough to be taken to the particleboard manufacturing and subsequent testing stage.

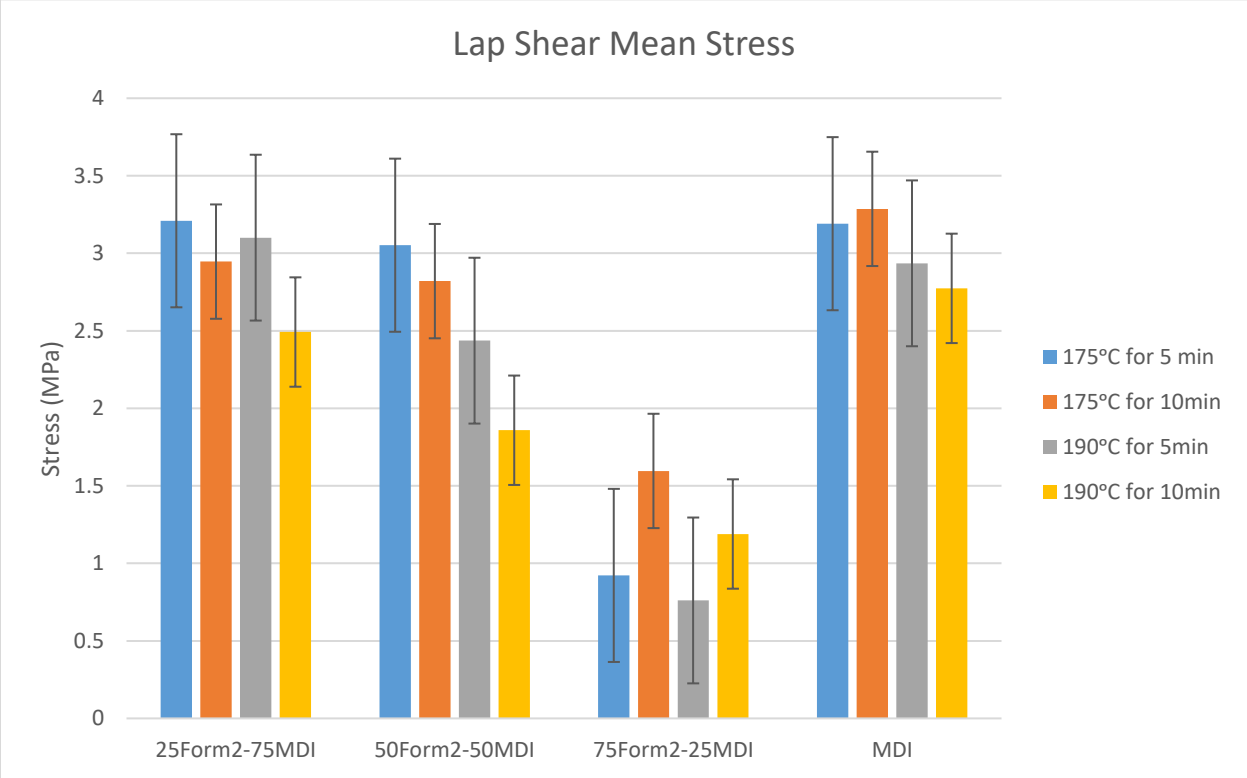

Figure 20: Mean Stress for all Formula2-MDI mixed formulas as compared to pure MDI

5.1.3. Fourier transform infrared spectroscopy results

FTIR was run to discern what chemical reactions if any were taking place in the primary resins used in particleboard manufacture. This was done by comparing the functional group found in Formula 2 and MDI to 25F2/75M, 50F2/50M, and 75F2/25M after being cured at 80^{o}C for 24 hours and seeing if any new functional groups were formed indicating a reaction took place.

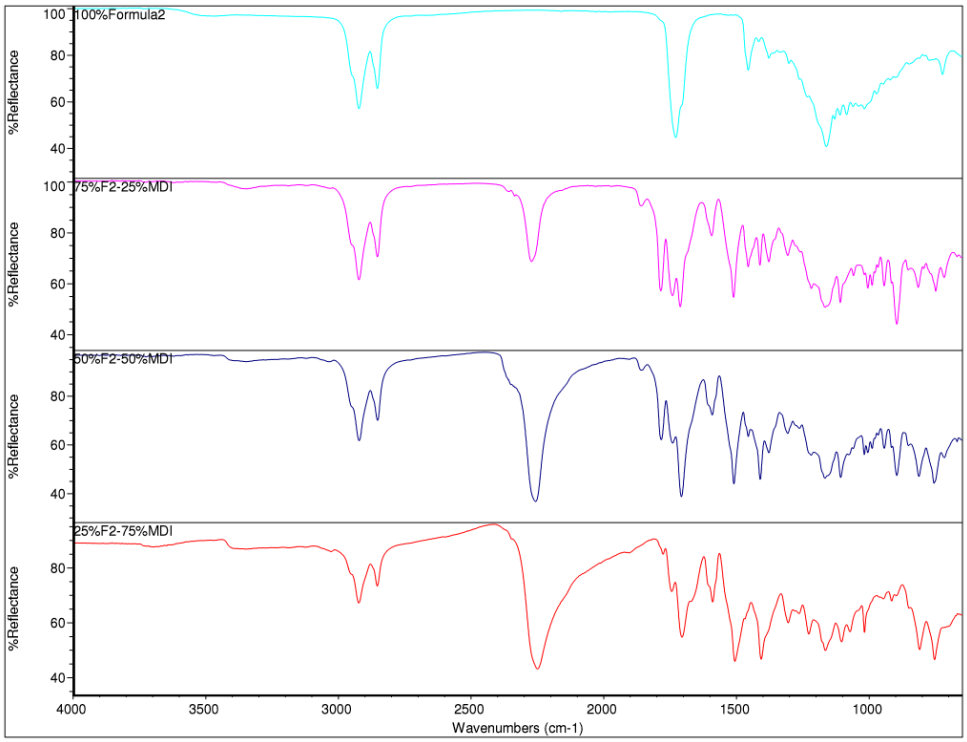

Figure 21: FTIR spectra for 100% Formula 2, 25F2/75M, 50F2/50M, and 75F2/25M

The key peaks found in the Formula 2 – MDI mixtures, shown in Figure 21, seem to be shared with the peaks of Formula 2 and MDI. This leads to the conclusion that no reaction occurred between the two resins. However, this is not the case and there are a couple of key peaks that are unique to the Formula 2 – MDI mixtures. The Formula 2 – MDI mixtures themselves (25F2/75M, 50F2/50M, 75F2/25M) all share these distinct peaks, but they vary in intensity.

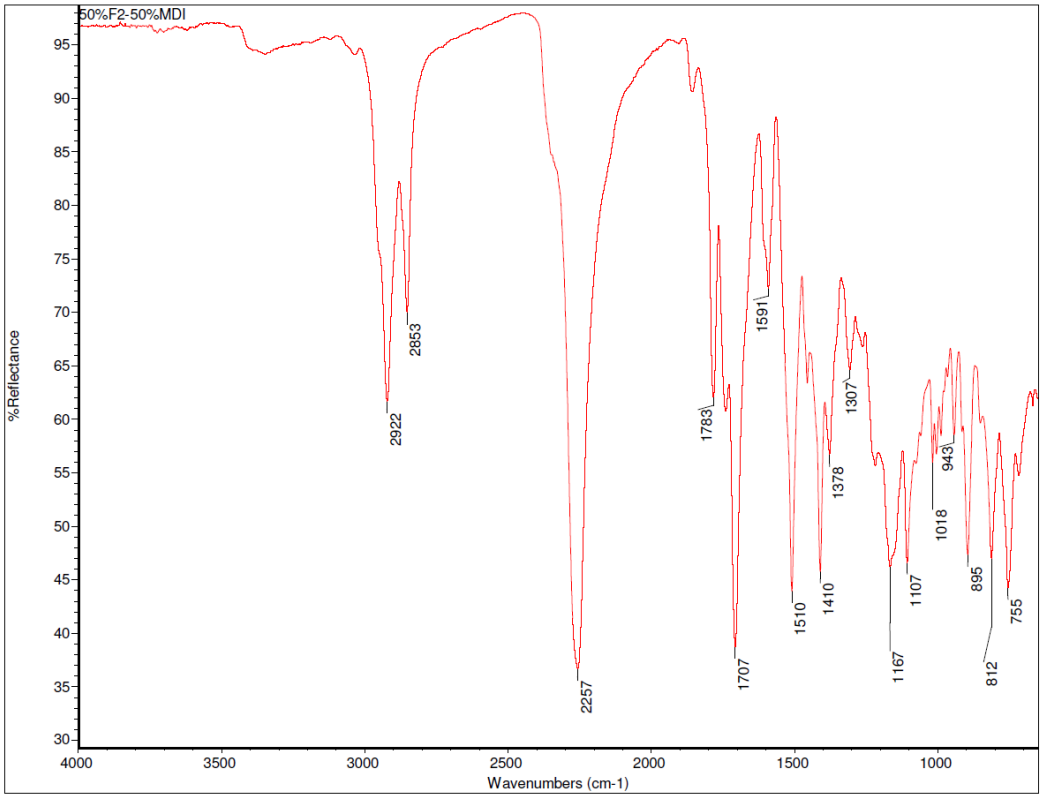

Figure 22: FTIR spectra of 50F2/50M

The three peaks at 1785, 1741, and 1712 cm^{-1} all have to do with the reaction between Formula 2 and MDI with 1785 cm^{-1} being left over anhydride, 1741 cm^{-1} being an ester formed from epoxy and anhydride bonding, and 1712 cm^{-1} are carbamate groups formed from isocyanate reaction with the OH molecule on the anhydride. These three peaks are simply one peak at 1729 cm^{-1}, in the Formula 2 spectra, which represents the ester molecule. The reason these other peaks form in the mixtures of Formula 2 and MDI is because of the isocyanate groups ability to reacted with the OH molecule created when the anhydride ring opens. This OH group is designed to react with the epoxy and create a chain reaction that creates the crosslinking network that is desired. However, when isocyanate attaches to the OH molecule there is no reactive group to continue the reaction because either a dimer or trimer ring forms, or a polyetherification side reaction occurs. This inability to further the reaction is one of the reason that so much isocyanate

ends up remaining unreacted as seen by the peak at 2257 cm^{-1} and given the time will hydrolyze into urea. A lower weight percentage of approximately 1% to 5% MDI is advised to minimize the amount of unreacted isocyanate. The remaining peaks are simply reaction groups of Formula 2 or MDI, these were the only peaks unique to the Formula 2-MDI mixture.

5.2. Physico-Mechanical Properties Testing Results and Analysis

5.2.1. Density results

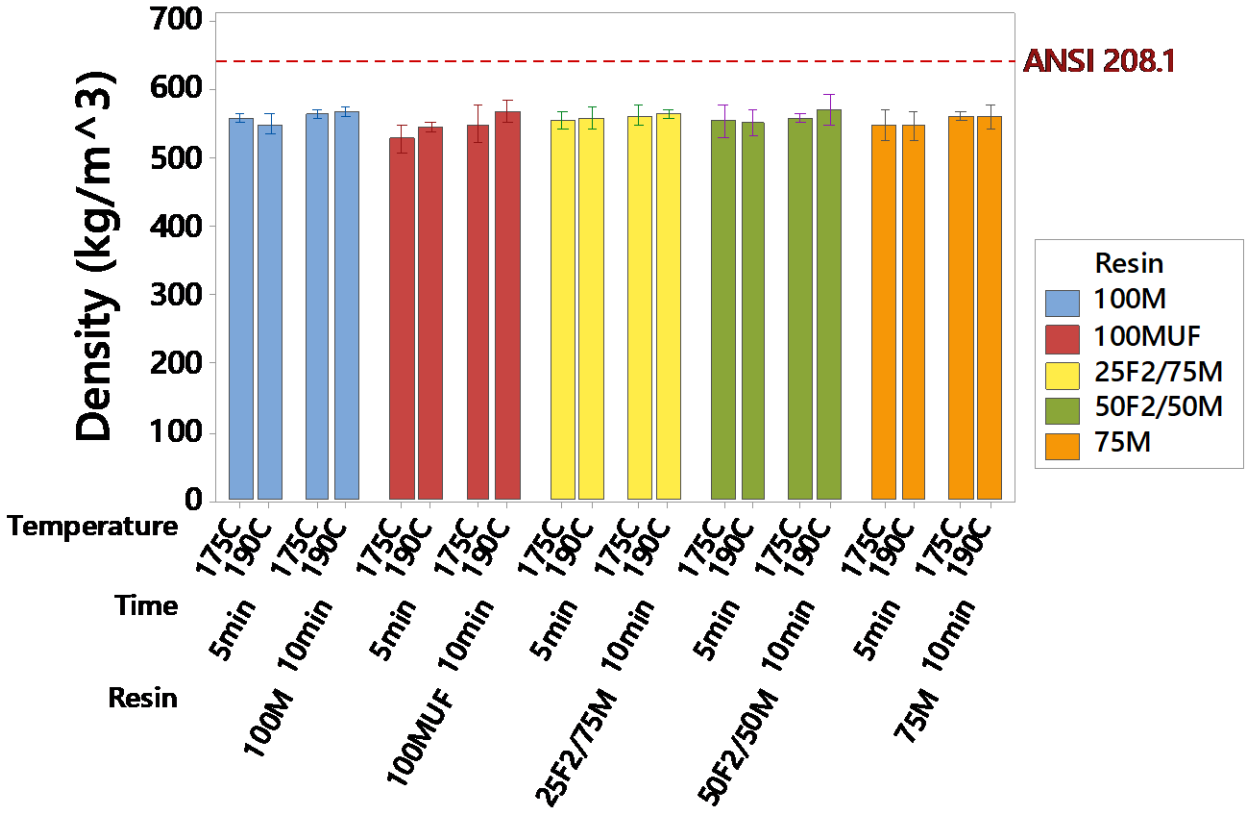

Figure 23: Mean and interval plot for density of particleboards

Table 5: ANOVA for Particleboard Density

Source	**DF**	**SS**	**MS**	**F**	**P**
Resin	4	1821.1	455.29	4.39	0.004
Time	1	3510.4	3510.42	33.88	0.000
Temperature	1	431.0	431.01	4.16	0.046
Resin*Time	4	392.6	98.14	0.95	0.443
Resin*Temperature	4	989.4	247.34	2.39	0.061
Time*Temperature	1	137.6	137.60	1.33	0.254
Resin*Time*Temperature	4	223.3	55.82	0.54	0.708
Error	60	6216.9	103.61		
Total	79	13722.3			
S	10.1791	**R-sq**	54.69%	**R-sq(adj)**	40.35%

Table 6: Tukey pairwise comparison test for density and resin

Resin	N	Mean	Grouping	
100MDI	16	558.788	A	
25F2/75MDI	16	558.787	A	
50F2/50MDI	16	557.542	A	
75MDI	16	553.245	A	B
100MUF	16	546.304		B
Means that do not share a letter are significantly different				

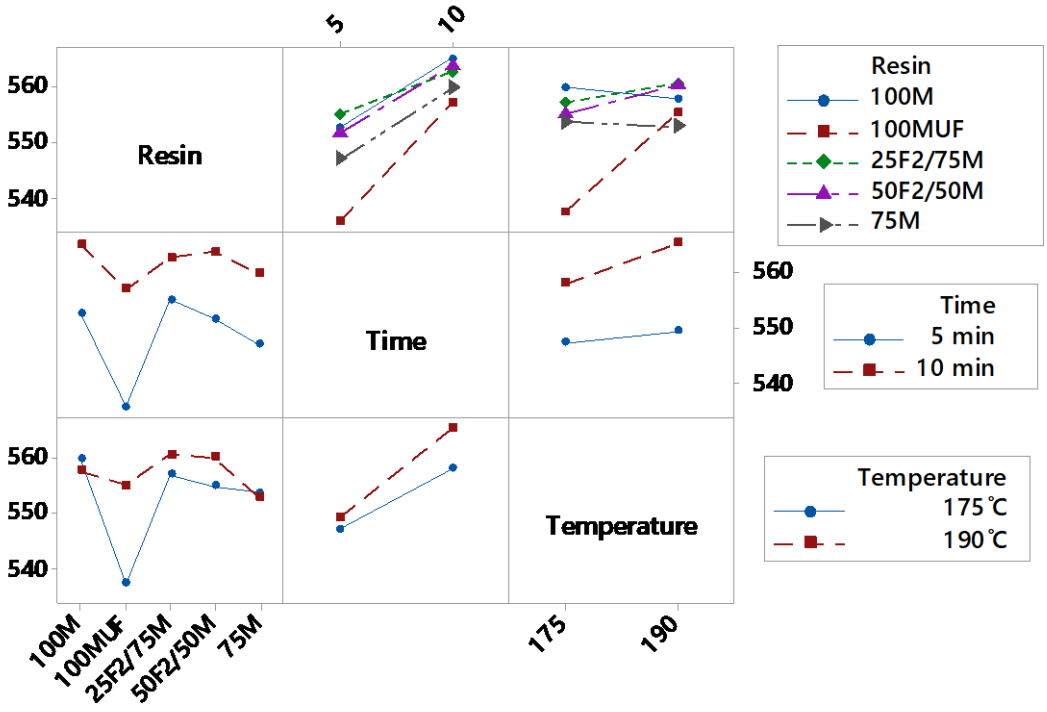

Figure 24: Interaction plot of resin, time and temperature for density

Table 5 shows that the significant effect were all the primary ones, resin, time, and temperature, with no interaction effects being shown to be significant. The interaction plot shows some interaction effects but since they were deemed to be insignificant in the ANOVA model it was deemed unimportant. The Tukey test for resin shows that density does not vary significantly between any resin types besides 100MUF which was just outside of this significance range as shown by the fact that it was statistically the same as 75M. It has also been shown that independent of the resin selection press time effects the density of the boards with longer press time yielding denser boards. It can also be seen that all the boards fall under the ANSI 208.1 standard of 640 kg/m^3 density needed for classification as medium density particleboard and as such fall within the low-density particleboard category though at the upper end of that.

5.2.2. Water absorption results

In this section 100MUF will not be included in the analysis. This is due to the samples completely falling apart after being submerged for 2-hours and so no meaningful measurements could be taken.

5.2.2.1. 2-hour change in volume test

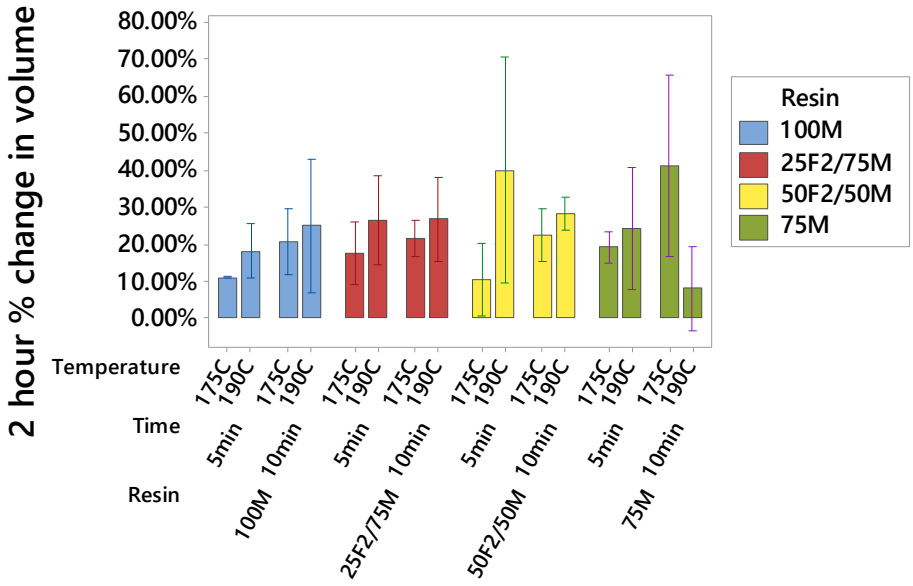

Figure 25: Mean and interval plots for percentage change in volume of particleboards after 2-hour submersion in water

Table 7: ANOVA for 2-hour % change in volume

Source	DF	SS	MS	F	P
Resin	3	0.03696	0.012319	1.69	0.181
Time	1	0.01876	0.018765	2.58	0.115
Temperature	1	0.02749	0.027487	3.78	0.058
Resin*Time	3	0.01414	0.004714	0.65	0.588
Resin*Temperature	3	0.21098	0.070327	9.67	0.000
Time*Temperature	1	0.11846	0.118459	16.29	0.000
Resin*Time*Temperature	3	0.08663	0.028878	3.97	0.013
Error	48	0.34900	0.007271		
Total	63	0.86243			
S	0.0852693	**R-sq**	59.53%	**R-sq(adj)**	46.89%

Table 8: Tukey pairwise comparison for impact of resin on the percentage volume change after 2-hour immersion in water

Resin	N	Mean	Grouping
50F2/50MDI	16	0.252379	A
75MDI	16	0.231314	A
25F2/75MDI	16	0.231030	A
100MDI	16	0.186472	A
Means that do not share a letter are significantly different			

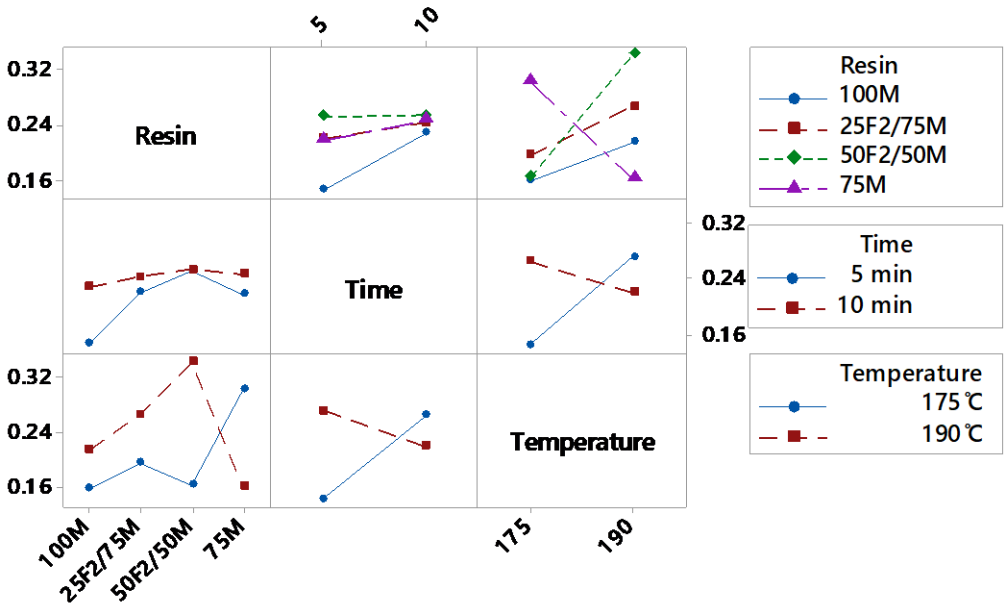

Figure 26: Interaction plot of resin, time and temperature for 2-hour % change in volume

Table 7 shows an interesting assertion, that all the interaction effects related to three primary factors were significant. This was further substantiated by the interval plot showing strong interactions across the board. These interaction effects were further reflected in the Tukey pairwise tests that showed that all factors for an individual factor were the same since the significant factor was the interaction effect between all the primary effects. As such the choice of resin has no significant impact on the boards change in volume after being submerged in water for 2-hours.

5.2.2.2. 2-hour change in mass test

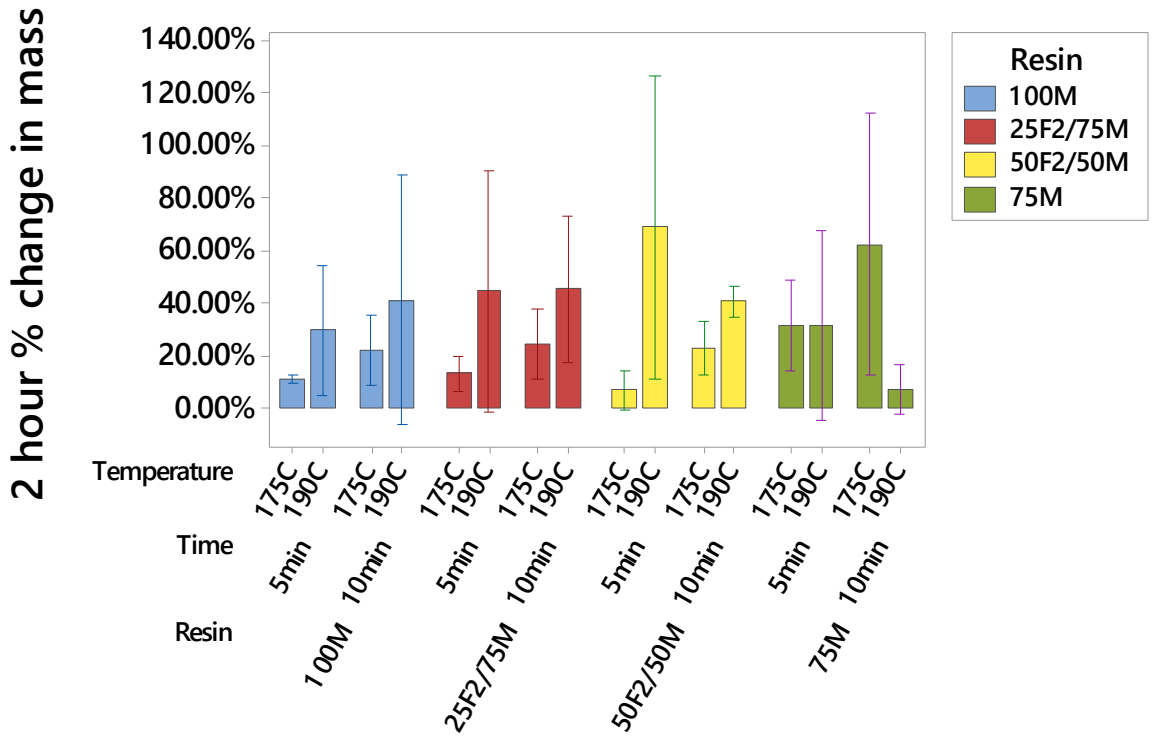

Figure 27: Mean and interval plot for percentage mass change in particleboards after 2-hour immersion in water

Table 9: ANOVA for 2-hour % change in mass

Source	**DF**	**SS**	**MS**	**F**	**P**
Resin	3	0.07091	0.02364	0.69	0.562
Time	1	0.01946	0.01946	0.57	0.454
Temperature	1	0.32562	0.32562	9.53	0.003
Resin*Time	3	0.06548	0.02183	0.64	0.594
Resin*Temperature	3	1.03158	0.34386	10.06	0.000
Time*Temperature	1	0.29730	0.29730	8.70	0.005
Resin*Time*Temperature	3	0.21443	0.07148	2.09	0.114
Error	48	1.63996	0.03417		
Total	63	3.66475			
S	0.184840	**R-sq**	55.25%	**R-sq(adj)**	41.27%

Table 10: Tukey pair wise comparison for impact of resin on the mass change of particleboards after 2-hour

Resin	N	Mean	Grouping
50F2/50MDI	16	0.348279	A
75MDI	16	0.332202	A
25F2/75MDI	16	0.319509	A
100MDI	16	0.260152	A
Means that do not share a letter are significantly different			

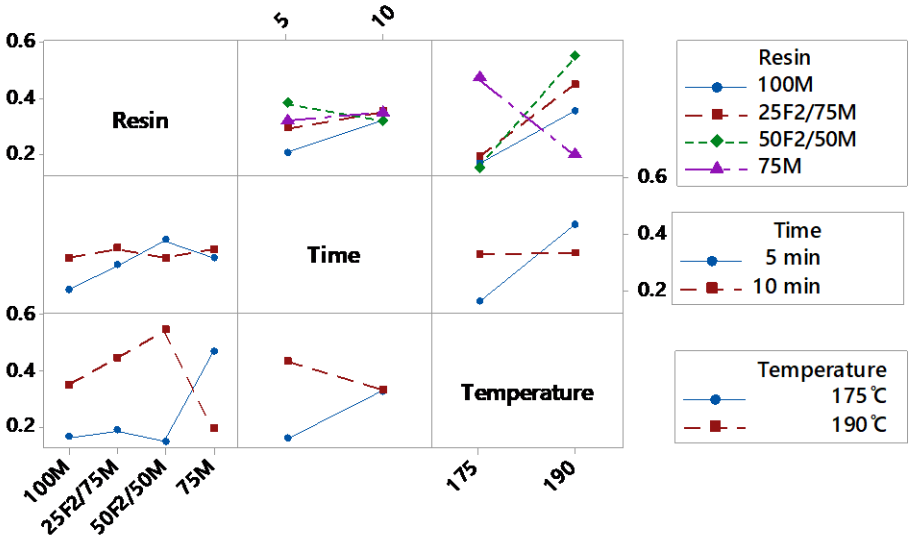

Figure 28: Interaction plot of resin, time and temperature for 2-hour % change in mass

Table 9 shows an interesting assertion, that being that none of the primary factors were significant outside of temperature, and that the interaction effects with temperature were quite significant. This was further supported by the interaction plots showing strong interactions between the temperature and the other factors. The Tukey tests also substantiate this claim in table 10 and appendix table A5 which show no significant difference between the populations as divided by resin, or time while showing a significant difference between temperatures. As such the choice of resin exhibits no significant impact on the particleboards change in mass after being submerged in water for 2-hours.

5.2.2.3. 24-hour change in volume test

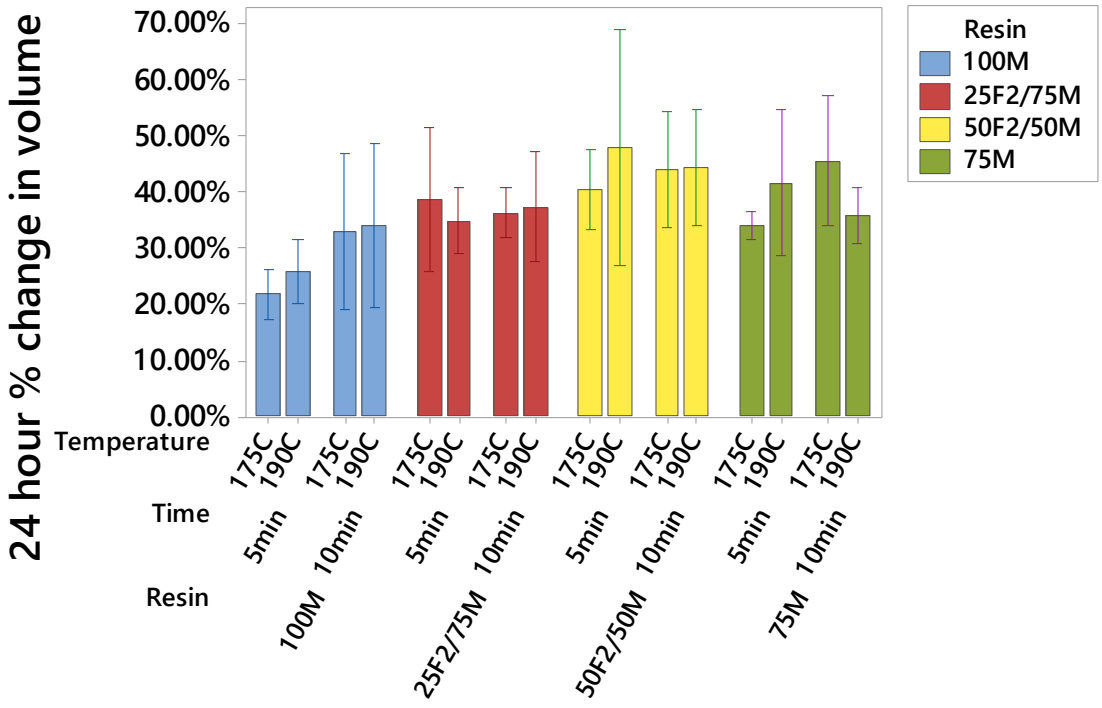

Figure 29: Mean and interval plot for percentage volume change in particleboards after 24-hour immersion in water

Table 11: ANOVA for 24-hour % change in volume

Source	**DF**	**SS**	**MS**	**F**	**P**
Resin	3	0.199984	0.066661	15.05	0.000
Time	1	0.014820	0.014820	3.35	0.074
Temperature	1	0.001582	0.001582	0.36	0.553
Resin*Time	3	0.024782	0.008261	1.87	0.148
Resin*Temperature	3	0.008539	0.002846	0.64	0.591
Time*Temperature	1	0.012573	0.012573	2.84	0.099
Resin*Time*Temperature	3	0.025863	0.008621	1.95	0.135
Error	48	0.212585	0.004429		
Total	63	0.500729			
S	0.0665497	**R-sq**	57.54%	**R-sq(adj)**	44.28%

Table 12: Tukey pair wise comparison for impact of resin on the volume change of particleboards after 24-hour

Resin	N	Mean	Grouping		
50F2/50MDI	16	0.440727	A		
75MDI	16	0.392139	A	B	
25F2/75MDI	16	0.367252		B	
100MDI	16	0.286279			C
Means that do not share a letter are significantly different					

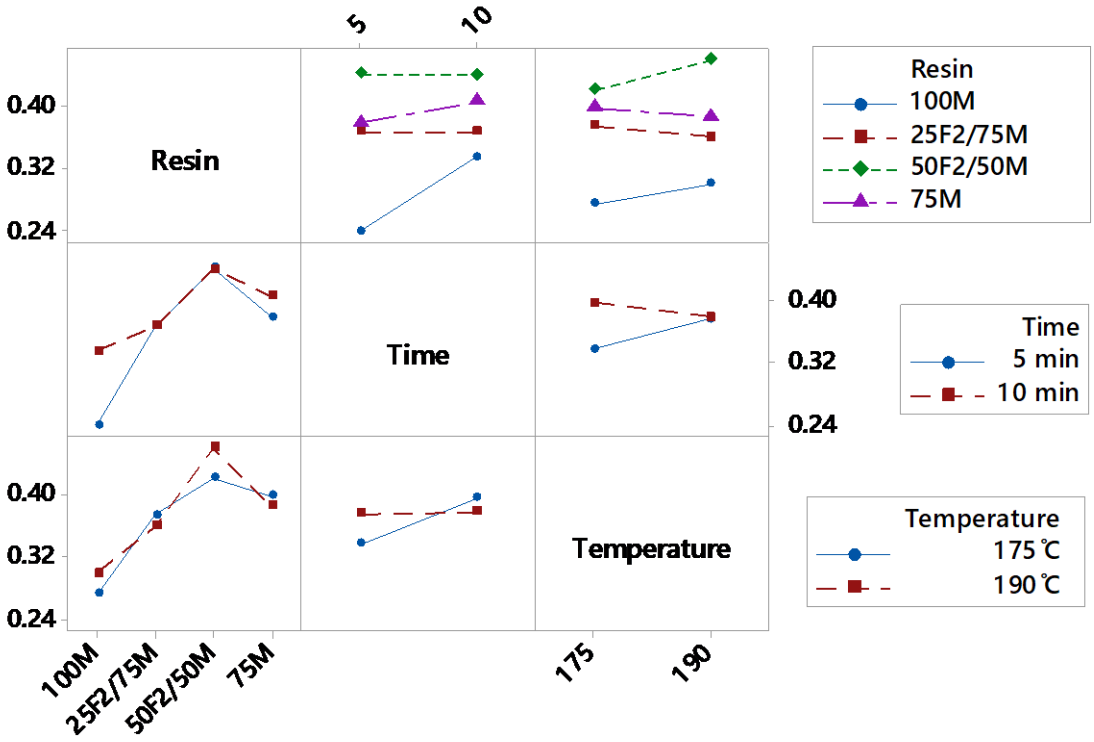

Figure 30: Interaction plot of resin, time and temperature for 24-hour % change in volume

Table 11 shows the primary factor, according to the ANOVA model was the resin, no other major influencers appear. This was further substantiated by the interaction plot which shows some interaction but none that were strong enough to warrant ignoring resin as the primary influencer. The Tukey test in Table 18 shows that the two test resin systems 25F2/75M and 50F2/50M were significantly different from each other while both being statistically the same as 75M and statistically worse the 100M.

5.2.2.4. 24-hour change in mass test

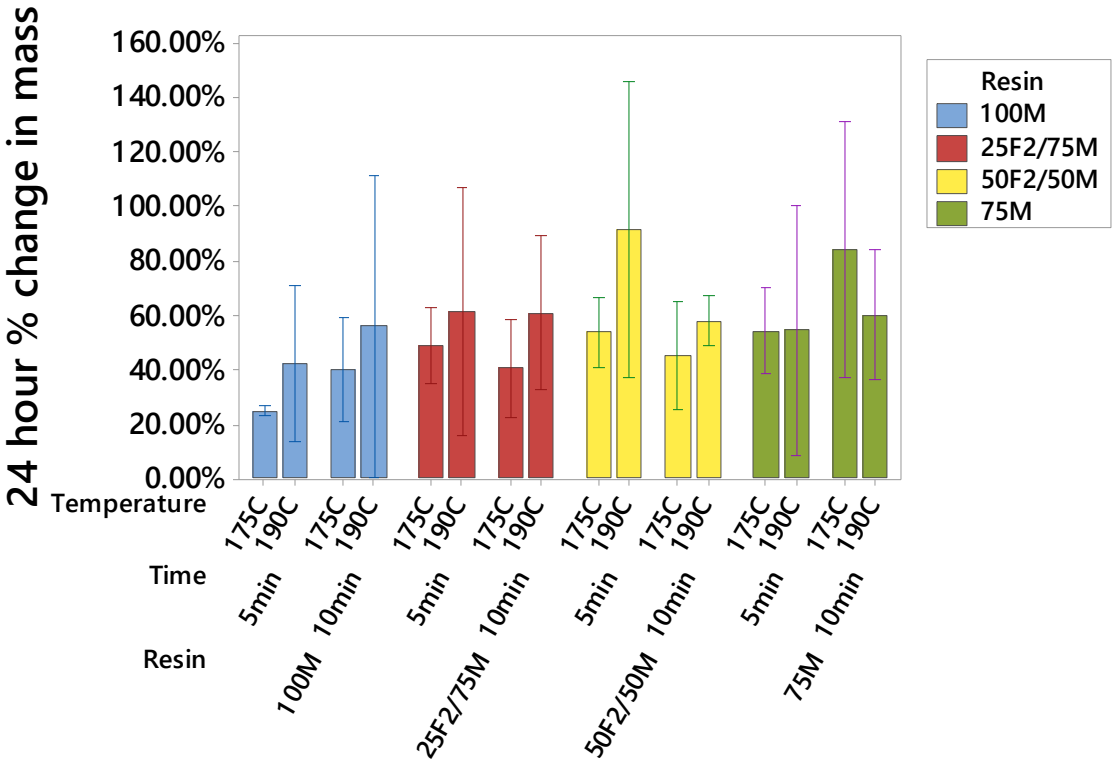

Figure 31: Mean and interval plot for percentage mass change in particleboards after 24-hour immersion in water

Table 13: ANOVA for 24-hour % change in mass

Source	**DF**	**SS**	**MS**	**F**	**P**
Resin	3	0.51714	0.172380	4.26	0.010
Time	1	0.00455	0.004554	0.11	0.739
Temperature	1	0.21323	0.213229	5.27	0.026
Resin*Time	3	0.38602	0.128673	3.18	0.032
Resin*Temperature	3	0.31558	0.105192	2.60	0.063
Time*Temperature	1	0.04492	0.044915	1.11	0.297
Resin*Time*Temperature	3	0.08176	0.027252	0.67	0.572
Error	48	1.94047	0.040426		
Total	63	3.50366			
S	0.201063	**R-sq**	44.62%	**R-sq(adj)**	27.31%

Table 14: Tukey pair wise comparison for impact of resin on the mass change of particleboards after 24-hour

Resin	N	Mean	Grouping	
75MDI	16	0.631406	A	
50F2/50MDI	16	0.619508	A	
25F2/75MDI	16	0.528337	A	B
100MDI	16	0.407029		B
Means that do not share a letter are significantly different				

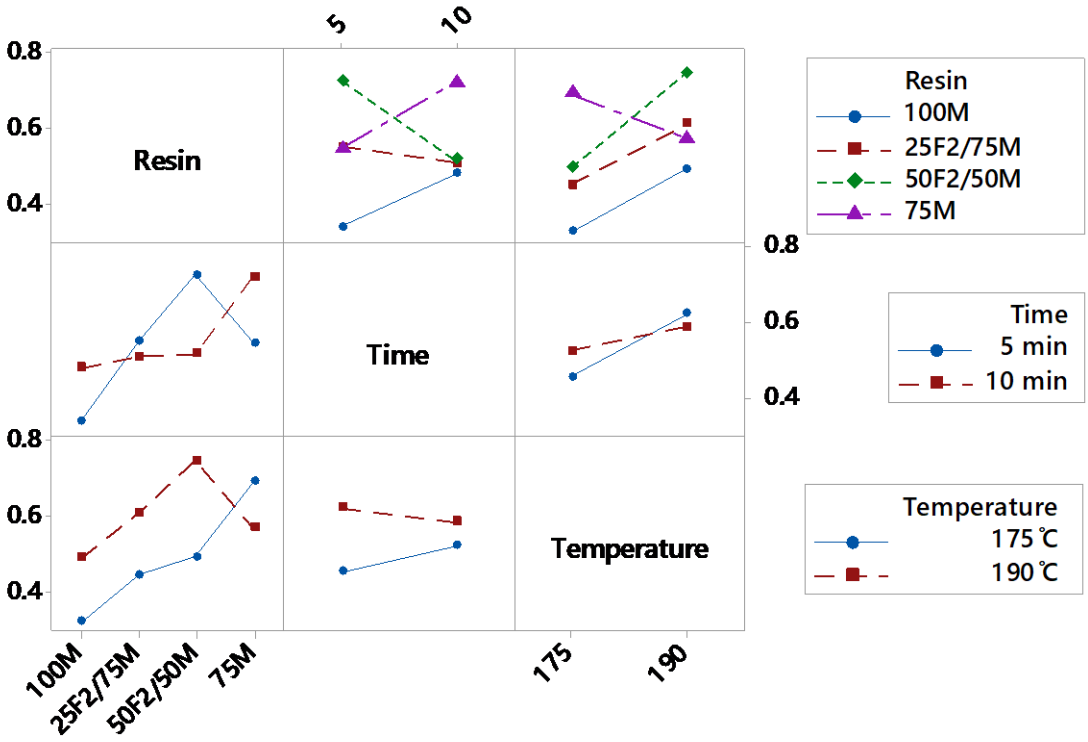

Figure 32: Interaction plot of resin, time and temperature for 24-hour % change in mass

The ANOVA test shows one interaction effect, resin*time, being significant along with resin and temperature being significant. The interaction plot shown in Figure 32 shows this interaction to be significant and strong. As such Tukey's pairwise comparison test cannot be used to determine significance as more than just the factor being compared plays a role. As such the statistical significance was a function of the resin, time, and temperature.

5.2.3. Linear expansion results

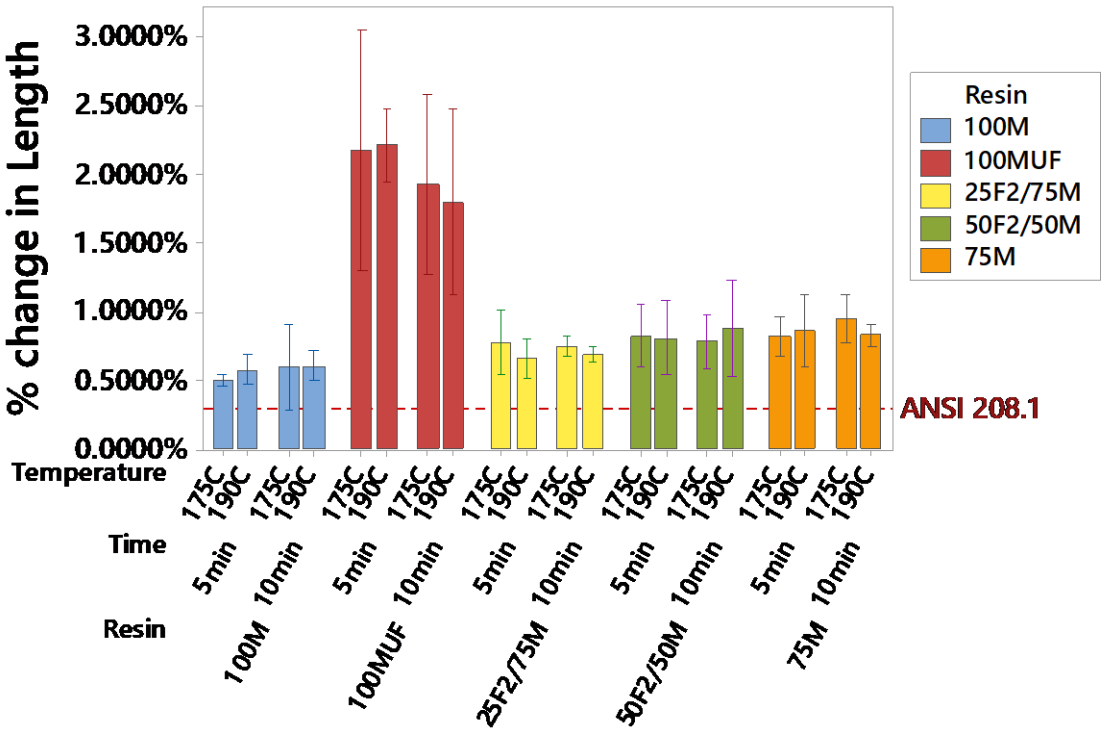

Figure 33: Mean and interval plot for linear expansion of particleboards

Table 15: ANOVA for linear expansion

Source	DF	SS	MS	F	P
Resin	4	0.002331	0.000583	95.55	0.000
Time	1	0.000001	0.000001	0.17	0.678
Temperature	1	0.000003	0.000003	0.42	0.522
Resin*Time	4	0.000025	0.000006	1.04	0.394
Resin*Temperature	4	0.000010	0.000002	0.40	0.810
Time*Temperature	1	0.000003	0.000003	0.53	0.470
Resin*Time*Temperature	4	0.000013	0.000003	0.52	0.720
Error	60	0.000366	0.000006		
Total	79	0.002752			
S	0.0024697	**R-sq**	86.70%	**R-sq(adj)**	82.49%

Table 16 Tukey pair wise comparison for impact of resin on the linear expansion particleboards

Resin	N	Mean	Grouping		
100MUF	16	0.0207029	A		
75MDI	16	0.0086816		B	
50F2/50MDI	16	0.0082626		B	
25F2/75MDI	16	0.0071814		B	C
100MDI	16	0.0056996			C

Means that do not share a letter are significantly different

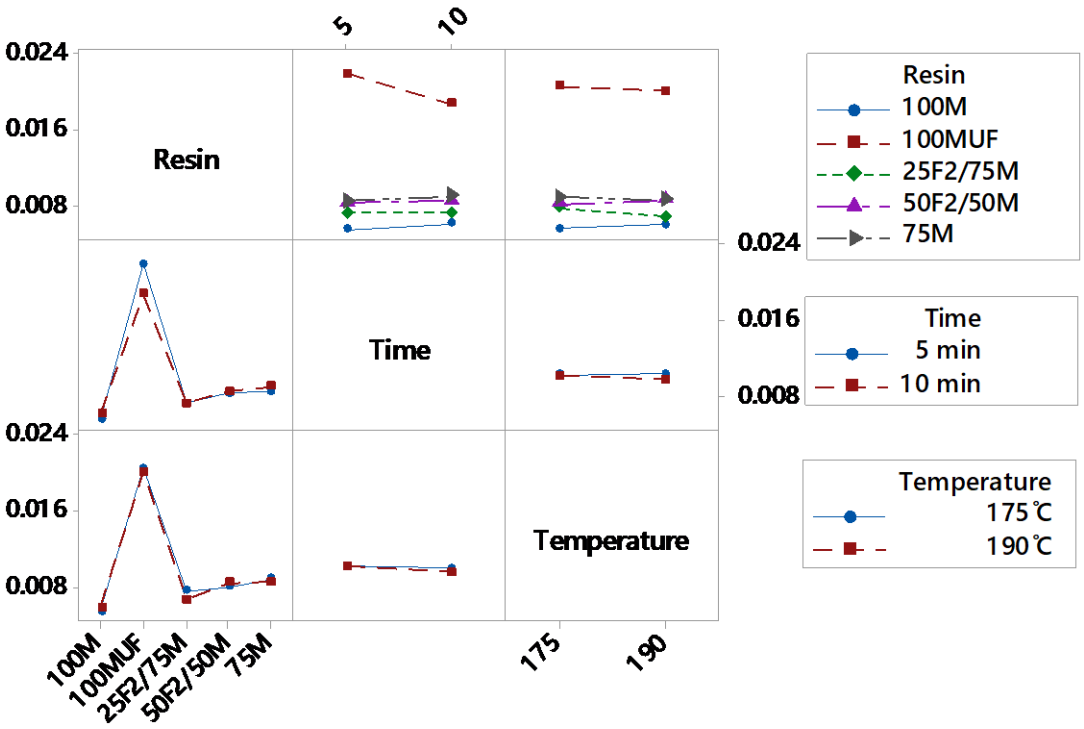

Figure 34: Interaction plot of resin, time and temperature for linear expansion

The ANOVA analysis found in Table 15 shows that only resin has a significant effect on the model. This means the interaction effects can be ignored but, looking at the interaction Plot for linear expansion shows no strong interactions occurring. This means that the Tukey test results for resin can be interpreted as being true. This shows that 100MUF which was notorious for being bad with water was the worst by a wide margin. The two resins of interest 50F2/50M and 25F2/75M were statistically the same as 75M. However, 25F2/75M still performs

comparably to 100M while the other two were significantly different from 100M. All the boards failed to expand less than the ANSI 208.1 standard of 0.30% change in length with the difference in expansion being at least twice as high as outlined by the standard.

5.2.4. Static bending results

5.2.4.1. Modulus of rupture

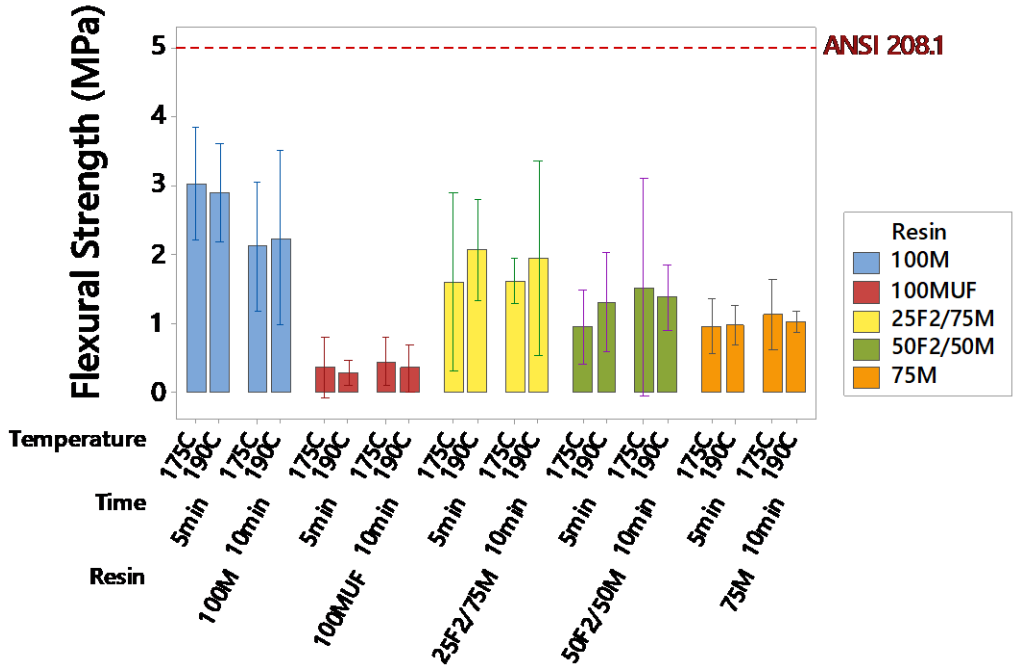

Figure 35: Mean and interval plot for modulus of rupture of particleboards

Table 17: ANOVA for modulus of rupture

Source	DF	SS	MS	F	P
Resin	4	1857339	464335	40.81	0.000
Time	1	718	718	0.06	0.802
Temperature	1	1670	1670	0.15	0.703
Resin*Time	4	149929	37482	3.29	0.017
Resin*Temperature	4	111512	27878	2.45	0.056
Time*Temperature	1	1163	1163	0.10	0.750
Resin*Time*Temperature	4	7947	1987	0.17	0.951
Error	60	682599	11377		
Total	79	2812877			
S	106.661	**R-sq**	75.73%	**R-sq(adj)**	68.05%

Table 18: Tukey pairwise comparison showing the impact of resin on the modulus of rupture of the particleboards

Resin	N	Mean	Grouping			
100MDI	16	2.56000	A			
25F2/75MDI	16	1.80000		B		
50F2/50MDI	16	1.28625			C	
75MDI	16	1.01875			C	
100MUF	16	0.35688				D
Means that do not share a letter are significantly different						

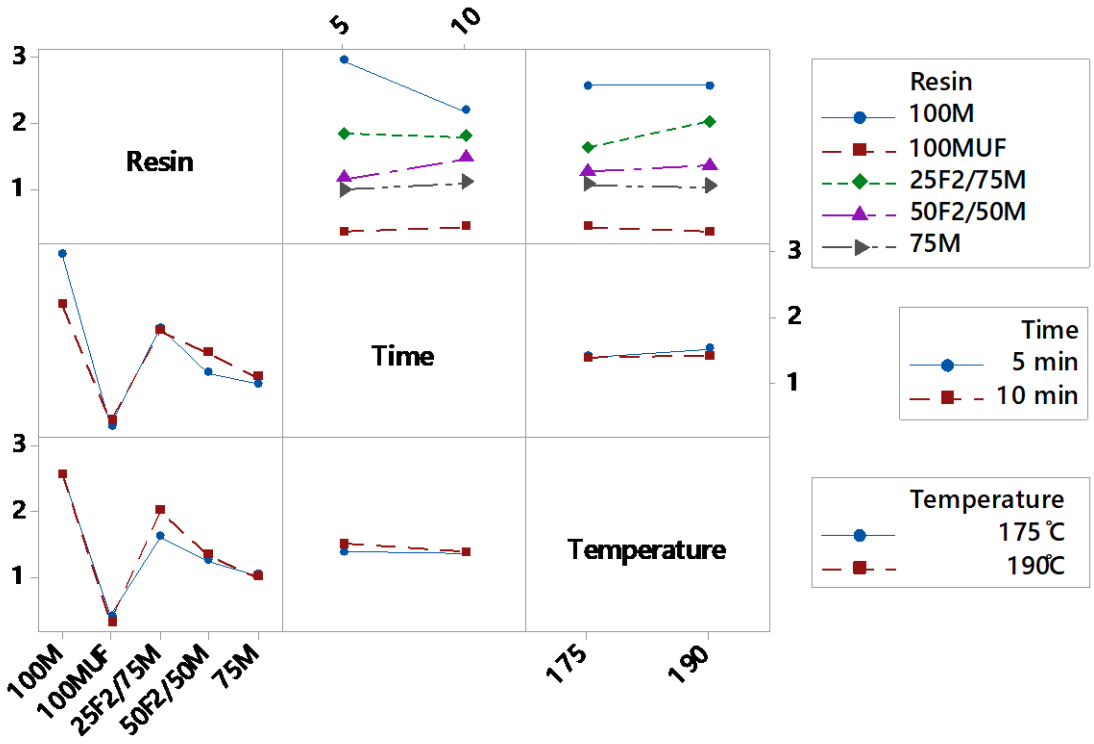

Figure 36: Interaction plot of resin, time and temperature for modulus of rupture

Resin*time was a significant interaction effect and resin itself was also seen as a significant interaction effect based on the ANOVA model in Table 17. The interaction plot shows weak interaction effects so the interaction between resin*time can be ignored and the resin effect can be looked at in isolation. Tukey's test for resin reveals that the two test resin systems 25F2/75M and 50F2/50M were significantly different from each other. With 50F2/50M be

statistically that same as 75M, statistically worse than 100M, and statistically better than 100MUF. Meanwhile 25F2/75M performs worse than 100M but better then every other resin. However, when comparing all these resins to the ANSI 208.1 standard of 5 MPa the different boards do not meet the standard with the best performing still being 2 MPa short of reaching this goal.

5.2.4.2. Modulus of elasticity

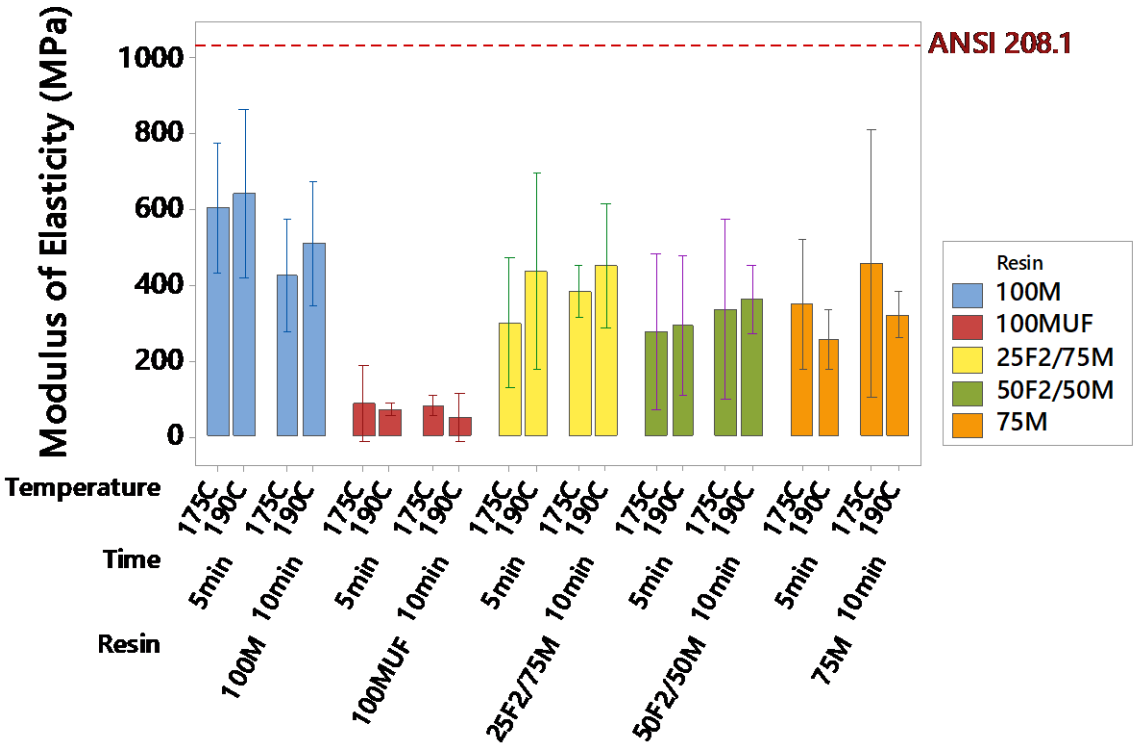

Figure 37: Mean and interval plot for modulus of elasticity of particleboards

Table 19: ANOVA for modulus of elasticity

Source	DF	SS	MS	F	P
Resin	4	44.0305	11.0076	44.92	0.000
Time	1	0.0800	0.0800	0.33	0.570
Temperature	1	0.1148	0.1148	0.47	0.496
Resin*Time	4	2.7878	0.6970	2.84	0.032
Resin*Temperature	4	0.5992	0.1498	0.61	0.656
Time*Temperature	1	0.0546	0.0546	0.22	0.639
Resin*Time*Temperature	4	0.2762	0.0691	0.28	0.889
Error	60	14.7042	0.2451		
Total	79	62.6474			
S	0.495046	**R-sq**	76.53%	**R-sq(adj)**	69.10%

Table 20: Tukey pairwise comparison showing the impact of resin on the modulus of elasticity of the particleboards

Resin	N	Mean	Grouping		
100MDI	16	542.966	A		
25F2/75MDI	16	390.714		B	
75MDI	16	344.529		B	
50F2/50MDI	16	315.882		B	
100MUF	16	71.769			C
Means that do not share a letter are significantly different					

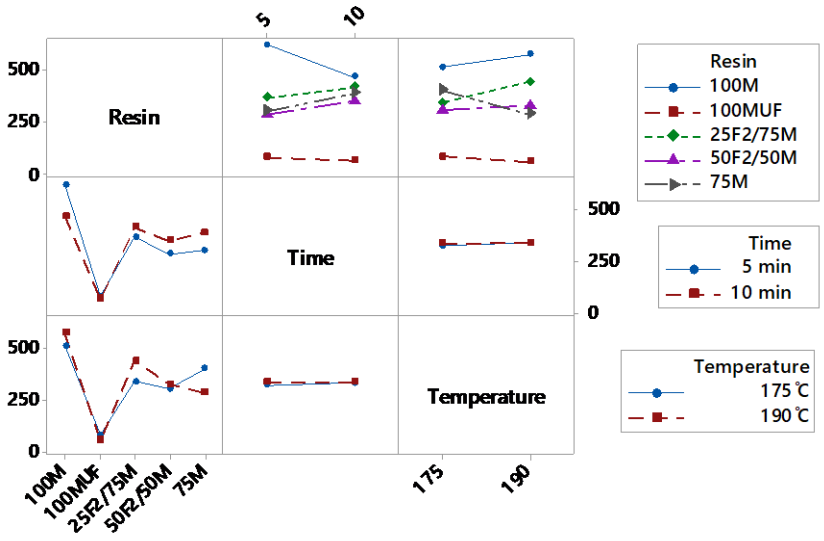

Figure 38: Interaction plot of resin, time and temperature for modulus of elasticity

From ANOVA table 19, it can be observed that resin itself and resin*time interaction had signification impact on the modulus of elasticity of the particleboards. The interaction plot shows weak interaction effects so the interaction between resin*time can be ignored. A strong interaction between temperature and time was shown but due to the ANOVA model showing it as insignificant it will be ignored, and the resin effect can be looked at in isolation. Tukey's test for resin reveals that 100M statistically outperforms all the other resins while 25F2/75M, 50F2/50M and 75M all perform statically the same while 100MUF performs the worst out of all resins tested. When compared to the ANSI 208.1 standard however all the different formulations fall short of the desired 1034 MPa called for.

5.2.5. Tension perpendicular to surface (Internal bond) results

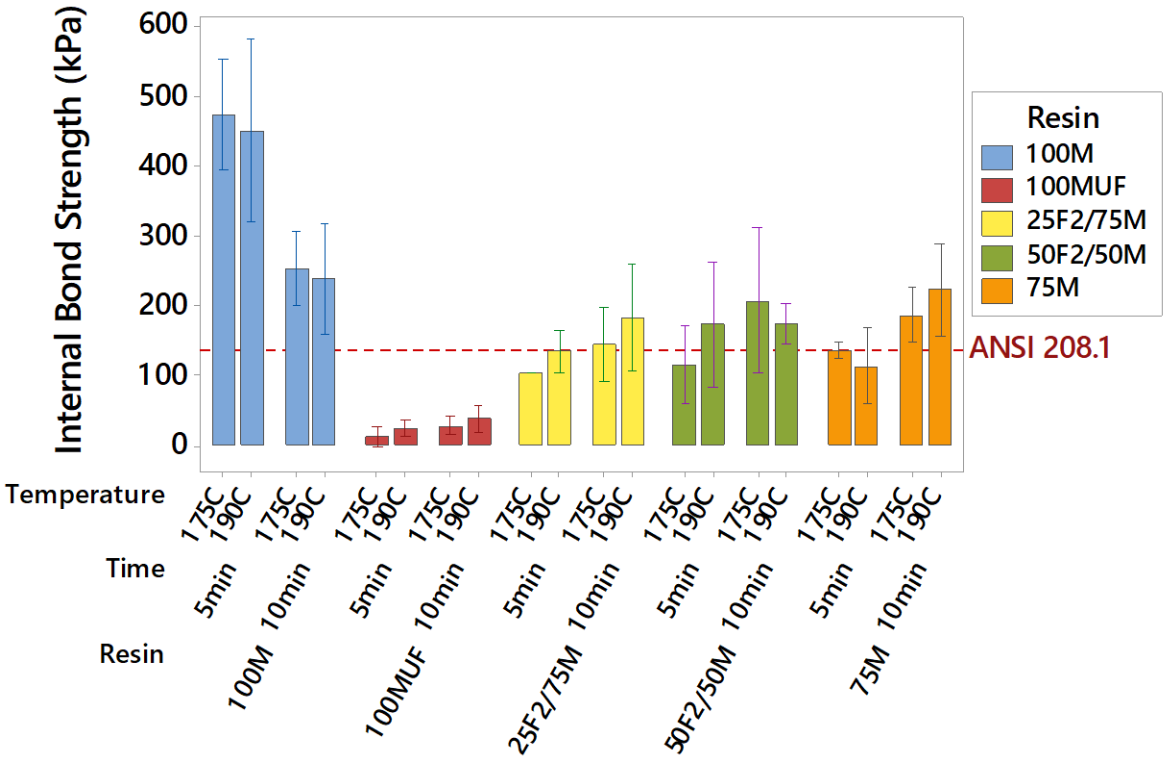

Figure 39: Mean plot with data interval bars based on a 95% confidence interval for internal bond strength of particleboards

Table 21: ANOVA for internal bond strength

Source	DF	SS	MS	F	P
Resin	4	1109413	277353	115.30	0.000
Time	1	994	994	0.41	0.522
Temperature	1	2022	2022	0.84	0.362
Resin*Time	4	287113	71778	29.84	0.000
Resin*Temperature	4	7010	1752	0.73	0.575
Time*Temperature	1	86	86	0.04	0.851
Resin*Time*Temperature	4	14833	3708	1.54	0.198
Error	80	192432	2405		
Total	99	1613903			
S	49.0449	**R-sq**	88.08%	**R-sq(adj)**	85.24%

Table 22: Tukey pairwise comparison showing the impact of resin on the internal bond strength of the particleboards

Resin	N	Mean	Grouping		
100MDI	20	353.830	A		
50F2/50MDI	20	167.076		B	
75MDI	20	164.578		B	
25F2/75MDI	20	141.521		B	
100MUF	20	25.675			C
Means that do not share a letter are significantly different					

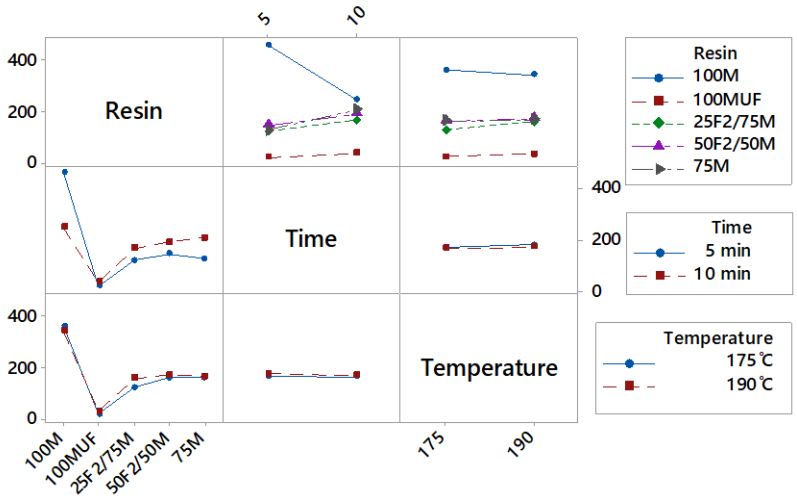

Figure 40: Interaction plot of resin, time and temperature for internal bond strength based on data means

The ANOVA test found in Table 21 shows a significant effect with resin*time and resin by itself. Figure 40 show that resin*time have an interaction effect, but it appears to be weak enough to ignore. This means that the results from the Tukey test can be used for interpreting the data. Thus Table 22 shows that 100M statistically outperforms all the other resins while 25F2/75M, 50F2/50M and 75M all perform statically the same and 100MUF performs the worst out of all resins tested. When comparing these formulations to the ANSI 208.1 standard they compare favorably with only 100MUF falling noticeably below the called for 137 kPa internal bond strength.

5.2.6. Screw withdrawal results

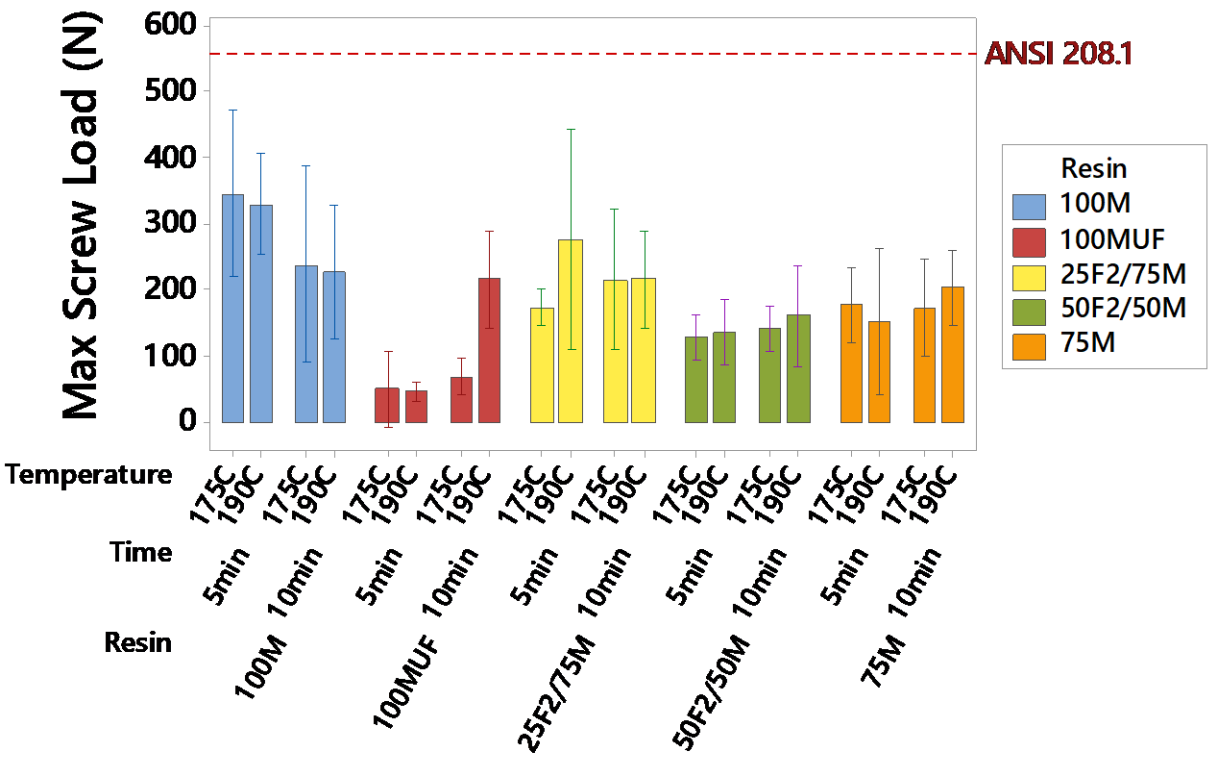

Figure 41: Mean and interval plot for maximum screw withdrawal force of particleboards

Table 23: ANOVA for maximum screw withdrawal force

Source	DF	SS	MS	F	P
Resin	4	338608	84651.9	29.67	0.000
Time	1	421	420.6	0.15	0.702
Temperature	1	12841	12840.8	4.50	0.038
Resin*Time	4	83578	20894.5	7.32	0.000
Resin*Temperature	4	21031	5257.7	1.84	0.132
Time*Temperature	1	3072	3072.5	1.08	0.304
Resin*Time*Temperature	4	33493	8373.3	2.94	0.028
Error	60	171164	2852.7		
Total	79	664207			
S	53.4109	**R-sq**	74.23%	**R-sq(adj)**	66.07%

Table 24: Tukey pairwise comparison showing the impact of resin on the maximum screw withdrawal force of the particleboards

Resin	N	Mean	Grouping			
100MDI	16	285.145	A			
25F2/75MDI	16	220.669	A	B		
75MDI	16	176.552		B	C	
50F2/50MDI	16	141.909			C	D
100MUF	16	95.904				D
Means that do not share a letter are significantly different						

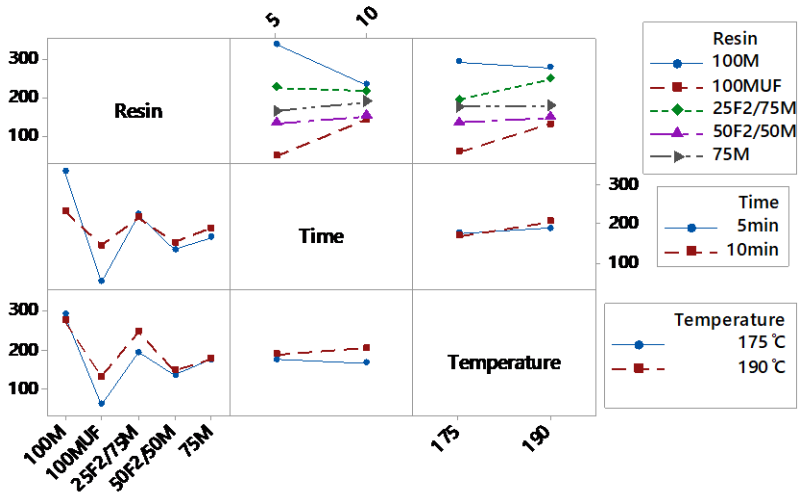

Figure 42: Interaction plot of resin, time and temperature for maximum screw withdrawal force

The interaction between resin, time, and temperature was shown to be statistically significant by the ANONVA test shown in Table 23. Along with resin*time, temperature, and resin. The interaction effect can be seen in to be average but since no significant crossing of multiple resins occurs the Tukey test can be used. This test for resin shows a bit of a step type significance grouping. With 25F2/75M being statistically equivalent to 100M and 75M and outperforming the other resins. Meanwhile 50F2/50M was shown to be statistically equivalent to 75M and 100MUF while preforming worse than all other resins. When comparing these formulations to the ANSI 208.1 standard of 556 N max screw withdrawal load all the formulations fall short of matching this by about double or more on average.

5.2.7. Hardness test results

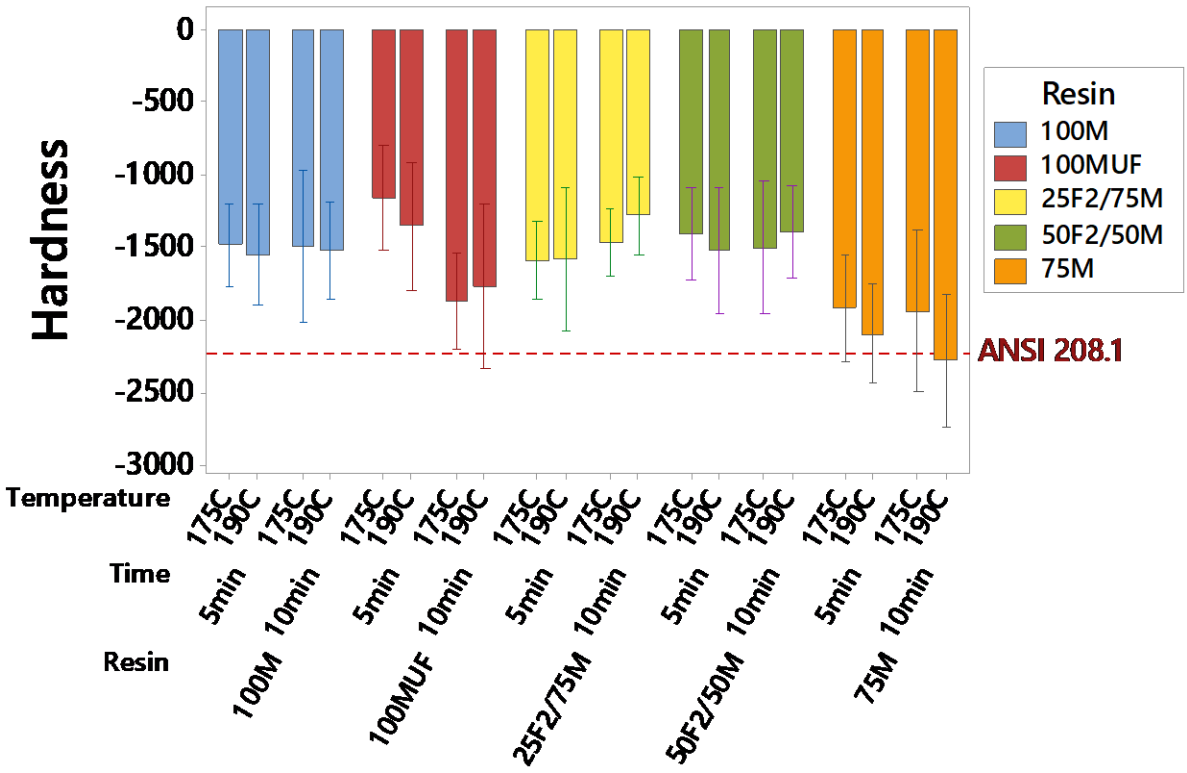

Figure 43: Mean and interval plot for hardness of particleboards

Table 25: ANOVA for hardness

Source	DF	SS	MS	F	P
Resin	4	8243235	2060809	9.11	0.000
Time	1	293439	293439	1.30	0.257
Temperature	1	105858	105858	0.47	0.495
Resin*Time	4	2697251	674313	2.98	0.021
Resin*Temperature	4	547863	136966	0.61	0.660
Time*Temperature	1	136195	136195	0.60	0.439
Resin*Time*Temperature	4	264547	66137	0.29	0.883
Error	140	31682291	226302		
Total	159	43970677			
S	475.712	**R-sq**	27.95%	**R-sq(adj)**	18.17%

Table 26: Tukey pairwise comparison showing the impact of resin on the hardness of the particleboards

Resin	N	Mean	Grouping	
50F2/50MDI	32	-1460.65	A	
25F2/75MDI	32	-1481.66	A	
100MDI	32	-1514.25	A	
100MUF	32	-1540.53	A	
75MDI	32	-2062.60		B
Means that do not share a letter are significantly different				

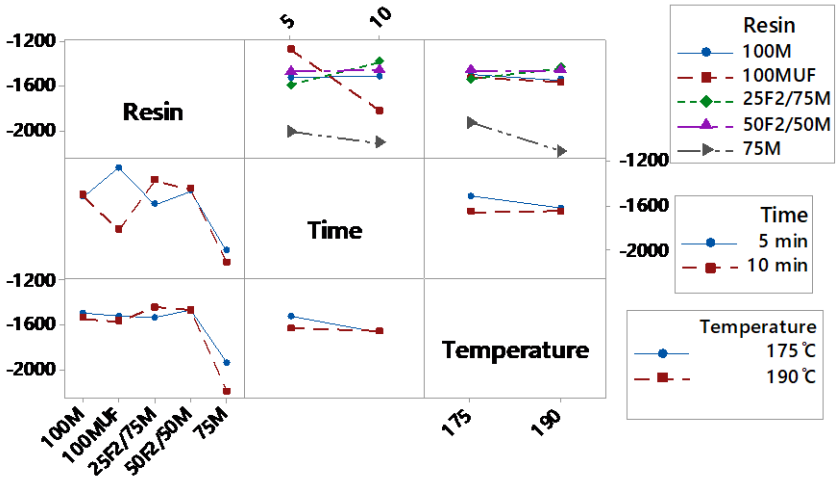

Figure 44: Interaction plot of resin, time and temperature for hardness

Table 25 shows a significant effect with resin*time and resin by itself. Figure 44 show that resin*time have a strong interaction effect, so the Tukey test results cannot be used. From the tests taken no strong conclusion can be inferred. One thing that stands out in this model however was the poor fit as compared to other models the amount of error and the lack of fit for this residual was particularly poor suggesting that the primary influential factor was not accounted for. One possibility is that it was influenced by wood content more than resin type. This was partially substantiated with the resin comparison test which also happens to compare wood content. Here it can be seen that the only statically significant resin was 75M which happens to have higher wood content. This cannot be said for certain until a model is made to add this as a factor, but it is something to consider. When comparing the hardness value of the different formulations to the ANSI 208.1 standard it can be seen from Figure 43 that effectively all the different formulations do not match the standard. It should be noted that no hardness value was given for low-density particleboard and therefore the most common required hardness was used that being 2225 N.

5.3. Summary of Results

5.3.1. Resin characterization and analysis results summary

- Peak heat flow was a better predictor of curing kinetics of a resin over total isothermal energy
- A peak heat flow of 0.8 W/g or above was indicative of a resin that will cure within a 5 min to 10 min cure time
- Lap shear testing as a means of resin strength characterization was an effective tool at deciding a resins viability as a particleboard binder

- Formula 2 – MDI mixtures do react, but the isocyanate inhibits chain growth by reacting with epoxy and anhydride
- Lower amounts of MDI would help reduce the excess isocyanate found within the Formula 2 – MDI mixtures spectra

5.3.2. Physico-mechanical properties testing results and analysis summary

- 2-hour volume change, 2-hour mass change, and 24-hour mass change were heavily influenced by interaction effects for the particleboards tested
- Resin has little to no influence on the density and hardness of the particleboards tested
- 50F2/50MDI, 25F2/75MDI, and 75MDI were statistically the same for linear expansion, modulus of elasticity, and internal bond strength
- 75MDI acts statistically the same as 50F2/50MDI and 25F2/75MDI for 24-hour change in volume, and screw withdrawal while 50F2/50MDI and 25F2/75MDI were significantly different from one another.
- Modulus of rupture for 25F2/75MDI outperforms all resins except 100MDI which was significantly better than 25F2/75MDI
- 100MDI outperformed all resins except for being statistically the same as 25F2/75MDI for screw withdrawal and linear expansion
- 100MUF underperformed compared to all other resins except for screw withdrawal where 50F2/50MDI was statistically the same as 100MUF
- When compared to the ANSI 208.1 standard all but internal bond strength was at least half the standard value
- Internal bond on average matched the ANSI 208.1 standard with 100M well outperforming the standard and 100MUF well underperforming

50F2/50MDI on average provides the same properties as 75MDI meaning a 25% reduction in MDI was statistically the same as a 50% substitution of MDI. Meanwhile, 25F2/75MDI performs the same as 75MDI on average but never performs worse than it while outperforming 50F2/50MDI on average. Meaning that 25F2/75MDI retains more mechanical properties then 75MDI as compared to 100MDI. Basically, 50F2/50MDI and 75MDI perform statistically the same, while 25F2/75MDI performs in-between 75MDI and 100MDI.

When it comes to the ANSI 208.1 standard almost every field underperformed this is due to several factors. The most obvious is that the processing conditions were not as controlled as commercial manufactured boards are due to the limitations in facilities. With those limited faculties comes the inability to manufacture multi-layer particleboard. This multi-layer board design increases the modulus of rupture and elasticity which accounts for at least some of the deficiency there. Hardness isn't even given as a parameter for low-density particleboard so not meeting this parameter was trivial and more included as a reference point. As for screw withdrawal and linear expansion it is unclear as to why these parameters fell below ANSI 208.1 standards. The last parameter, internal bond strength, was equal to or greater than the ANSI 208.1 standard. The internal bond strength of a particleboard primarily tests the bond strength of the resin binder and is less influenced by other factors such as particle distribution. This shows that these resins have potential and warrant further investigation.

6. CONCLUSION

The goals of the research were to:

H1: An ESS resin binder system that includes a crosslinker and a catalyst can be made that can cure within a 5 to 10 min cure window

H2: An ESS based resin system can be used as the sole binder in particleboards and be comparable to industrial resins (MUF, UF, PF, MDI)

H3: An ESS resin system can be partially substituted for MDI in particleboards while maintaining properties

H1 was met by the standards set out by this research. All told six different resin systems were found that cured within a 5 to 10 min window. Of these six only one, Formula 2, was seen as having potential as a resin binder. As the sole binder the properties did not meet the criteria laid out in H2. However, most wood composite binders are used in concentrations of 8% to 12% where all the testing for these particleboards used resin concentrations of 4%. These higher resin percentages are something that might be worth exploring in future research.

H3 was met when comparing 50F2/50MDI and 25F2/75MDI, to the 75MDI particleboards while it did not meet the requirements when compared to 100MDI. When looking at the two resins tested the 50F2/50MDI and 75MDI perform statistically the same while 25F2/75MDI performs in-between 75MDI and 100MDI. Meaning that a higher amount of MDI can be cut through substitution over resin reduction while maintaining properties. It is currently unclear what would happen if a small amount of MDI, 1% to 3%, was used in conjunction with a larger Formula 2 resin content of 8% to 12% and might be worth further investigation.

All the formulations tested had high internal bond strength that met or exceeded the ANSI 208.1 standard. This means substitution might be a viable option for particleboard binder

systems addressing the health concerns with the potential to also reduce costs. Substitution can help ease the adoption process as it gives time for the infrastructure to grow to make this material commercially available and economically viable. For the wood composites industry this might lower the risk to the point of being a worthwhile adoption.

REFERENCES

[1] Wool, R.P. and X.S. Sun. 2005, Biobased Polymers and Composites, MA, USA: Elsevier Science publisher, 2005.

[2] Food and Agriculture Organization of the United Nations, "The North American Forest Sector Outlook Study 2006 - 2030," 2006.

[3] ASTM International, "ASTM D1554 - 10: Standard Terminology Relating to Wood-Base Fiber and Particle Panel Materials 1," vol. 3. pp. 31–34, 2013.

[4] S. Oswalt, M. Thompson, and W. B. Smith, "U.S. Forest Resource Facts and Historical Trends," 2010.

[5] Forest Products Laboratory, "Wood Handbook: Wood as an Engineering Material," U.S. Department of Agriculture, 2010.

[6] Eram Sharmin, Fahmina Zafar, Deewan Akram, Manawwer Alam, Sharif Ahmad, "Recent advances in vegetable oils based environment friendly coatings: A review", Industrial Crops and Products, Volume 76, 15 December 2015, Pages 215-229, ISSN 0926-6690.

[7] N. Boquillon, C. Fringant, "Polymer networks derived from curing of epoxidised linseed oil: influence of different catalysts and anhydride hardeners", Polymer, Volume 41, Issue 4, 2000, Pages 8603-8613, ISSN 0032-3861.

[8] Alan A. Mara, Technologies of Wood Bonding: Principles in Practice, New York, NY: Van Nostrand Reinhold, 1992.

[9] E. Sitz, Processing and Manufacture of Soybean and Wheat Straw Medium Density Fiberboard Utilizing Epoxidized Sucrose Soyate, Fargo: North Dakota State University, 2016.

[10] Healthy Building Network, "Alternative Resin Binders," Global Health & Safety Initiative, 2008.

[11] Nuryawan A, Risnasari I, Sucipto T, Iswanto AH, Dewi RR. Urea-formaldehyde resins: production, application, and testing. InIOP Conference Series: Materials Science and Engineering 2017 Jul (Vol. 223, No. 1, p. 012053). IOP Publishing.

[12] Formaldehyde Emission Standards for Composite Wood Products. In: Agency EP, editor. 2016-27987 ed: U.S. Government; 2016. p. 89674-743 (70 pages).

[13] H. Lei and C. E. Frazier, "Curing behavior of melamine-urea-formaldehyde (MUF) resin adhesive," International Journal of Adhesion and Adhesives, vol. 62, pp. 40-44, 2015.

[14] “Particleboard and medium-density fiberboard: Choose Green Report,” 2001.

[15] X. Pan, P. Sengupta and D. Webster, "Novel biobased epoxy compounds: epoxidized sucrose esters of fatty acids," Green Chemistry, vol. 13, pp. 965-975, 2011.

[16] Shida Miao, Ping Wang, Zhiguo Su, Songping Zhang, “Vegetable-oil-based polymers as future polymeric biomaterials”, Acta Biomaterialia, Volume 10, Issue 4, April 2014, Pages 1692-1704, ISSN 1742-7061.

[17] E. Monono, Pilot Scale Production, Characterization, and Optimization of Epoxidized Vegetable Oil-Based Resin, Fargo: North Dakota State University, 2015.

[18] X. Pan, P. Sengupta and D. Webster, "High Biobased Content Epoxy — Anhydride Thermosets from Epoxidized Sucrose Esters of Fatty Acids," BioMacromolecules, vol. 12, no. 6, p. 2416–2428, 2011.

[19] Adlina Paramarta, Dean C. Webster, “Bio-based high performance epoxy-anhydride thermosets for structural composites: The effect of composition variables”, Reactive and Functional Polymers, Volume 105, August 2016, Pages 140-149, ISSN 1381-5148.

[20] Sudheer Kumar, Sushanta K. Samal, Smita Mohanty, Sanjay K. Nayak, “Study of curing kinetics of anhydride cured petroleum-based (DGEBA) epoxy resin and renewable resource based epoxidized soybean oil (ESO) systems catalyzed by 2-methylimidazole”, Thermochimica Acta, Volume 654, 2017, Pages 112-120, ISSN 0040-6031.

[21] H. Miyagawa, A.K. Mohanty, M. Misra, L.T. Drzal Macromol. Mater. Eng., 289 (2004), pp. 629-641.

[22] Nassibeh Hosseini, Dean C. Webster, Chad Ulven, “Advanced biocomposite from highly functional methacrylated epoxidized sucrose soyate (MAESS) resin derived from vegetable oil and fiberglass fabric for composite applications”, European Polymer Journal, Volume 79, June 2016, Pages 63-71, ISSN 0014-3057.

[23] Christopher Taylor, Ali Amiri, Adlina Paramarta, Chad Ulven, Dean Webster, “Development and weatherability of bio-based composites of structural quality using flax fiber and epoxidized sucrose soyate”, Materials & Design, Volume 113, 5 January 2017, Pages 17-26, ISSN 0264-1275.

[24] Hughes, Mark. “Wood and Wood Products: Manufacture of wood-based panels.” 2016.

[25] Kelly MW. Critical literature review of relationships between processing parameters and physical properties of particleboard. US Department of Agriculture, Forest Service, Forest Products Laboratory; 1977 May 10.

[26] Kamke, Frederick A. “Physics of Hot-Pressing.” US Forest Products Laboratory, Fundamentals of Composites Processing Workshop, 2003.

[27] L. Sangyeob, T. Shupe and C. Hse, "Properties of Bio-Based Medium Density Fiberboard," Recent Developments in Wood Composites, pp. 51-58, 2006.

[28] P. Evon, J. Vinet, L. L and R. L, "Influence of thermo-pressing conditions on the mechanical propertiesof biodegradable fiberboards made from a deoiled sunflower cake," Industrial Crops and Products, vol. 65, pp. 117-126, 2015.

[29] Heinemann C, Frühwald A, Humphrey PE. Evaluation of adhesive cure during hot pressing of wood-based composites. na; 2003.

[30] R. Widyorini, J. Xu, K. Umemura, and S. Kawai, “Manufacture and properties of binderless particleboard from bagasse I: effects of raw material type, storage methods, and manufacturing process,” J. Wood Sci., vol. 51, no. 6, pp. 648–654, Dec. 2005.

[31] T. Tabarsa, S. Jahanshahi, and A. Ashori, “Mechanical and physical properties of wheat straw boards bonded with a tannin modified phenol–formaldehyde adhesive,” Compos. Part B, vol. 42, no. 2, pp. 176–180, Mar. 2011.

[32] J. Xu, R. Widyorini, H. Yamauchi, and S. Kawai, “Development of binderless fiberboard from kenaf core,” J. Wood Sci., vol. 52, no. 3, pp. 236–243, Jun. 2006.

[33] Carll CG. Wood particleboard and flakeboard: Types, grades, and uses. (General technical report FPL; 53): 9 p.. 1986;53.

[34] ASTM D1554: Standard Terminology Relating to Wood-Base Fiber and Particle Panel Materials, West Conshohocken, PA: ASTM International, 2010.

[35] American National Standard, ANSI Standard 208.1 Particleboard, Gaithersburg, MD, 2009.

[36] Composite Panel Association, ANSI 208.2 Medium Density Fiberboard (MDF) for Interior Applications, Gaithersburg, MD, 2002.

[37] ASTM D2339: Standard Test Method for Strength Properties of Adhesives in Two-Ply Wood Construction in Shear by Tension Loading, West Conshohocken, PA: ASTM International, 2011.

[38] T, Arunkumar & Ramachandran, S. (2016). Surface Coating and Characterisation of Polyurea for Liquid Storage. International Journal of Ambient Energy. 1-14. 10.1080/01430750.2016.1222966.

[39] ASTM D1037: Standard Test Methods for Evaluating Properties of Wood-Base Fiber and Particle Panel Materials, West Conshohocken, PA: ASTM International, 2012.

[40] D. Sundquist, Dried Distillers Grains with Solubles as a Multifunctional Filler in Wood Particleboards, Fargo: North Dakota State University, 2015.

[41] Levine, David M. Applied Statistics for Engineers and Scientists: Using Microsoft Excel and Minitab. Prentice Hall, 2001.

[42] Montgomery, Douglas C. Design and Analysis of Experiments. John Wiley, 2017.

APPENDIX A. TUKEY TESTS FOR TIME AND TEMPERATURE

Table A1: Tukey pairwise comparison showing the impact of time on the density of the particleboards

Time	N	Mean	Grouping	
10	40	561.557	A	
5	40	548.309		B
Means that do not share a letter are significantly different				

Table A2: Tukey pairwise comparison showing the impact of temperature on the density of the particleboards

Temperature	N	Mean	Grouping
190	40	557.254	A
175	40	552.612	A
Means that do not share a letter are significantly different			

Table A3: Tukey pairwise comparison for impact of time on the percentage volume change after 2-hour immersion in water

Time	N	Mean	Grouping
10	32	0.242422	A
5	32	0.208176	A
Means that do not share a letter are significantly different			

Table A4: Tukey pairwise comparison for impact of temperature on the percentage volume change after 2-hour immersion in water

Temperature	N	Mean	Grouping
190	32	0.246023	A
175	32	0.204575	A
Means that do not share a letter are significantly different			

Table A5: Tukey pairwise comparison for impact of time on the percentage mass change after 2-hour immersion in water

Time	N	Mean	Grouping
10	32	0.332474	A
5	32	0.297597	A
Means that do not share a letter are significantly different			

Table A6: Tukey pairwise comparison for impact of temperature on the percentage mass change after 2-hour immersion in water

Temperature	N	Mean	Grouping	
190	32	0.386364	A	
175	32	0.243707		B
Means that do not share a letter are significantly different				

Table A7: Tukey pairwise comparison for impact of time on the percentage volume change after 24-hour immersion in water

Time	N	Mean	Grouping
10	32	0.386816	A
5	32	0.356383	A
Means that do not share a letter are significantly different			

Table A8: Tukey pairwise comparison for impact of temperature on the percentage volume change after 24-hour immersion in water

Temperature	N	Mean	Grouping
190	32	0.376572	A
175	32	0.366627	A
Means that do not share a letter are significantly different			

Table A9: Tukey pairwise comparison for impact of time on the percentage mass change after 24-hour immersion in water

Time	N	Mean	Grouping
10	32	0.555005	A
5	32	0.538135	A
Means that do not share a letter are significantly different			

Table A10: Tukey pairwise comparison for impact of temperature on the percentage mass change after 24-hour immersion in water

Temperature	N	Mean	Grouping	
190	32	0.604291	A	
175	32	0.488849		B
Means that do not share a letter are significantly different				

Table A11: Tukey pairwise comparison showing the impact of time on the linear expansion of the particleboards

Time	N	Mean	Grouping
5	40	0.0102208	A
10	40	0.0099904	A
Means that do not share a letter are significantly different			

Table A12: Tukey pairwise comparison showing the impact of temperature on the linear expansion of the particleboards

Temperature	N	Mean	Grouping
175	40	0.0102836	A
190	40	0.0099277	A
Means that do not share a letter are significantly different			

Table A13: Tukey pairwise comparison showing the impact of time on the modulus of rupture of the particleboards

Time	N	Mean	Grouping
5	40	1.43600	A
10	40	1.37275	A
Means that do not share a letter are significantly different			

Table A14: Tukey pairwise comparison showing the impact of temperature on the modulus of rupture of the particleboards

Temperature	N	Mean	Grouping
190	40	1.44225	A
175	40	1.36650	A
Means that do not share a letter are significantly different			

Table A15: Tukey pairwise comparison showing the impact of time on the modulus of elasticity of the particleboards

Time	N	Mean	Grouping
10	40	336.168	A
5	40	330.175	A
Means that do not share a letter are significantly different			

Table A16: Tukey pairwise comparison showing the impact of temperature on the modulus of elasticity of the particleboards

Temperature	N	Mean	Grouping
190	40	337.741	A
175	40	328.603	A
Means that do not share a letter are significantly different			

Table A17: Tukey pairwise comparison showing the impact of time on the internal bond strength of the particleboards

Time	N	Mean	Grouping
5	50	173.688	A
10	50	167.383	A
Means that do not share a letter are significantly different			

Table A18: Tukey pairwise comparison showing the impact of temperature on the internal bond strength of the particleboards

Temperature	N	Mean	Grouping
190	50	175.033	A
175	50	166.039	A
Means that do not share a letter are significantly different			

Table A19: Tukey pairwise comparison showing the impact of time on the maximum screw withdrawal force of the particleboards

Time	N	Mean	Grouping
10	40	186.329	A
5	40	181.743	A
Means that do not share a letter are significantly different			

Table A20: Tukey pairwise comparison showing the impact of temperature on the maximum screw withdrawal force of the particleboards

Temperature	N	Mean	Grouping
190	40	196.705	A
175	40	171.367	A
Means that do not share a letter are significantly different			

Table A21: Tukey pairwise comparison showing the impact of time on the hardness of the particleboards

Time	N	Mean	Grouping
5	80	-1569.11	A
10	80	-1654.76	A
Means that do not share a letter are significantly different			

Table A22: Tukey pairwise comparison showing the impact of temperature on the hardness of the particleboards

Temperature	N	Mean	Grouping
175	80	-1586.22	A
190	80	-1637.66	A
Means that do not share a letter are significantly different			

APPENDIX B. DSC CURVES

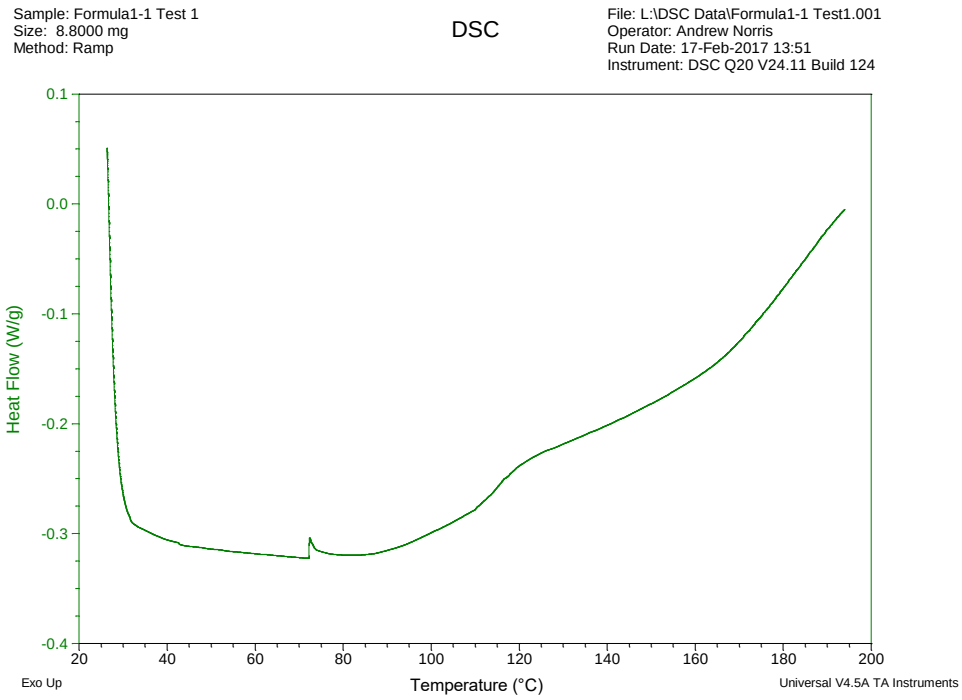

Figure B1: Formula 1 ramp DSC curve

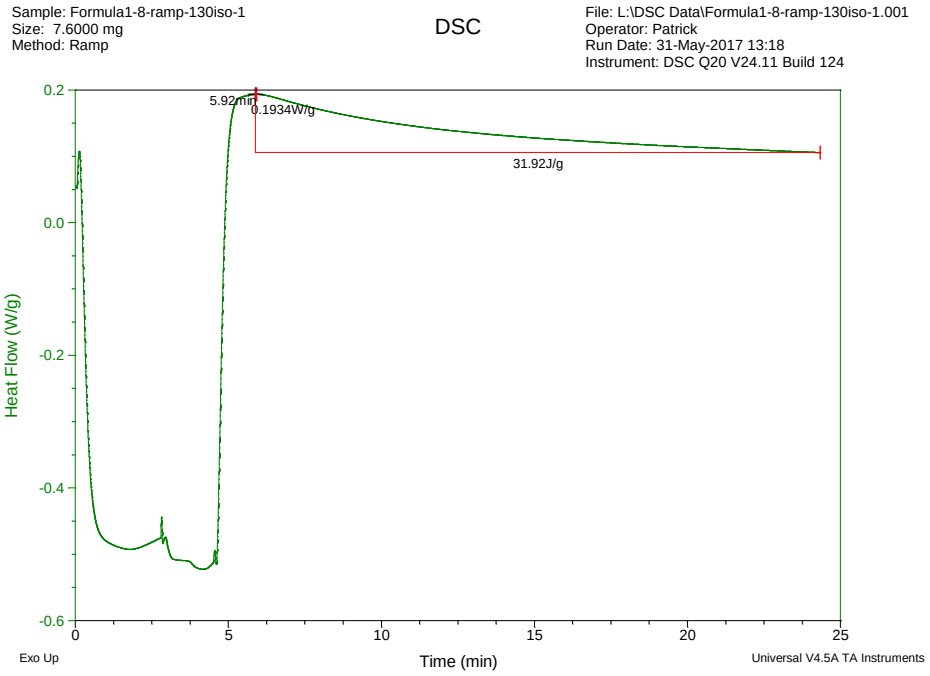

Figure B2: Formula 1 130°C isothermal DSC curve

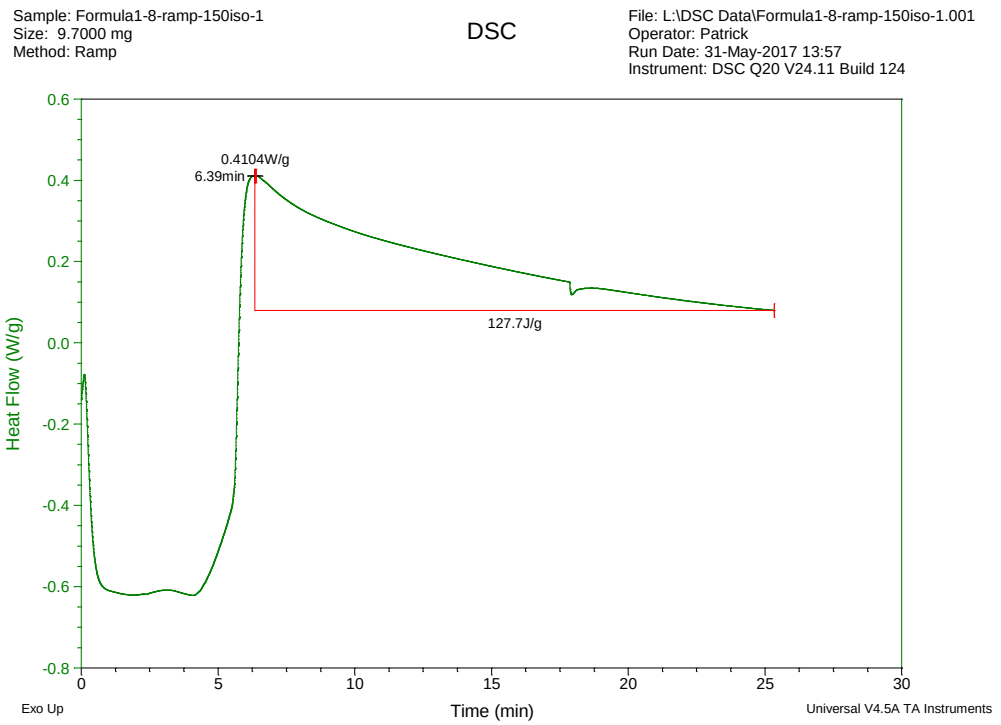

Figure B3: Formula 1 150°C isothermal DSC curve

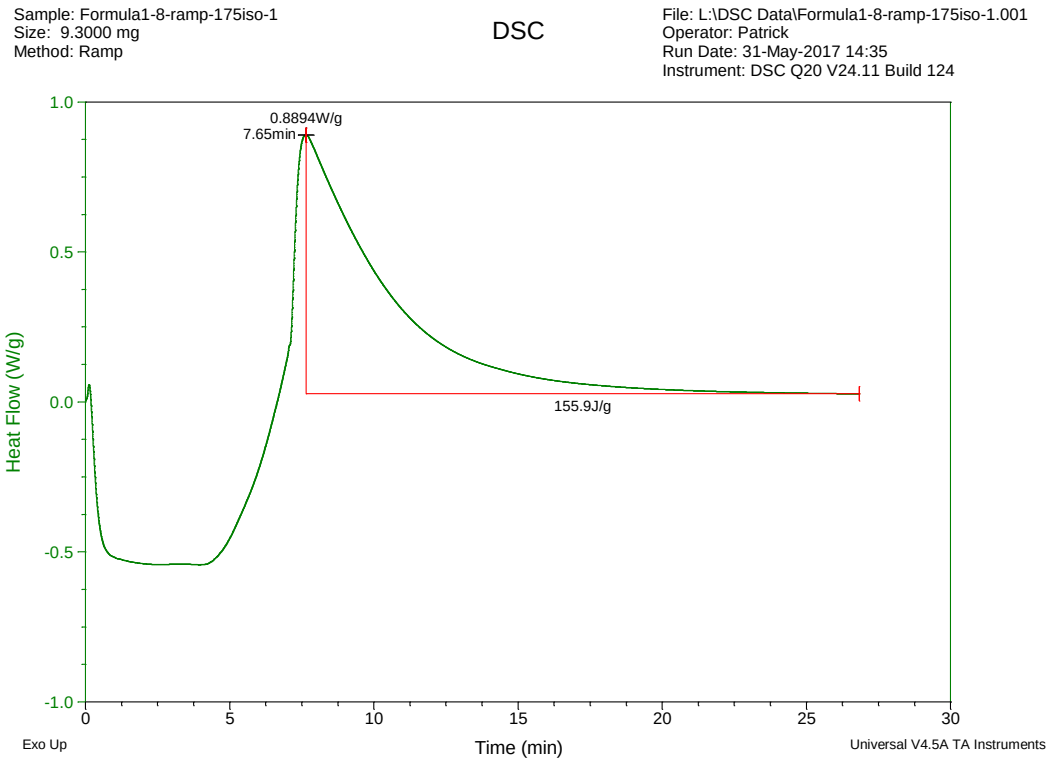

Figure B4: Formula 1 175°C isothermal DSC curve

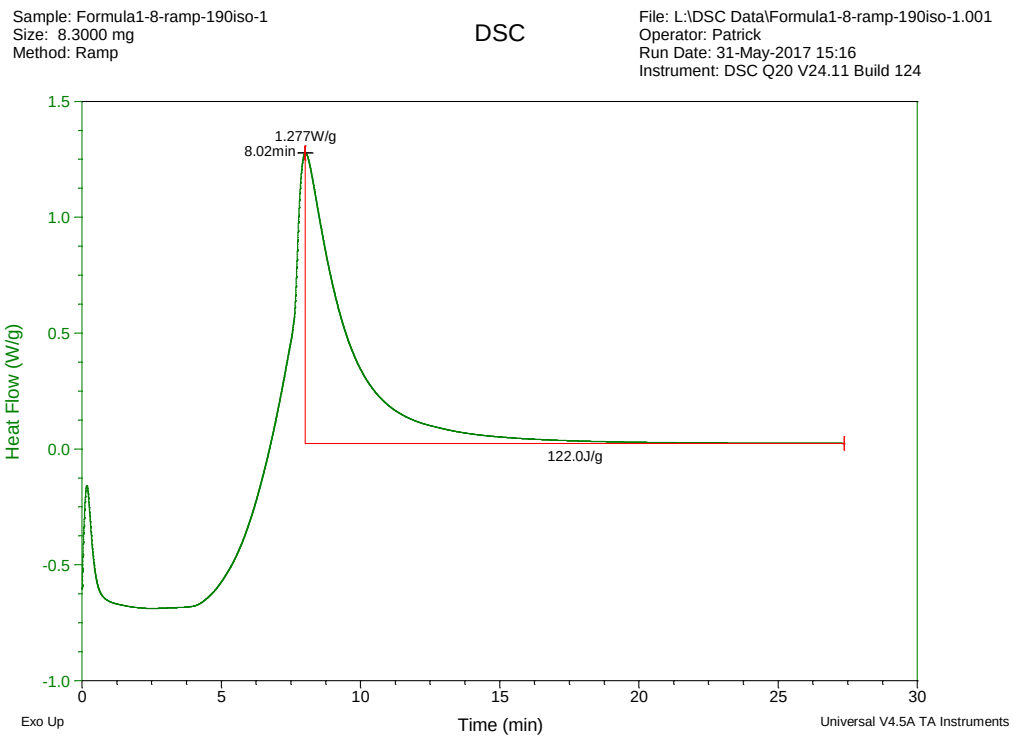

Figure B5: Formula 1 190^{o}C isothermal DSC curve

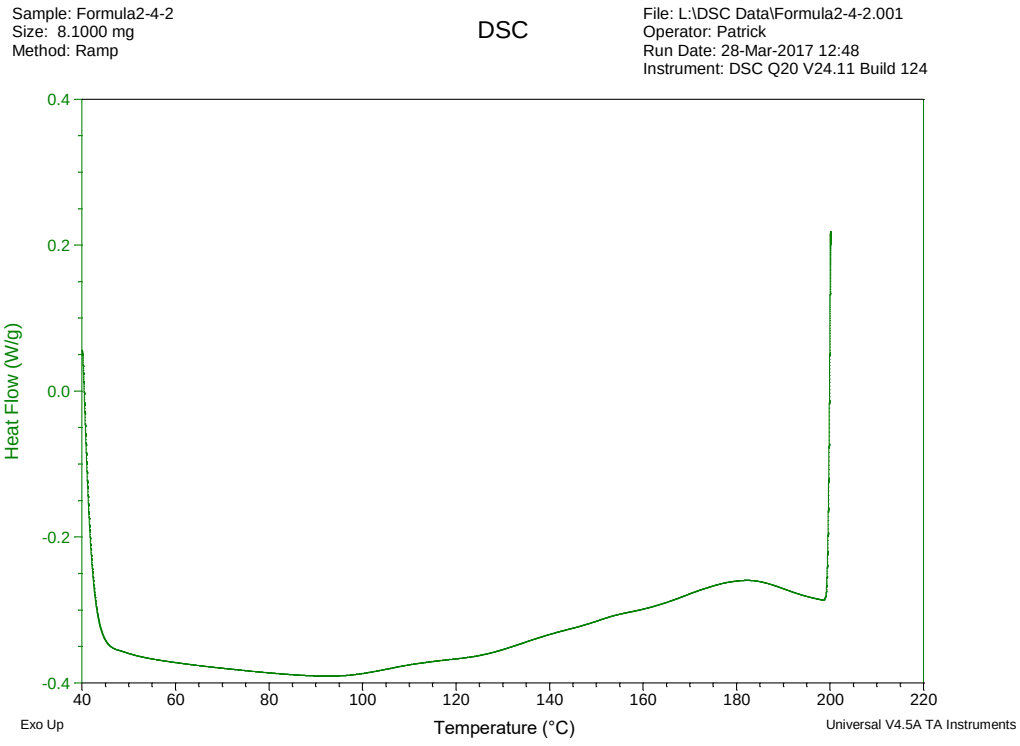

Figure B6: Formula 2 ramp DSC curve

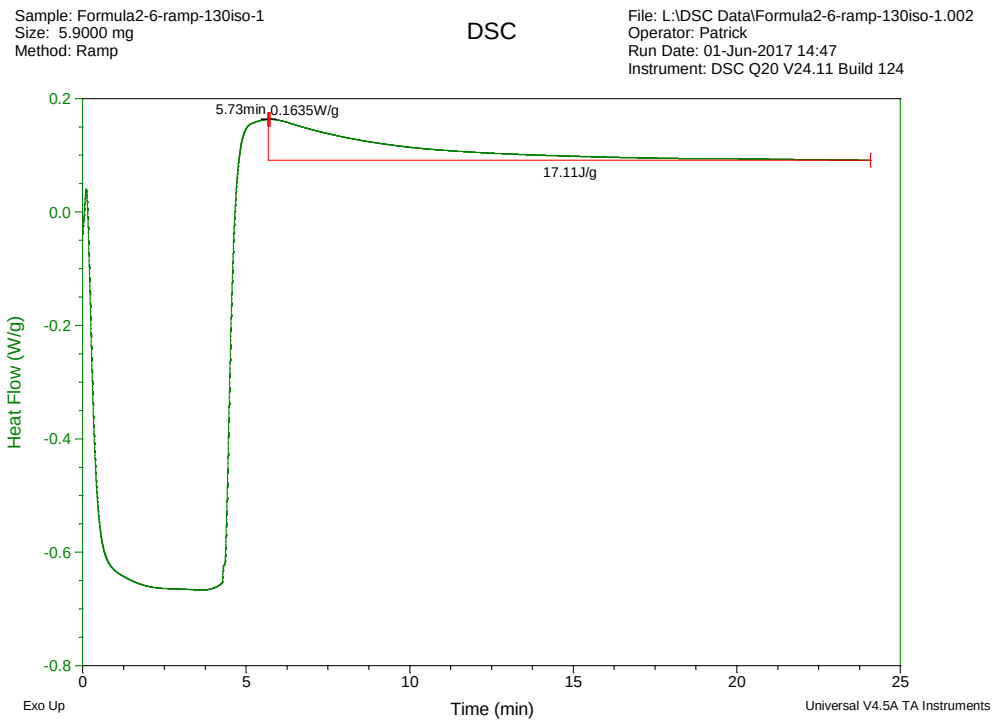

Figure B7: Formula 2 130ºC isothermal DSC curve

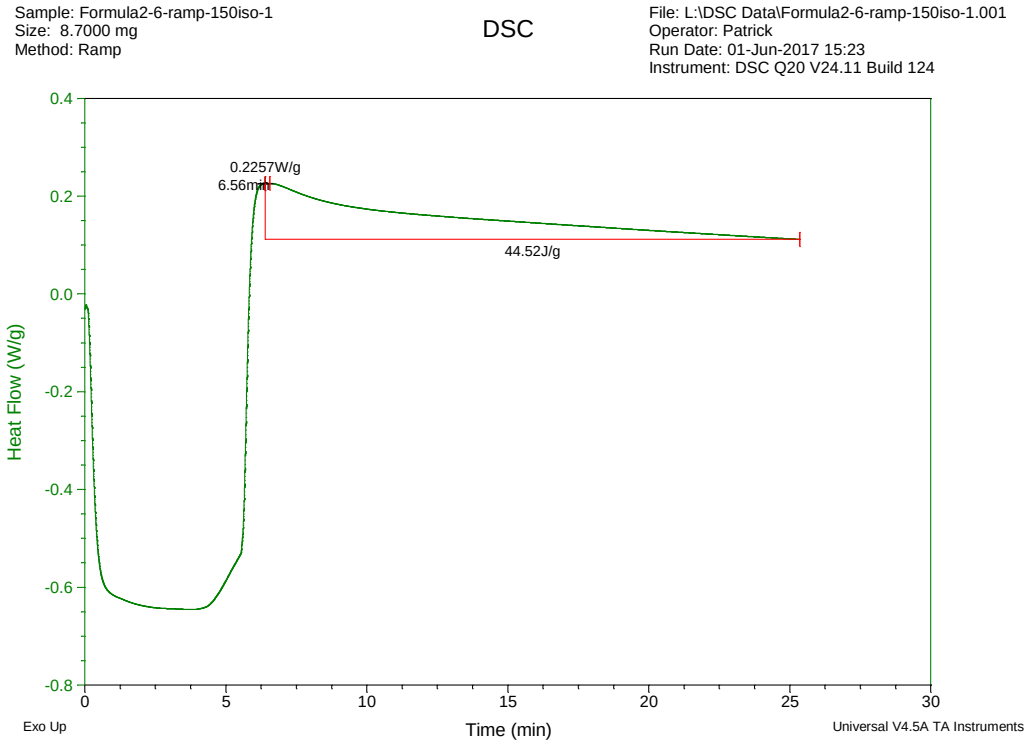

Figure B8: Formula 2 150ºC isothermal DSC curve

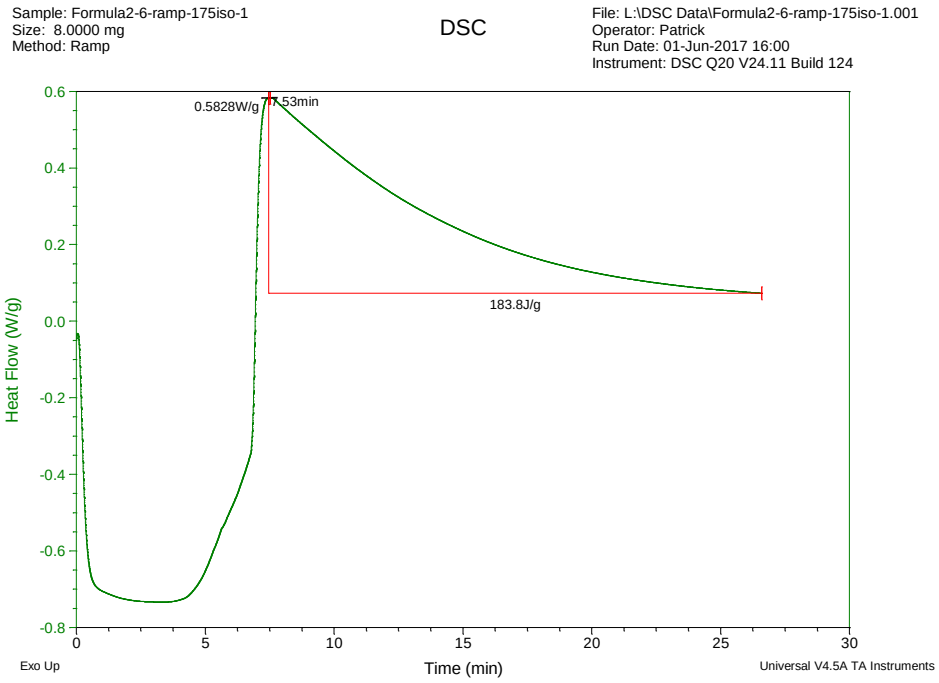

Figure B9: Formula 2 175°C isothermal DSC curve

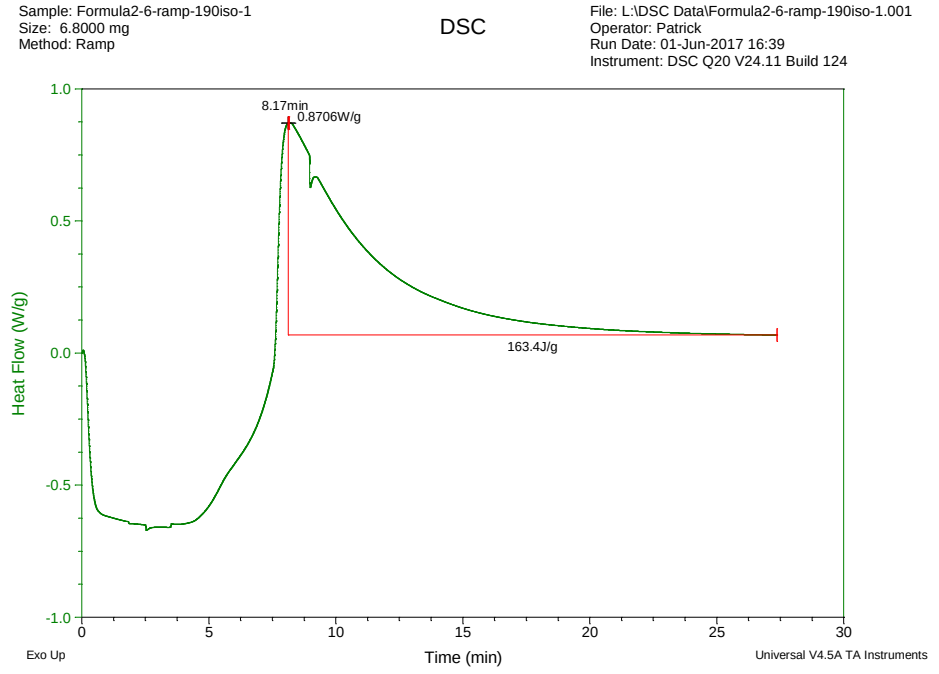

Figure B10: Formula 2 190°C isothermal DSC curve

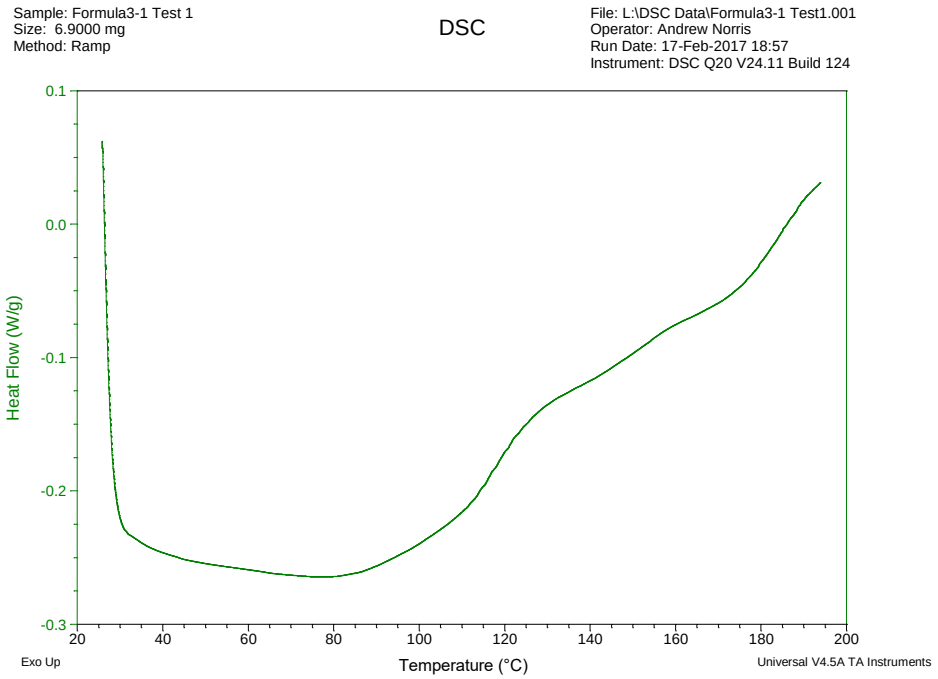

Figure B11: Formula 3 ramp DSC curve

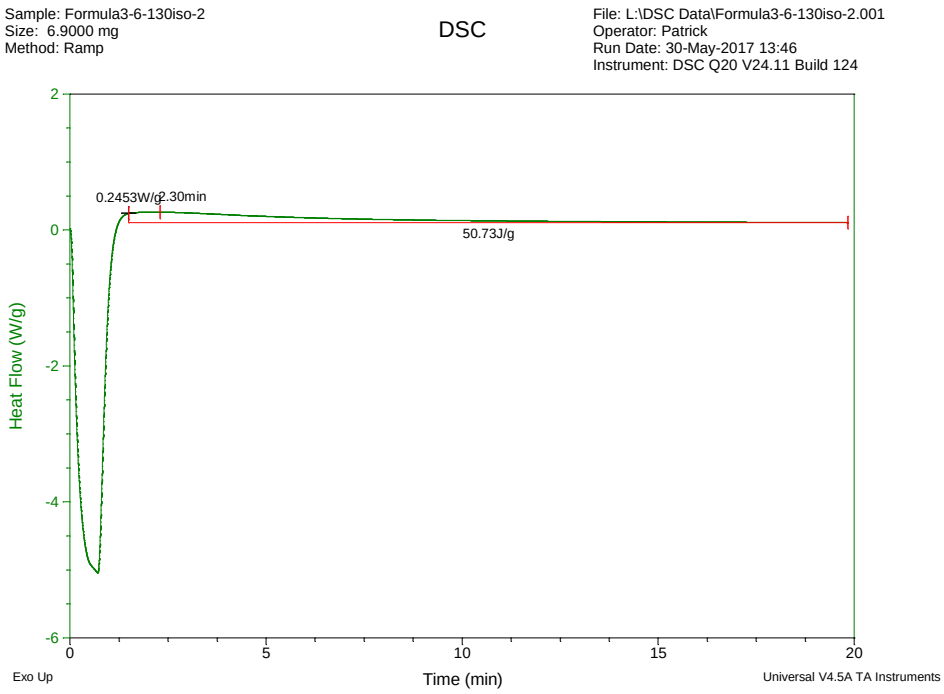

Figure B12: Formula 3 130°C isothermal DSC curve

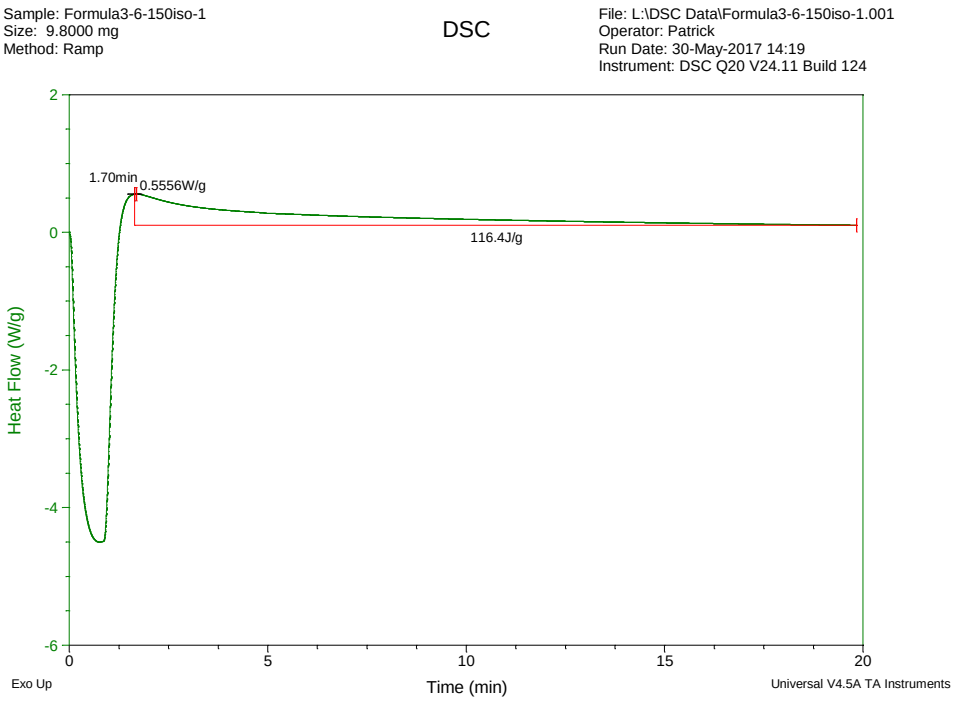

Figure B13: Formula 3 150^{o}C isothermal DSC curve

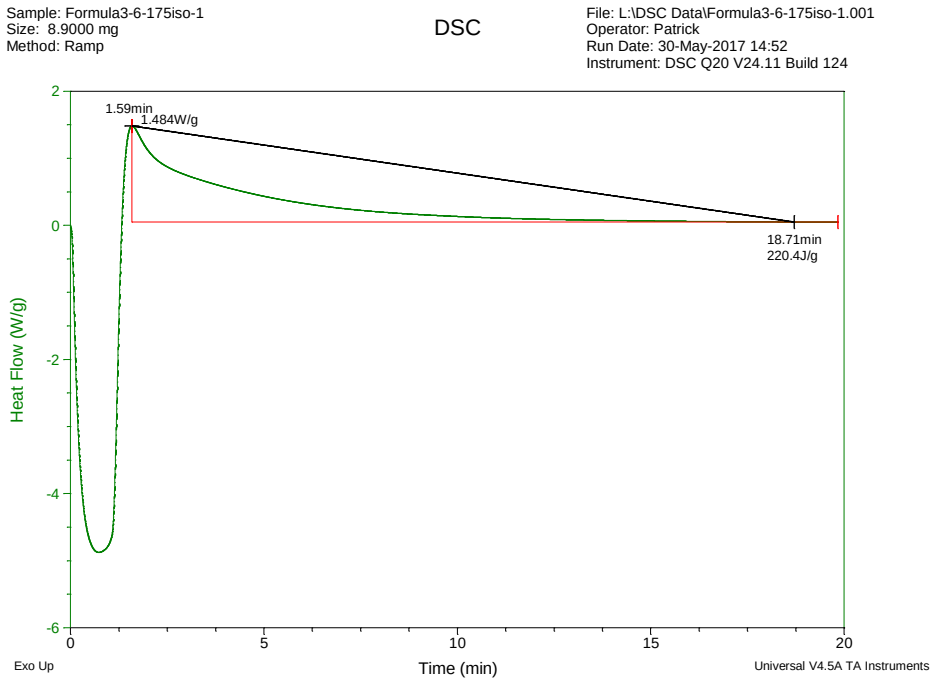

Figure B14: Formula 3 175^{o}C isothermal DSC curve

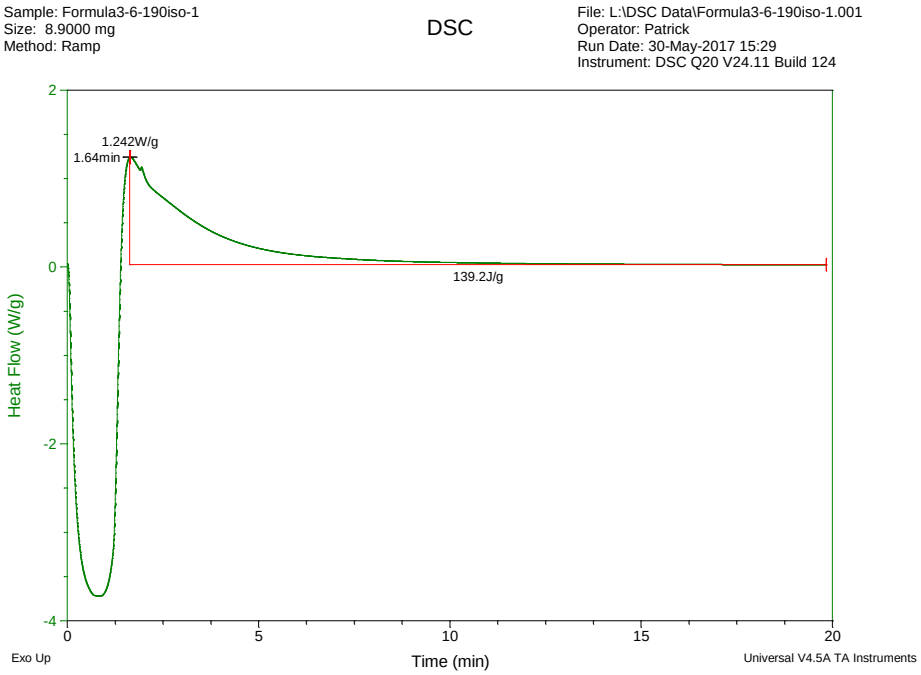

Figure B15: Formula 3 190ºC isothermal DSC curve

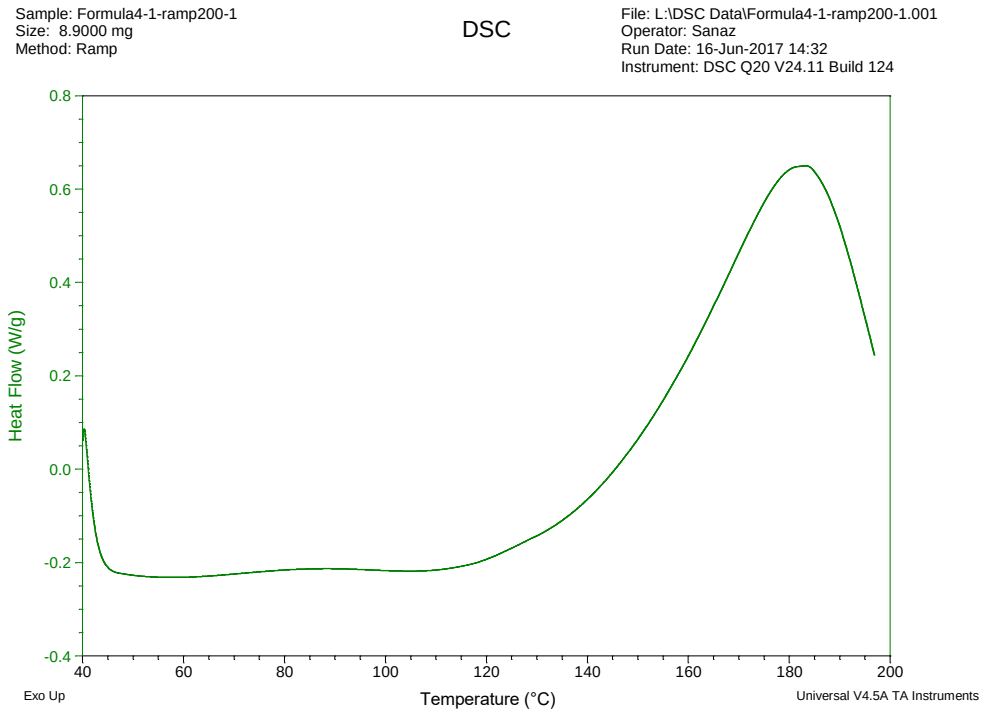

Figure B16: Formula 4 ramp DSC curve

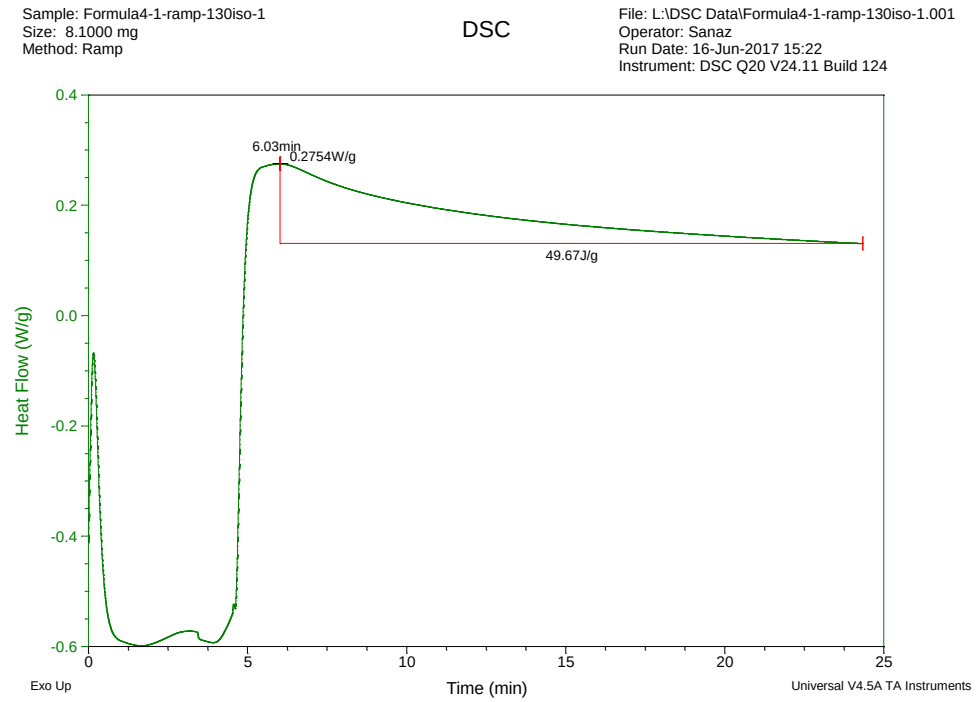

Figure B17: Formula 4 130^{o}C isothermal DSC curve

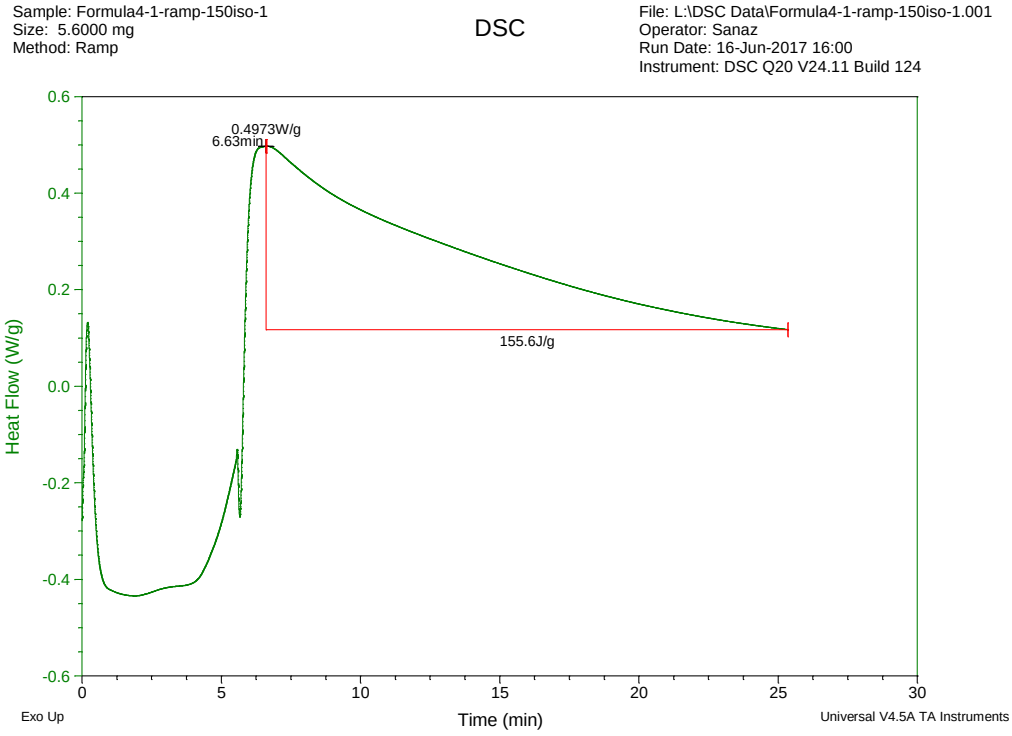

Figure B18: Formula 4 150^{o}C isothermal DSC curve

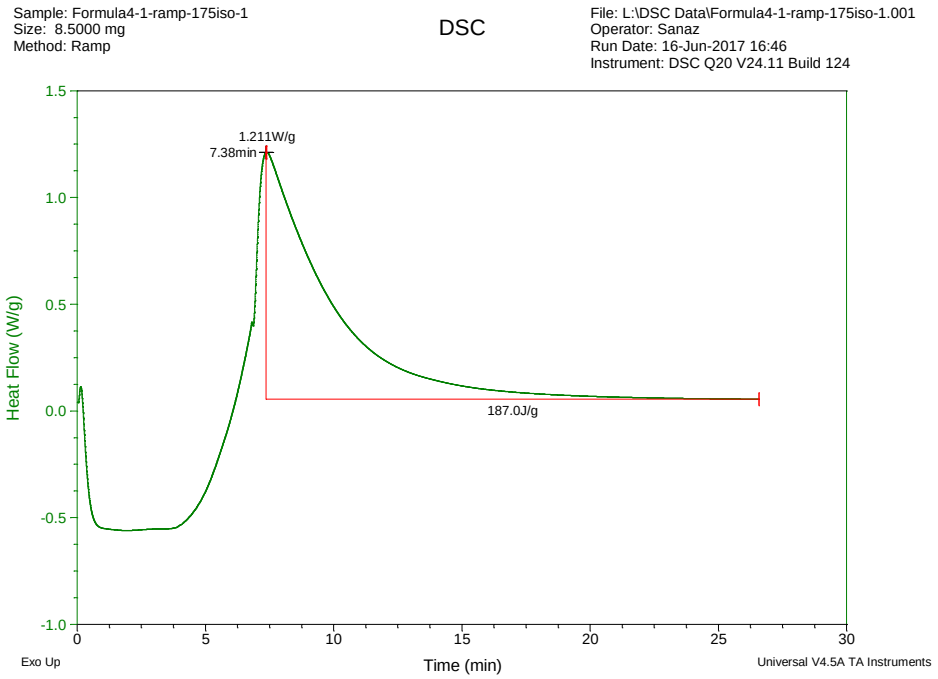

Figure B19: Formula 4 175^{o}C isothermal DSC curve

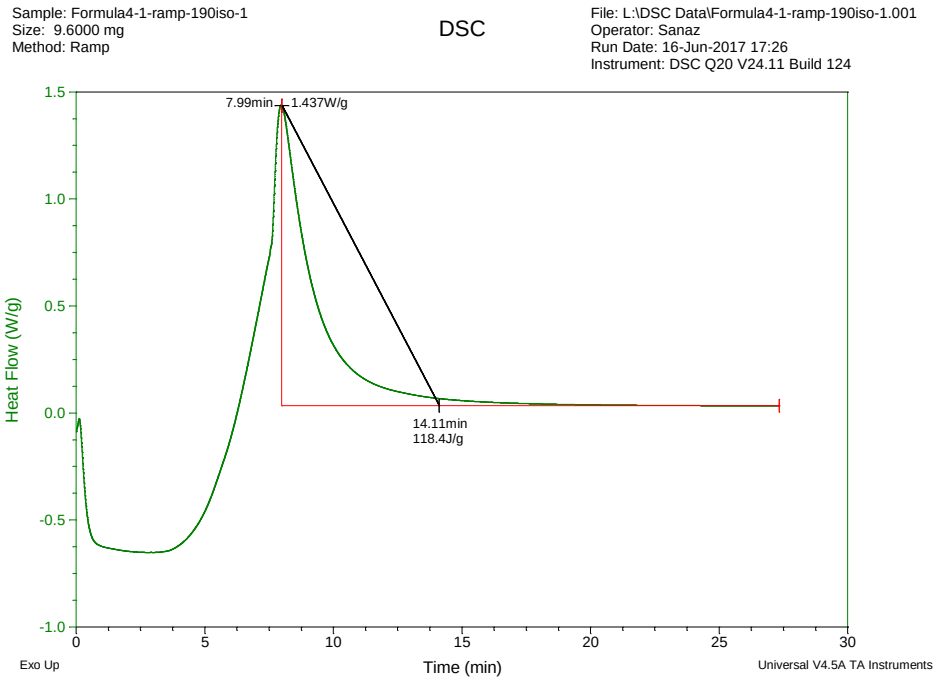

Figure B20: Formula 4 190^{o}C isothermal DSC curve

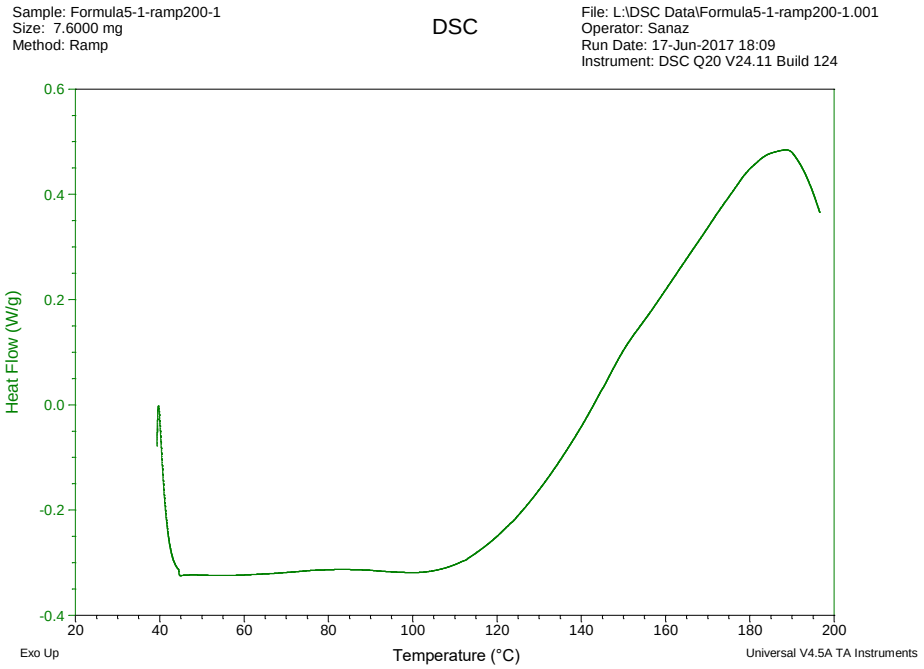

Figure B21: Formula 5 ramp DSC curve

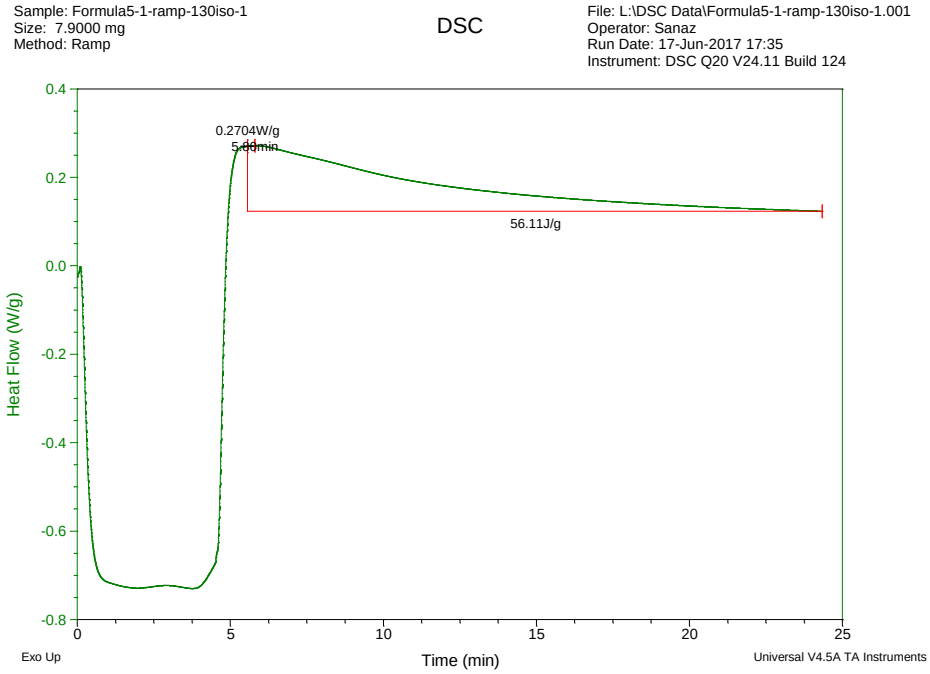

Figure B22: Formula 5 130^{o}C isothermal DSC curve

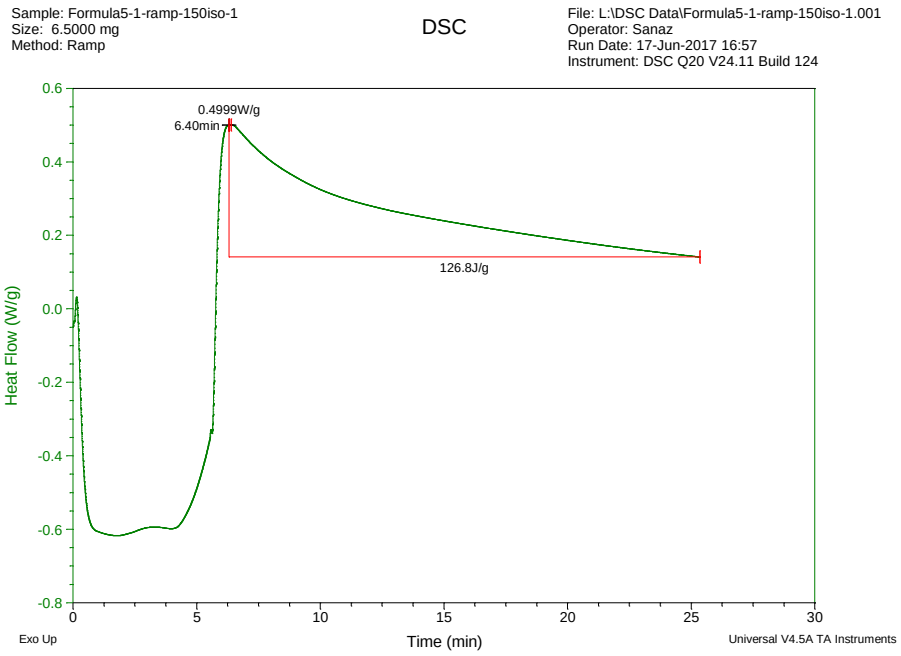

Figure B23: Formula 5 150^{o}C isothermal DSC curve

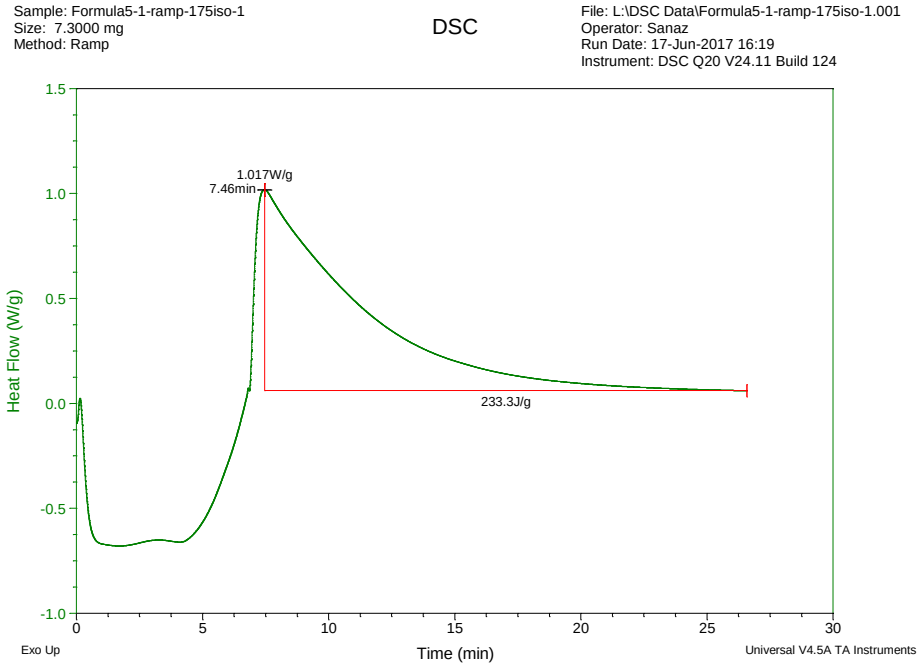

Figure B24: Formula 5 175^{o}C isothermal DSC curve

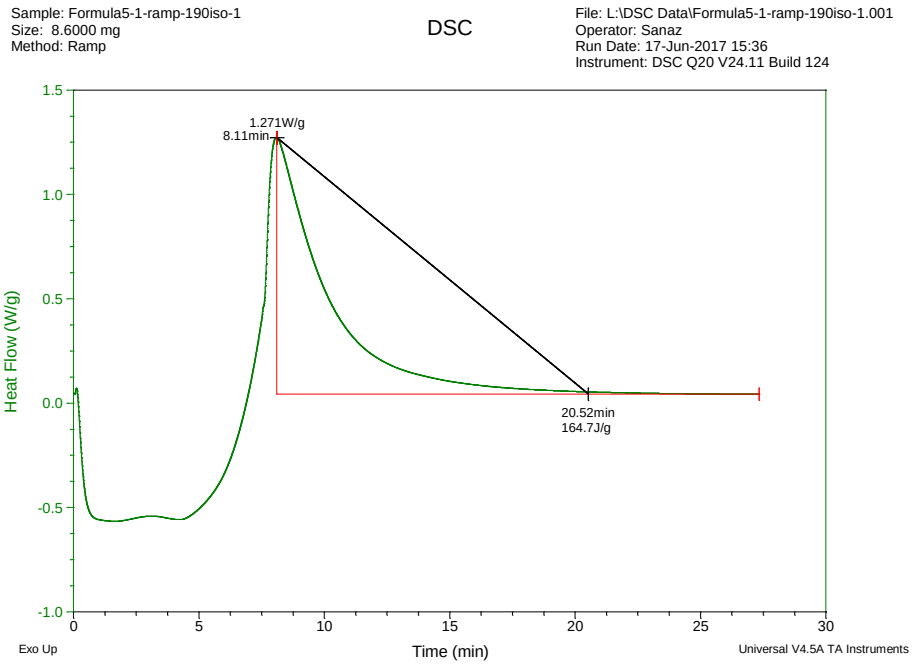

Figure B25: Formula 5 190^{o}C isothermal DSC curve

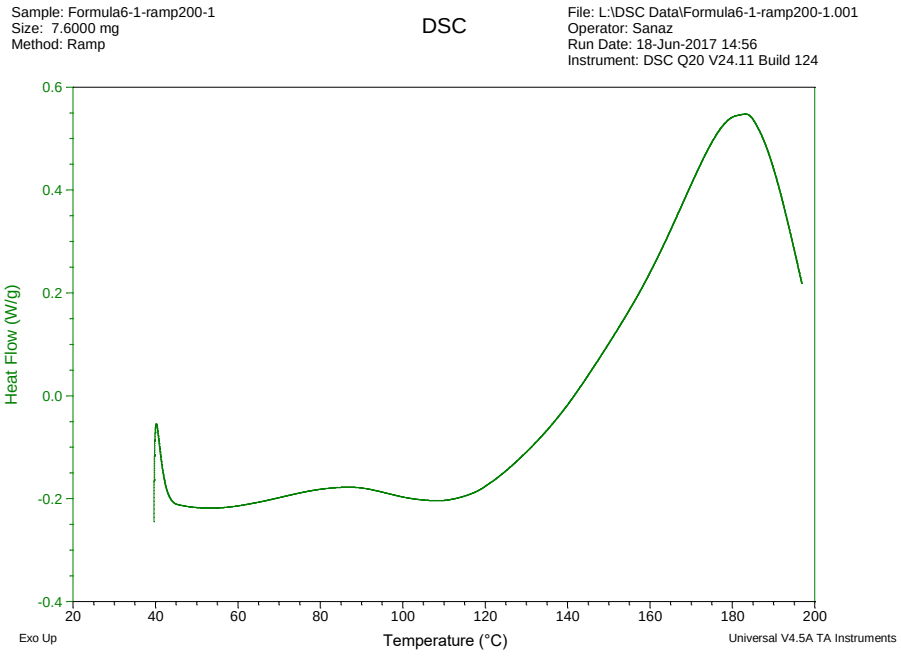

Figure B26: Formula 6 ramp DSC curve

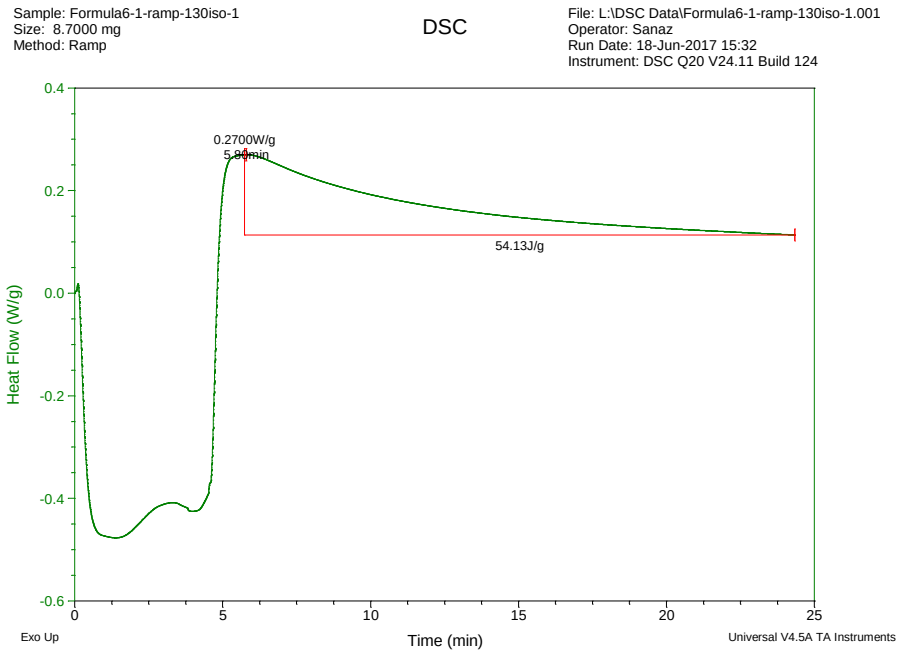

Figure B27: Formula 6 130ºC isothermal DSC curve

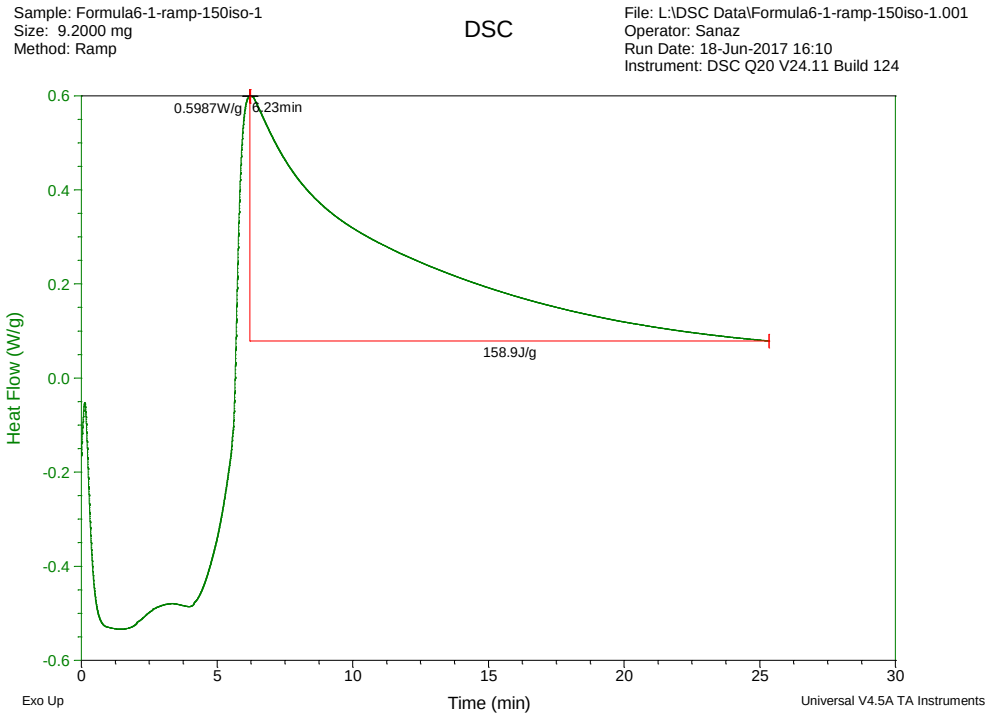

Figure B28: Formula 6 150ºC isothermal DSC curve

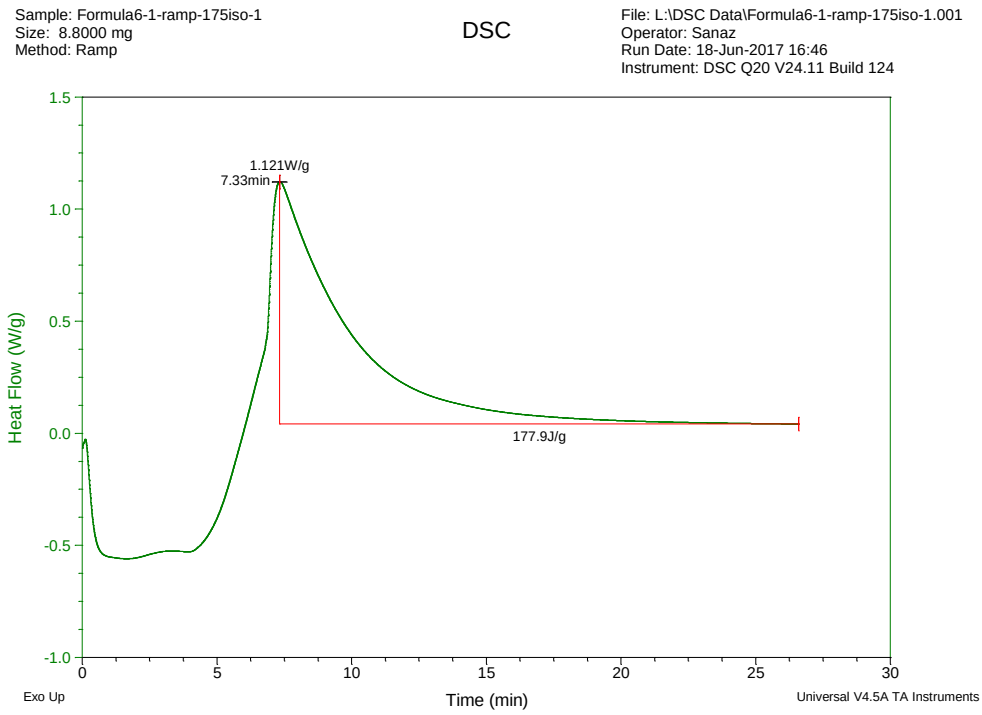

Figure B29: Formula 6 175°C isothermal DSC curve

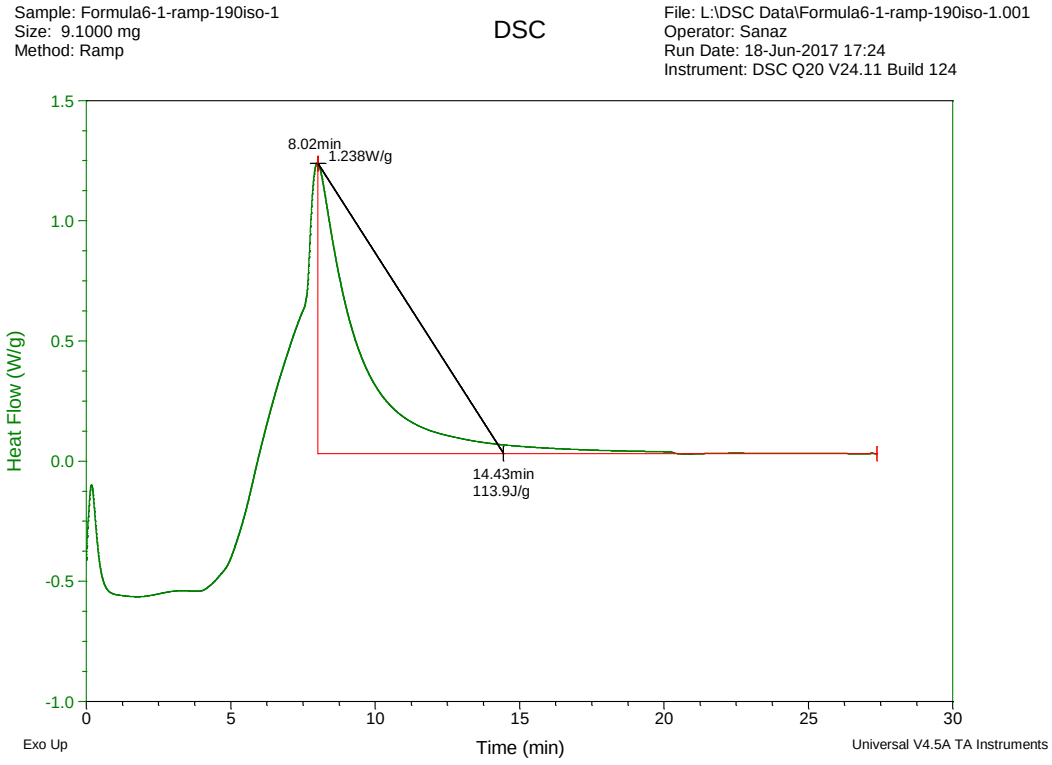

Figure B30: Formula 6 190°C isothermal DSC curve

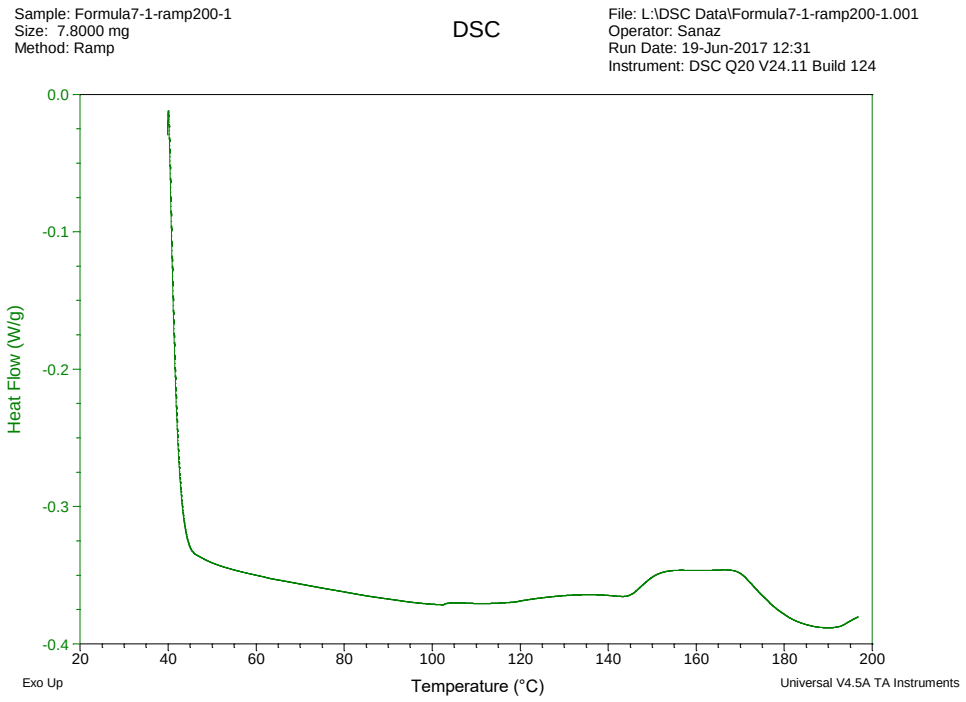

Figure B31: Formula 7 ramp DSC curve

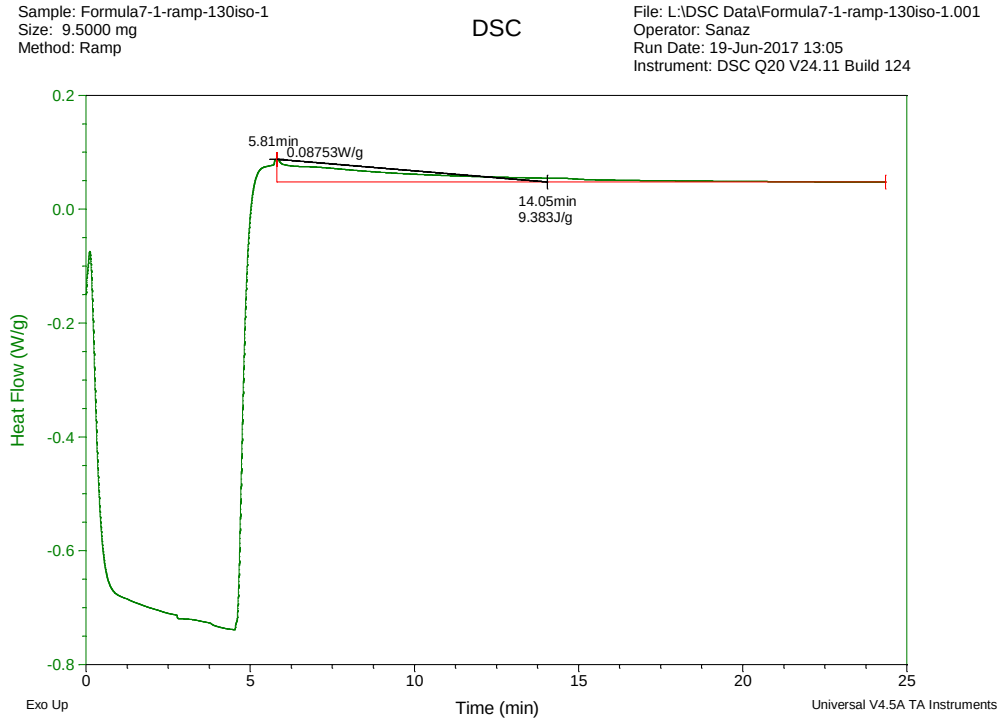

Figure B32: Formula 7 130^{o}C isothermal DSC curve

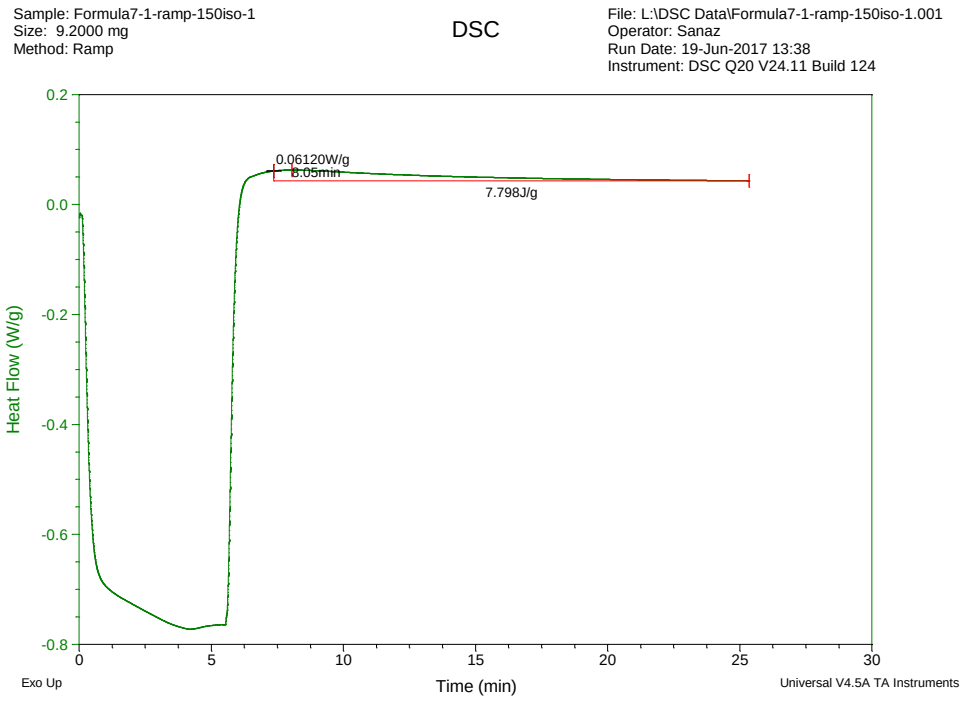

Figure B33: Formula 7 150^{o}C isothermal DSC curve

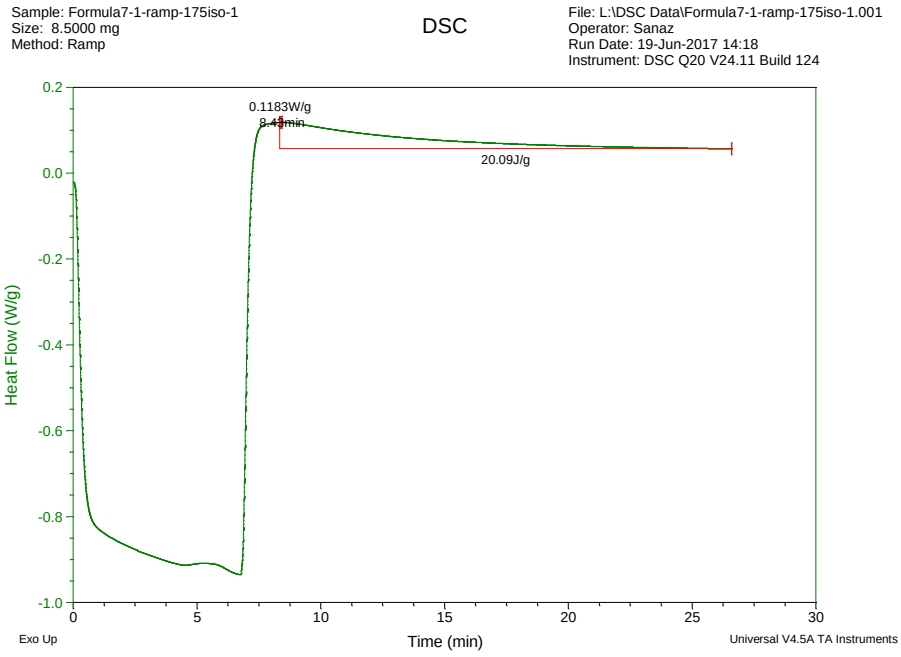

Figure B34: Formula 7 175^{o}C isothermal DSC curve

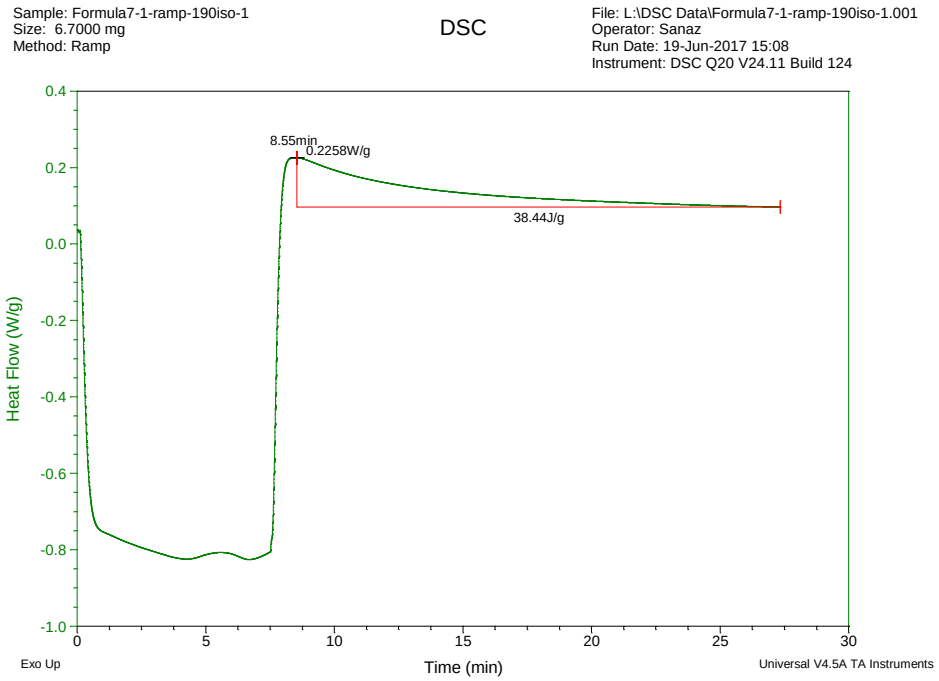

Figure B35: Formula 7 190°C isothermal DSC curve

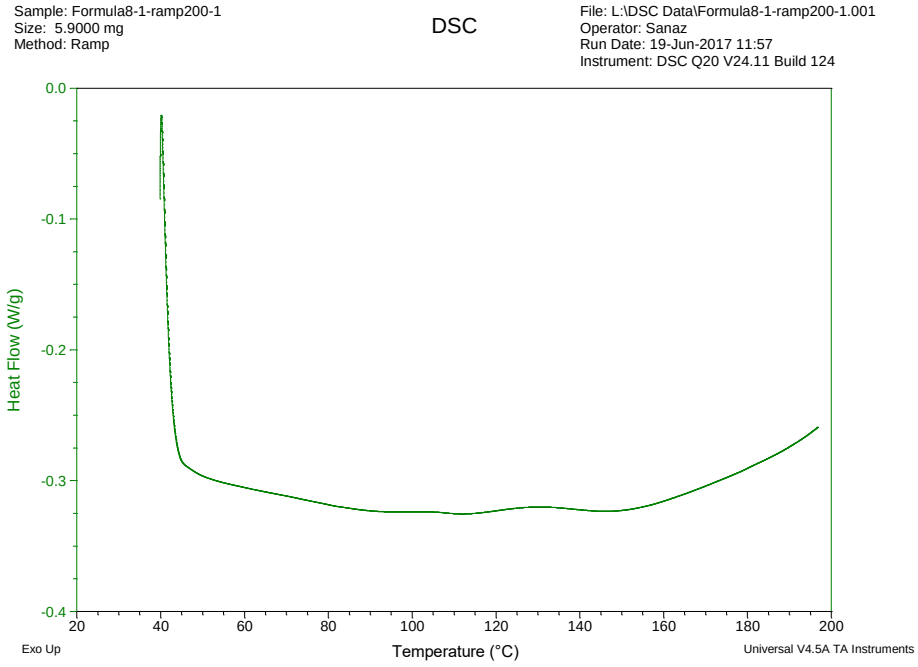

Figure B36: Formula 8 ramp DSC curve

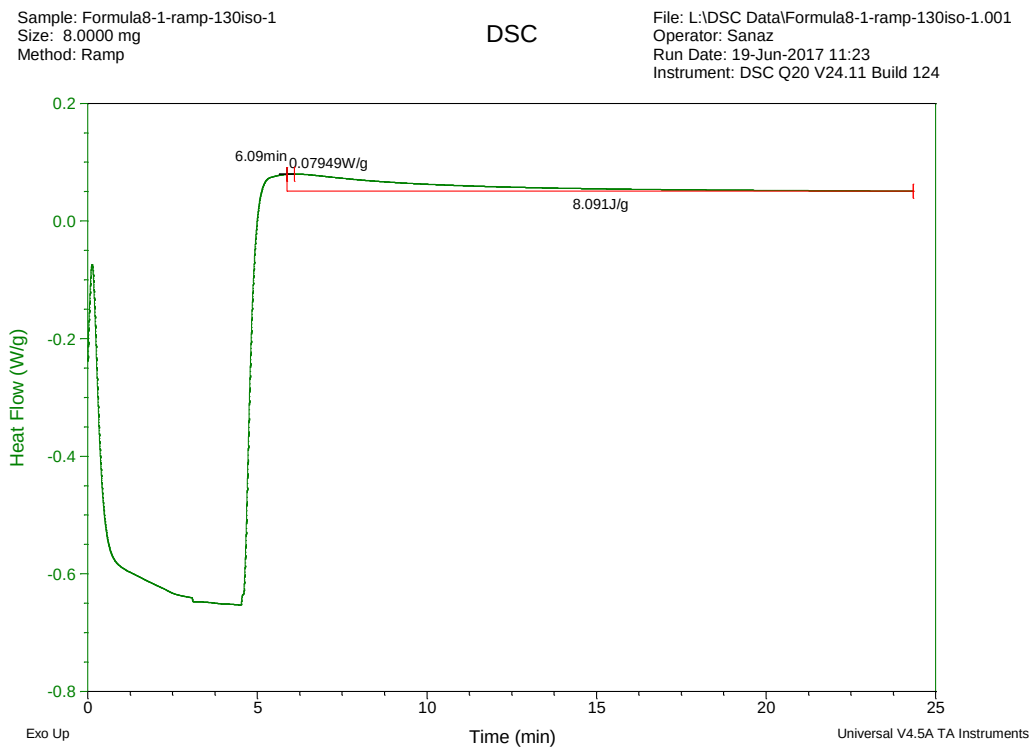

Figure B37: Formula 8 130^{o}C isothermal DSC curve

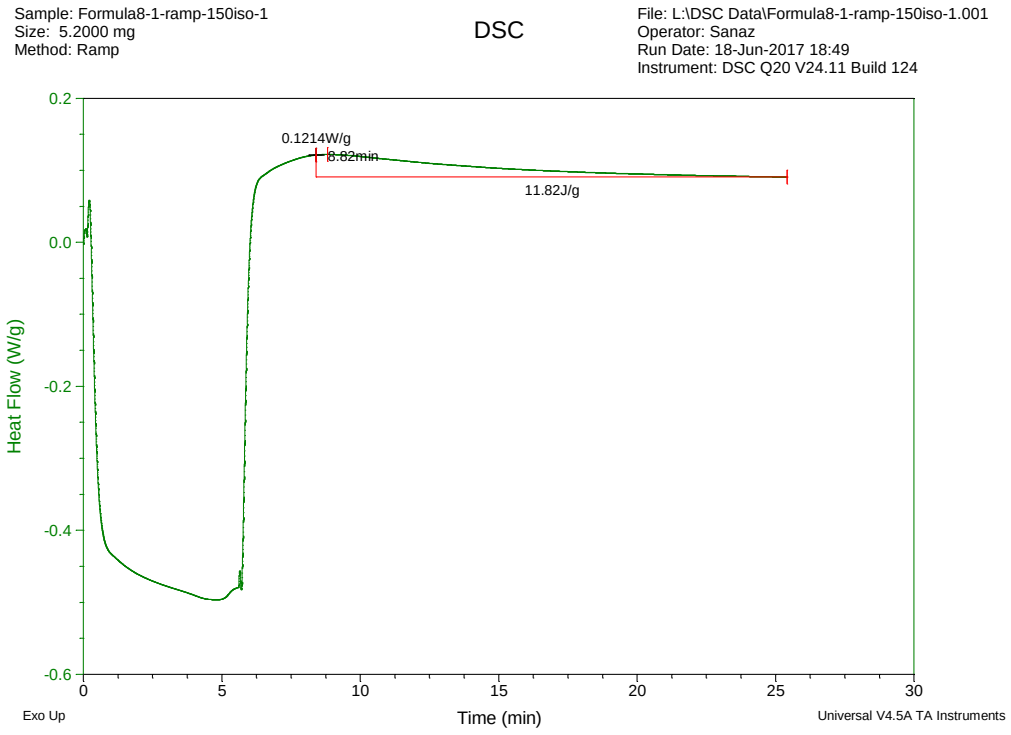

Figure B38: Formula 8 150^{o}C isothermal DSC curve

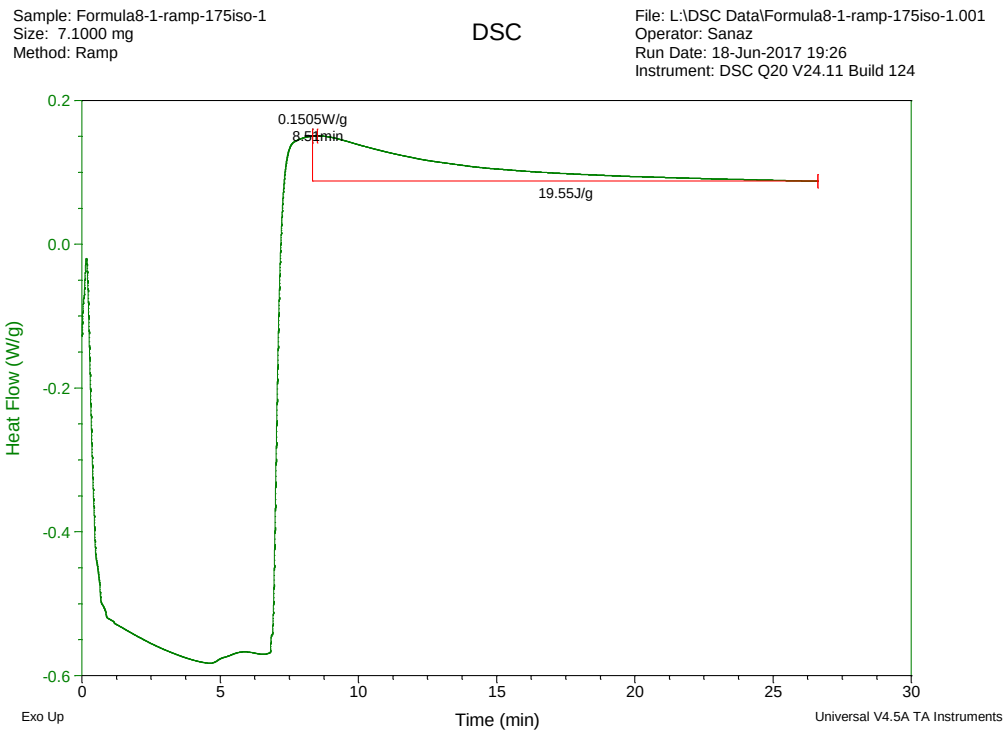

Figure B39: Formula 8 175°C isothermal DSC curve

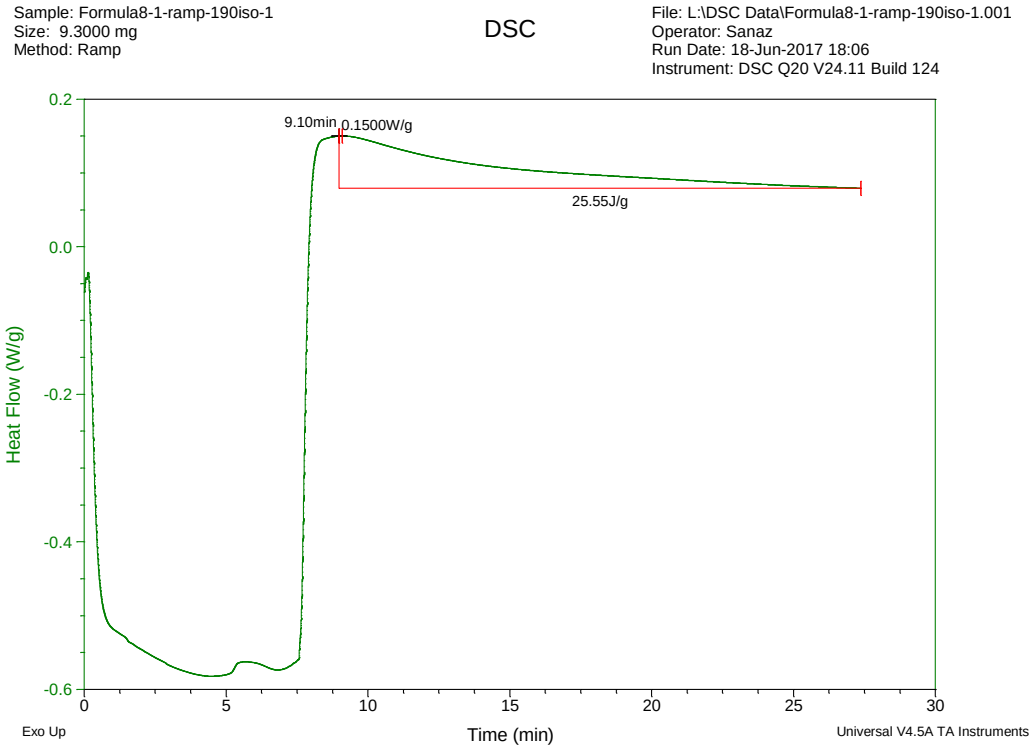

Figure B40: Formula 8 190°C isothermal DSC curve

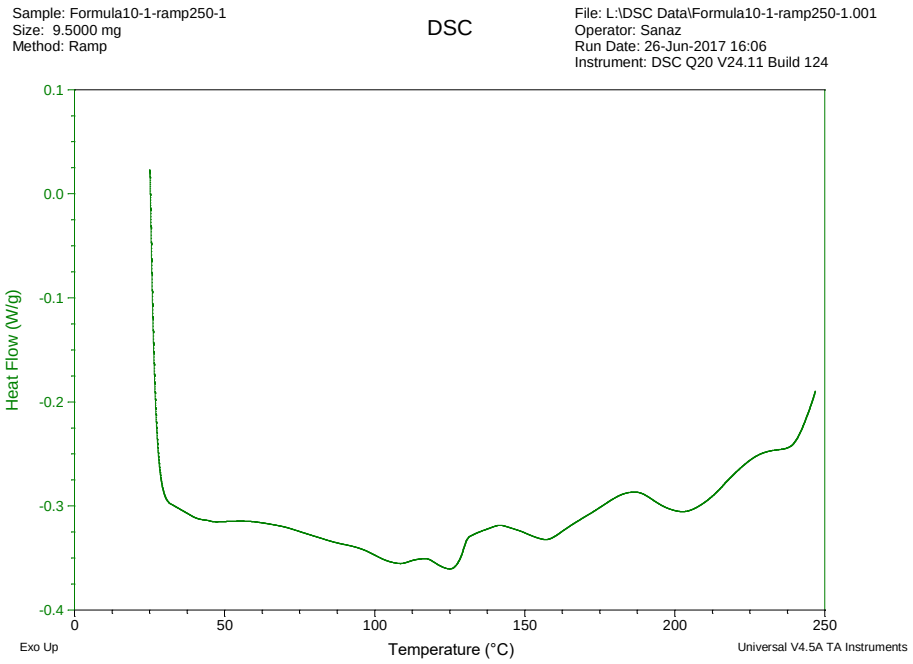

Figure B41: Formula 9 ramp DSC curve

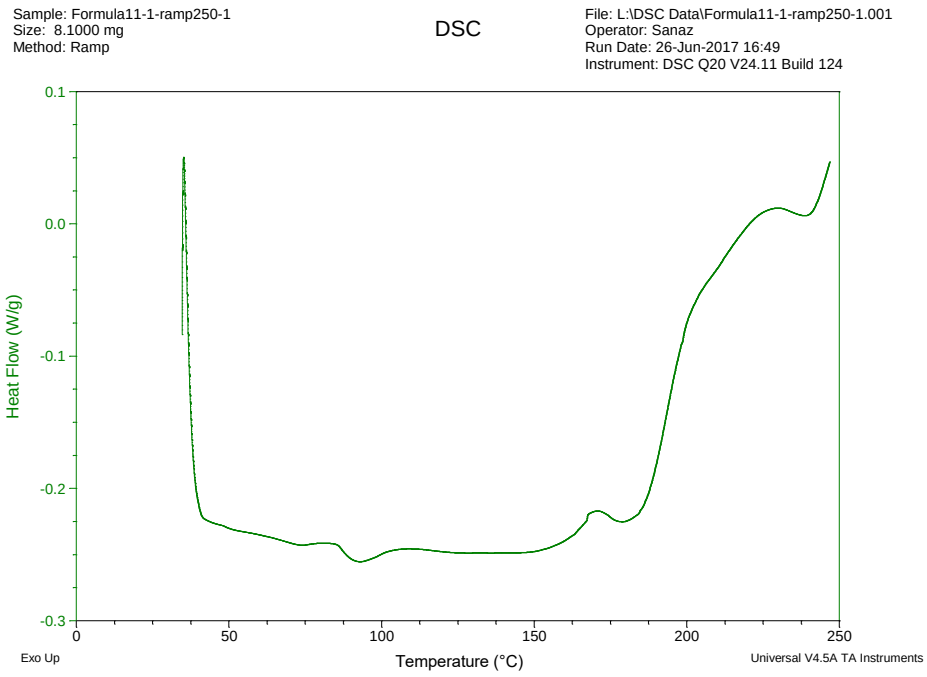

Figure B42: Formula 10 ramp DSC curve

APPENDIX C. FTIR SPECTRA

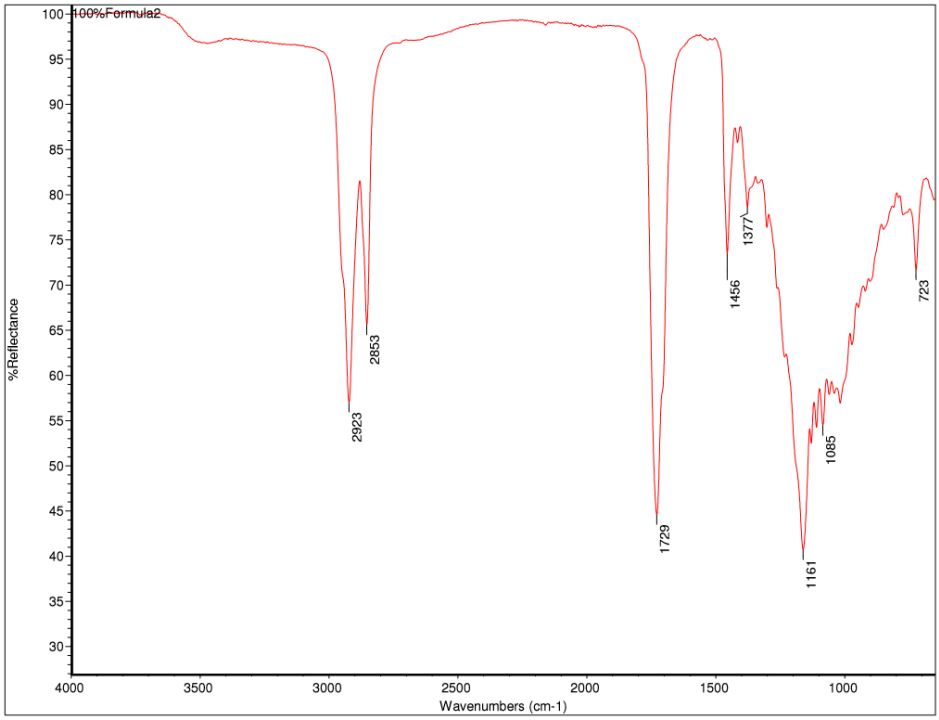

Figure C1: FTIR spectra of 100F2

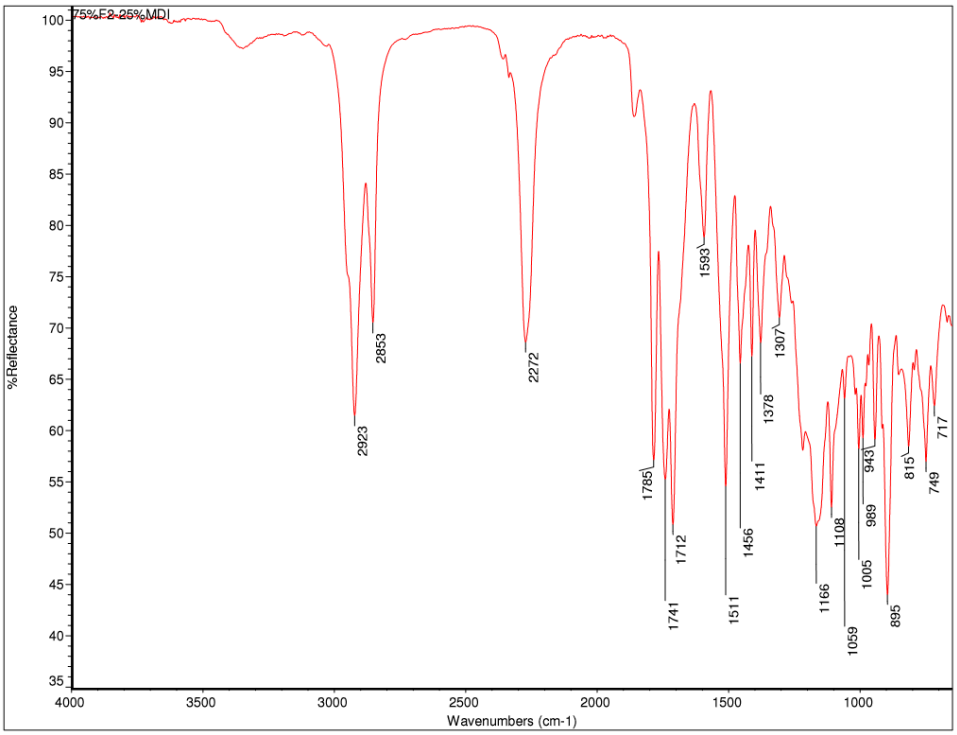

Figure C2: FTIR Spectra of 75F2/25M

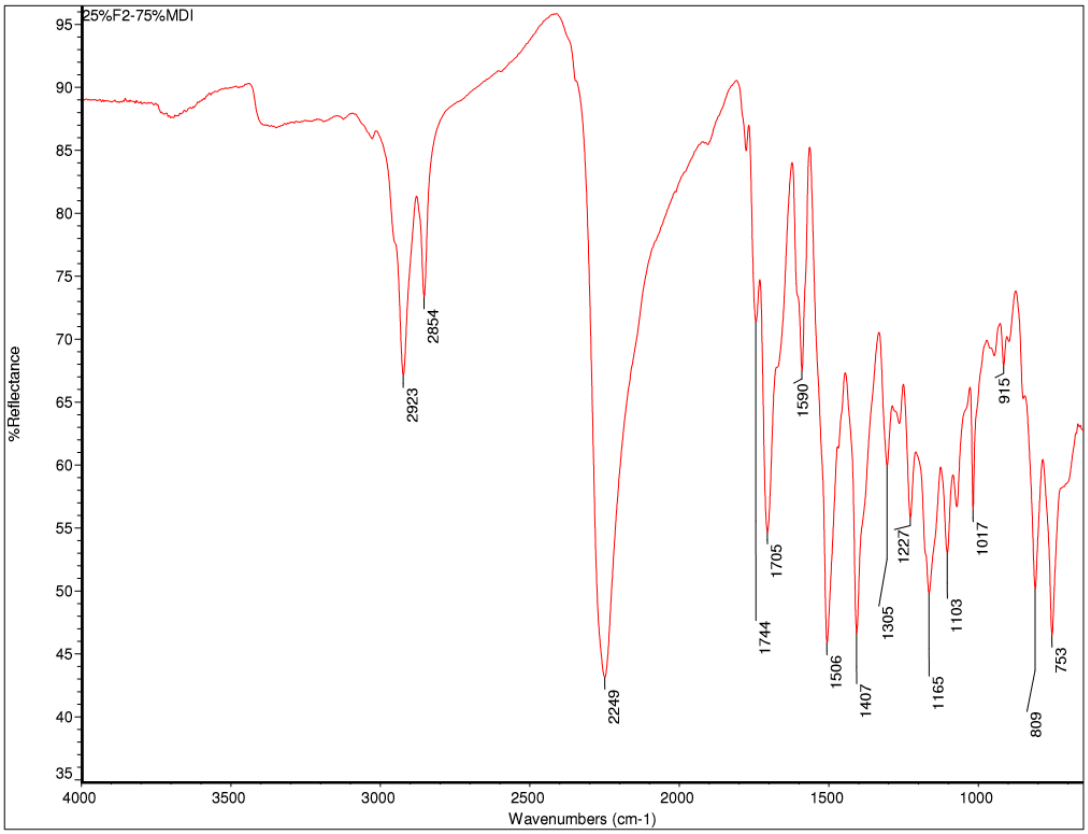

Figure C3: FTIR Spectra of 25F2/75M

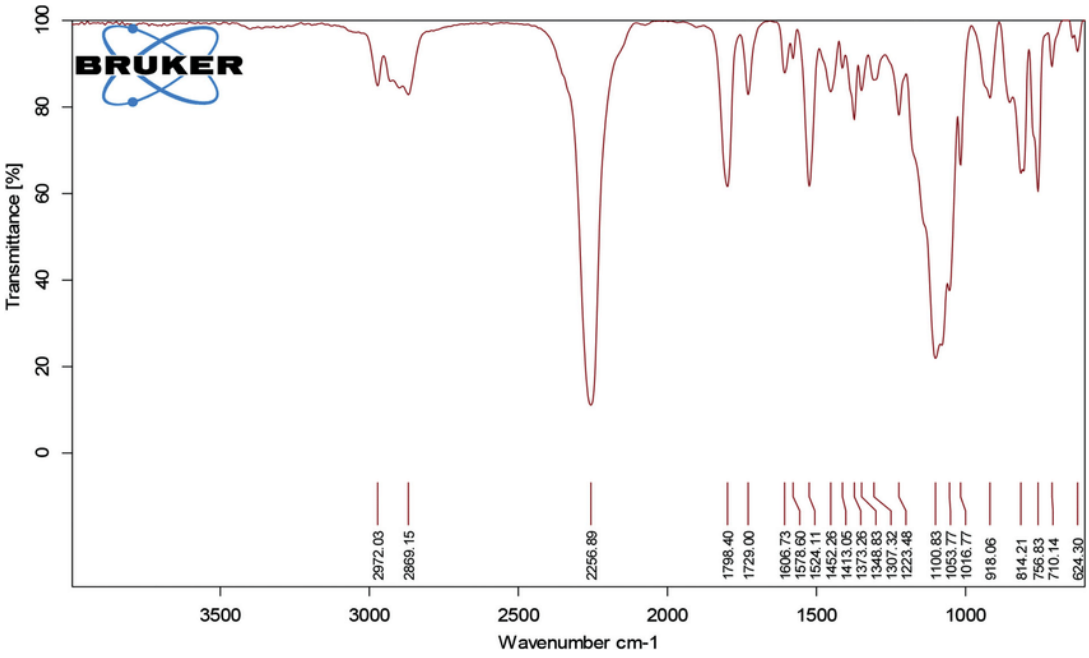

Figure C4: FTIR Spectra of 100M [38]